

Solvent removal from biodegradable microparticles prepared by solvent extraction/evaporation methods

Inaugural-Dissertation
to obtain the academic degree
Doctor rerum naturalium (Dr. rer. nat.)

submitted to the Department of Biology, Chemistry, Pharmacy
of Freie Universität Berlin

by
Florian Kias

Berlin 2024

The enclosed doctoral research work was accomplished from March 2020 until June 2024 under the supervision of Prof. Dr. Roland Bodmeier at the College of Pharmacy, Freie Universität Berlin.

1st Reviewer: Prof. Dr. Roland Bodmeier

2nd Reviewer: Prof. Dr. Philippe Maincent

Date of defense: July 12, 2024

Declaration of Authorship

I hereby declare that I alone am responsible for the content of my doctoral dissertation titled “Solvent removal from biodegradable microparticles prepared by solvent extraction/evaporation methods” and that I have only used the sources or references cited in said dissertation. I declare that I have never submitted this dissertation as part of another doctoral procedure.

Berlin, June 19, 2024

Florian Kias

“Do not waste your time looking for an obstacle - maybe there is none.”

Franz Kafka

Acknowledgements

During my studies and the work on this dissertation, I was very lucky to have family and long-time friends behind me and to meet great colleagues, students and new friends. They have all somehow contributed to how this work and I have developed over the last years. I would like to take this opportunity to acknowledge the following people in particular:

First, I would like to express my sincere thanks to my supervisor Prof. Dr. Roland Bodmeier. He shaped me and this work through his perspicacity, focus on scientific relevance, clarity and conciseness. I thank him for his guidance, inspiring impulses, willingness to discuss on the one hand and for giving me the space to develop to professionally and personally independence on the other.

I thank Prof. Dr. Philippe Maincent, for reading and co-evaluating my dissertation.

I acknowledge all my colleagues at the College of Pharmacy, former and current members of our working group for the pleasant and productive working atmosphere. In particular, I would like to thank Dr. Friederike Bach, Neele Dietrich, Zilin Mo, Lukas Preußel, Alexandra Lechermeier and Stefan Walther for the cordial conversations during spontaneous lab meetings, coffee breaks, or afterworks, which sometimes brought clarity, inspiration and new insights and sometimes (perhaps even more importantly) diversion. Special thanks to Giulia Cappelletti and Alexandra Lechermeier for their practical assistance in the lab and to Dr. Friederike Bach, Neele Dietrich and Zilin Mo for proofreading parts of this dissertation. I would also like to thank Anke Schindler from the Core Facility BioSupraMol for her assistance with the scanning electron microscopy.

I am grateful for having family and long-time friends always giving me their support and listening ear. In particular, I would like to thank my parents for their loving upbringing, the values they taught me and their trust in me and my decisions. Lastly, I thank Darlin from the bottom of my heart for her love, support, trust, patience and for making me feel at home when I am by her side.

Thank you all!

Table of Contents

1. Introduction	1
1.1. Long-acting injectables	2
1.2. Poly(lactide-co-glycolide)	5
1.3. Overview: Preparation of PLGA microparticles	8
1.4. Emulsification in the solvent extraction/evaporation method	11
1.4.1. Droplet formation by the batch process	12
1.4.2. Droplet formation by microfluidic flow focusing	14
1.5. Solvent removal in the solvent extraction/evaporation method	17
1.5.1. Initial solvent extraction	18
1.5.2. Final solvent extraction & free volume theory	23
1.5.3. Secondary drying	29
1.5.4. Solvent residues	31
1.6. Research objectives	33
2. Materials and Methods	34
2.1. Materials	35
2.1.1. Drugs	35
2.1.2. Biodegradable polymers	35
2.1.3. Solvents and others.....	35
2.2. Methods	36
2.2.1. Preparation of microparticles and films	36
2.2.2. In-process monitoring with focused beam reflectance measurement and video microscopy.....	39
2.2.3. Alcohol vapor-assisted fluidized bed drying	39
2.2.4. Residual Solvent content.....	40
2.2.5. Solubility.....	41
2.2.6. Optical Microscopy	42
2.2.7. Droplet and particle size analysis	42
2.2.8. Drug loading and encapsulation efficiency.....	43
2.2.9. In-vitro release.....	43

2.2.10.	Morphology	43
2.2.11.	Viscosity	43
2.2.12.	Surface tension	44
2.2.13.	Differential scanning calorimetry (DSC)	44
3.	Results	45
3.1.	Initial removal in the solvent extraction/evaporation method.....	46
3.1.1.	Phase-ratio limited solvent extraction and drug encapsulation.....	46
3.1.2.	Diafiltration-driven solvent extraction	49
3.1.3.	Effect of co-solvent methanol on the initial extraction	60
3.2.	Final solvent removal in the solvent extraction/evaporation method ..	64
3.2.1.	Effect of temperature and PLGA grade on the final solvent extraction .	64
3.2.2.	Effect of alcohols in the continuous phase on the final solvent extraction	71
3.3.	Secondary drying in an alcohol vapor-assisted fluidized bed.....	81
3.4.	Microfluidic microparticle preparation	94
3.4.1.	Drug encapsulation in microfluidic microparticle preparation	94
3.4.2.	Comparison of microparticles prepared by microfluidic flow focusing and the classical batch process.....	98
3.4.3.	Continuous solvent removal	100
4.	Summary.....	105
5.	Zusammenfassung	110
6.	Reference.....	116
	List of Figures	133
	List of Tables	138
	Publications.....	139

1. Introduction

The present dissertation focuses on the removal of solvents from biodegradable microparticles, a long-acting injectable dosage form. The following introduction begins with an overview about the relevance and variance of long-acting injectables in Chapter 1.1, followed by a presentation of poly(lactide-co-glycolide) (PLGA) as the most important biodegradable polymer for drug delivery and excipient for microparticle preparation in Chapter 1.2. An overview of the common manufacturing techniques for PLGA microparticles is given in Chapter 1.3. The extraction/evaporation method, which is the focus of this work, is then described in detail, divided into the emulsification process, described in Chapter 1.4 and the solvent removal described in Chapter 1.5. Based on this introduction, the research objectives are finally specified in Chapter 1.6.

1.1. Long-acting injectables

Parenteral administration of drug formulations is often superior compared to other administration routes in terms of bioavailability and targeted drug delivery [1–6]. Especially when administered orally, low solubility, permeability or stability limit the absorption of drugs [6–8]. Injections can circumvent these challenges but usually require repeated administration at short intervals due to the metabolism and systemic clearance of drugs. Long-acting injectables (LAI) are depot formulations, also called long-acting drug delivery systems (LADDS), for parenteral use, which reduce the frequency of administration by controlled release of the drug over a period of several days to several months [1–6]. This improves the patient compliance and the therapy adherence. In addition, uniform release avoids fluctuations in the plasma concentration of the drug and prevents it from falling below the minimum effective or exceeding the minimum toxic concentration. This increases the efficacy and safety of the therapy and minimizes side-effects [6,9,10].

Typically, LAI are injected subcutaneously or intramuscularly to achieve a systemic effect. It is also possible to administer directly into or close to the target tissue, such as the vitreous body of the eye [3,5,6]. Depending on the requirements, for example the release profile, there are different LAI of varying complexity. Oily solutions of drugs are easy to prepare, and final sterilization can be performed by sterile filtration instead of often for LAI required gamma sterilization. The drug is released by partitioning from the formulation, depending on its concentration, the surface area of the oily depot and

the partitioning coefficient between the tissue fluid and the formulation. Crystal suspensions are prepared by milling (top-down) or precipitation (bottom-up), allow high dosage of the drug per volume and release the drug by the rate of dissolution [4,5,11]. Suspensions and oily solutions can release drug over several days to weeks depending on the drug and formulation properties [4,5]. From more complex polymer or lipid-based solid formulations, drug is usually released by diffusion and/or erosion, which usually results in a prolonged release of weeks to months [4–6,12].

Biocompatible polymers used for LAI are differentiated based on whether they are biodegradable or not. Non-biodegradable polymers such as ethylene vinyl acetate, polyimide, poly(vinyl alcohol), poly(vinyl acetate) have to be surgically removed from the tissue after therapy. Drug release from such systems occurs by diffusion. Biodegradable polymers eliminate the need for resurgery of LAI. Natural and semi-synthetic polysaccharides (e.g., cellulose derivatives, sodium alginate, dextran, chitosan, and hyaluronic acid) and polypeptides (e.g., collagen, elastin, and albumin) or synthetic polyesters (e.g., methacrylates, poly(lactide-co-glycolide) (PLGA), polylactide, and polycaprolactone) are being researched for this purpose [6,13]. The release from polymer-based systems is often not or not only controlled by diffusion, but also by erosion. A distinction can be made between surface and bulk erosion [5,14].

PLGA is the most widely used biodegradable polymer on the market, with more than 20 approved LAI formulations for human use [5,12,15]. These are solid implants (e.g., Zoladex[®], Ozurdex[®], Propel[®]), in-situ forming implants (e.g., Atridox[®], Eligard[®], Perseris[®]) and, as the largest group in terms of numbers, microparticles (e.g., Lupron Depot[®], Risperidal Consta[®], Zilretta[®]) [5,12,15]. PLGA-LAI can be used as carriers for small drugs as well as for large complex biomolecules for various indications including mental disorders, metabolic disorders, pain, infections, etc. [5,6,15].

Solid PLGA implants are usually small cylindrical rods with 10 - 35 mm length and 1 - 3 mm diameter [5]. Commonly used preparation methods for implants include hot melt extrusion (HME), compression molding, injection molding and solvent casting [6,16]. More complex shapes are also possible, in particular through molding processes or 3D-printing, which may allow the control of the drug release or application in tissue engineering [6,17,18]. A major advantage of solid implants is the ease of manufacturing and the high drug loading capacity and release retardation due to the

small surface area to volume ratio. A disadvantage is the large size, which necessitates the use of large, painful cannulas or small surgical interventions for application [5].

In-situ forming implants are liquid or semi-solid PLGA solutions, which are easy to inject and solidify/gel after application [6,19–21]. Solvents used here to dissolve PLGA must be biocompatible and dissolve to a certain extent in aqueous body fluid. Commonly used solvents for in-situ systems include dimethylformamide (DMF), dimethyl sulfoxide (DMSO), ethyl benzoate, N-methyl-2-pyrrolidone (NMP), and triacetin [16,20,22]. A variation of this concept are in-situ forming microparticles, in which an O/W- or O/O-emulsion with PLGA and drug in the inner phase is injected [21–23]. At the application site in-situ forming implants/microparticles solidify fast due to fast diffusion of the solvent into the surrounding tissue. A significant proportion of drug can also be released during this step. Due to the high and possibly fluctuating burst release, in-situ forming systems may not be suitable for drugs with a small therapeutic window [5,21]. Furthermore, high solvent concentrations after application may cause myotoxicity [22].

Microparticles are dispersible particles of a size of 1 - 1000 μm . Microparticles made of PLGA with a size of approximately 1 - 250 μm , often 10 - 125 μm , are most commonly used for drug delivery to achieve good cannula mobility and to prevent phagocytosis of particles smaller than 10 μm [5,24,25]. Microparticles, in which drug is encapsulated dissolved or dispersed throughout the entire matrix, are called microspheres [5,24,25]. If the drug is deposited in the form of a reservoir system only in the inner core, covered by a drug-free polymer layer, microparticles are called microcapsules [5,24,25]. The administration of PLGA microparticles is less invasive compared to PLGA implants, because small needles can be used due to the small particle size instead. Surgical insertion or the use of large needles can therefore be avoided [5,25]. Disadvantages of microparticles, compared to implants, are that they cannot be removed to terminate the therapy, the maximum drug loading is usually lower and the release faster due to a larger surface area and shorter diffusion pathways. Furthermore, the manufacturing of microparticles is in general more complex compared to solid or in-situ forming implants. Most manufacturing methods for microparticles require several manufacturing steps, long process times and the use of organic solvents to dissolve the PLGA, which then must be removed again (Chapter 1.5).

1.2. Poly(lactide-co-glycolide)

The polyester PLGA consists of the monomers lactic acid and glycolic acid, typically arranged in blocks of polylactic acid and polyglycolic acid. Since the bond between two lactic acids forms an asymmetric stereochemical center, two enantiomers poly L-lactic acid and poly D-lactic acid can be divided. PLGA usually contains both forms in equal ratio and is therefore called poly(D,L-lactic-co-glycolic acid) [26]. PLGA can be produced by polycondensation of lactic acid and glycolic acid, whereby only a limited molecular weight is achieved. Therefore, ring-opening polymerization from the cyclic dimers lactide and glycolide, catalyzed by organometallic compounds, is used industrially to produce high-molecular weight PLGA efficiently (Figure 1) [27,28].

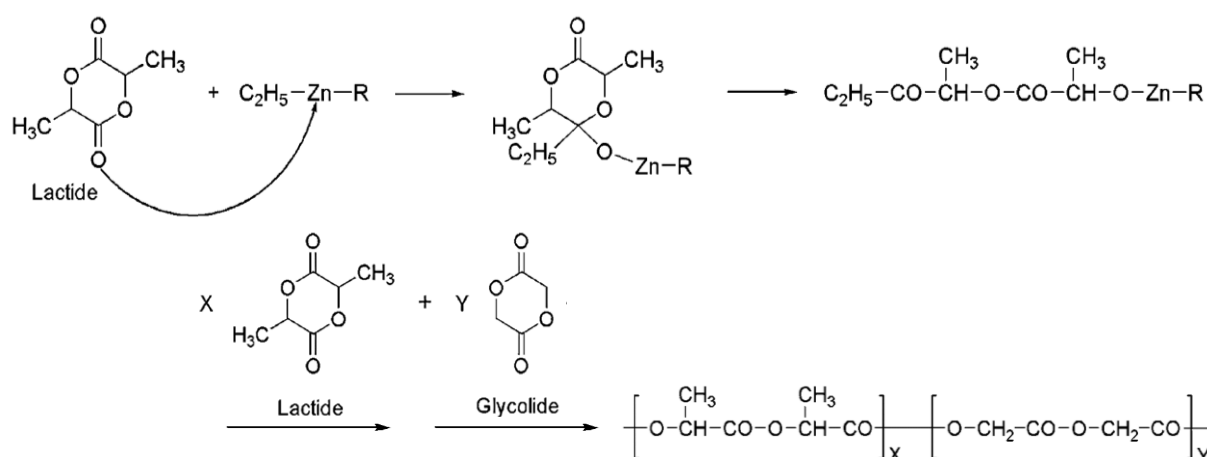


Figure 1: Synthesis of PLGA by ring-opening polymerization of lactide and glycolide (adapted from [27])

The physico-chemical properties of PLGA are mainly affected by its molecular weight, lactic to glycolic ratio and chemical groups at the polymer chain ends [12,15,27,28]. Furthermore, the distribution and length of polylactide and polyglycolide blocks, both strongly dependent on the synthesis process, can affect for example solubility, crystallinity and degradation behavior [28,29]. In general, increasing molecular weight, lactic content and end-capping increase the hydrophobicity of PLGA, thus altering its affinity for solvents, additives and drugs [12,15]. The molecular weight refers to the chain length of the polymer. An increase of molecular weight increases, for example, the viscosity of PLGA solutions, having a major effect on particle size of microparticles. Therefore, the inherent viscosity of a PLGA grade is often given as an indication of the molecular weight.

PLGA degrades primarily through hydrolysis of its ester bonds, which link the lactic acid and glycolic acid monomers, in the presence of water [27,30–32]. Progressing degradation results in monomers and oligomers which become water soluble below a critical molecular weight of about 1100 Da [30]. As degradation progresses, the PLGA matrix loses its mechanical strength until visible bulk erosion starts. As long as the matrix is not eroded, the monomers are only released slowly and accumulate, thus lowering the inner micro-pH of the matrix and promoting the hydrolytic degradation in the form of autocatalysis [27,30–32]. The degradation products of PLGA can be eliminated by renal excretion or metabolized from the body. Lactic acid and glycolic acid can be converted into pyruvate via a number of intermediate reactions and then metabolized into carbon dioxide and water by the tricarboxylic acid cycle (also known as Krebs cycle) [26,27].

The morphology of a PLGA matrix and the physicochemical properties of the PLGA grade affect degradation [32]. An increased hydrophobicity of PLGA delays the hydration and therefore the hydrolysis [30–33]. In addition, the methylene group of lactic acid impedes the hydrolysis sterically, resulting in a 1.3 times faster hydrolysis of the ester bonds of the glycolic unit compared to the lactic unit [31,33]. Thus PLGA with a high blockiness, i.e. an uneven distribution of lactic and glycolic units, degrades faster, due to a larger number of sterically easy accessible glycolic-glycolic bonds [28,29]. Increasing molecular weight may increase degradation rate due to an increased number of ester bonds, which can be hydrolyzed [31]. However, due to the initially higher molecular weight, it still takes more time until cleavage products have fallen below the critical molecular weight being water soluble and the integrity of the PLGA matrix is retained longer compared to an initially low molecular weight [14,29,31].

The release of drugs from PLGA microparticles is based on the diffusion through the polymer or water-filled pores and the erosion of the matrix [34]. The release depends primarily on the physicochemical properties of the drug and PLGA grade, the microparticle size and morphology [29,34,35]. The release profile can be monophasic linear, biphasic or most commonly triphasic [34–37]. During the first phase, the burst, drug, which is encapsulated close to the surface or in contact with surface-connected pores, is released rapidly by dissolution and diffusion. The burst is increased by a high drug loading, a small particle size or a high porosity [29,35,37,38]. Percolation, which

can occur at high loading with drug undissolved in the polymer (above so-called percolation threshold), greatly increases the burst. Dissolution of drug crystals close to the surface, create pores that allow media access to further drug crystals, creating a pore network that enables the rapid initial release of large amounts of the encapsulated drug [39]. The release in the second phase is almost constant and controlled by the diffusion of the drug through the slowly swelling PLGA-matrix [36,37]. Depending on the solubility and diffusivity of the drug in the polymer, little to almost all of the encapsulated drug is released within the second phase [37]. The last phase is controlled by substantial swelling and bulk erosion of the matrix due to progressed degradation of PLGA, so that remaining drug is released fast [29,36].

1.3. Overview: Preparation of PLGA microparticles

For the preparation of PLGA microparticles different methods can be used. For most manufacturing processes, PLGA must be dissolved in an appropriate organic solvent, for example chloroform, dichloromethane (DCM), or ethyl acetate (EtAc) [16,40].

The most common process is the solvent extraction/evaporation method, where a solution of PLGA in an organic solvent is emulsified in an aqueous continuous phase, which usually contains a surfactant or stabilizer (e.g., Polyvinyl alcohol (PVA) polyethylene glycol sorbitan monolaurate (Tween), sorbitan monooleate (Span), sodium dodecyl sulfate (SDS)) [41–43]. The resulting emulsion droplets solidify into microparticles through extraction and evaporation of the organic solvent. The various modifications of this manufacturing method might be differentiated by the targeted emulsion system, the process of emulsification (Chapter 1.4) and the solvent removal (Chapter 1.5). The simplest emulsion system is oil (drug:PLGA:organic solvent) in water (usually containing a stabilizer), abbreviated as O/W. A distinction can be made as to whether the drug is dissolved in the organic phase or dispersed, i.e. as a solid in oil in water (S/O/W) system. The drug can also be dissolved or dispersed in a second aqueous phase, which is emulsified into the organic phase to form a water in oil in water (W/O/W) system, also called double emulsion [16]. Challenges of the solvent extraction/evaporation method include the low encapsulation efficiency of water-soluble drugs, instabilities of drugs and PLGA due to the presence of water or organic solvent, and the removal of residual solvents [16].

In the phase separation method, the solubility of a dissolved polymer is decreased, for example by the addition of non-solvents, salts, incompatible polymers, complex-forming polymers, or temperature change to form coacervates onto the surface of drug crystals, that where subsequently solidified into particles [40]. For the preparation of PLGA microparticles by the organic phase separation method, the gradual addition of a solvent-miscible PLGA non-solvent (e.g., liquid methacrylic polymers, silicone oil, vegetable oil, or light liquid paraffine oils) to a stirred solution of PLGA in an organic solvent (e.g., dichloromethane, ethyl acetate, or acetonitrile), initiating liquid-liquid phase separation is most commonly performed [40,44,45]. Resulting droplets of PLGA-rich phase are solidified into microparticles by addition of an extractant (e.g., hexane,

heptane, or petroleum ether). The absence of water in this process may improve the encapsulation of hydrophilic drugs and stability of proteins, but process stability, scale-up and removal of non-volatile organic solvent residues are challenging [16,40].

In the spray drying method, a solution of PLGA in an organic solvent is atomized into fine droplets in a spray drying apparatus [40,46]. Warm drying gas facilitates fast solvent evaporation and thus solidification of the droplets. The need for fast solidification and a high risk of particle aggregation typically limit the flexibility of formulation and process development [16]. Even if the thermal stress is short-term and rather low due to evaporation cooling, it can be critical for some drugs. To avoid the use of heat, droplets can be sprayed into a cryogenic liquid such as nitrogen or argon, during so called spray freeze drying (SFD). The atomized droplets solidify immediately and organic solvent is removed in a subsequent process by lyophilization, or cryogenic solvent extraction in a non-solvent, as in the ProLease[®] process, used for manufacturing the discontinued Nutropin DEPOT[®] [40,43,47]. Microparticles prepared by spray drying or SFD typically have a high encapsulation efficiency, but may be porous, have significant burst release and low yield [40,48,49].

Methods that do not involve dissolution of PLGA in organic solvents are rarely used. In the so-called rapid expansion of supercritical solutions (RESS) method a polymer is dissolved in a supercritical fluid at high pressure and precipitated by a rapid decompression, due to a loss of the liquid-like solvent power [40]. Due to the limited solvent power of common supercritical fluids for high molecular weight polymers, this process is not commonly used for PLGA. Instead, supercritical fluids or compressed gas are more likely to be used to precipitate atomized or emulsified PLGA: or PLA:organic solvent droplets [40,50,51] or to extract residual solvent from formed microparticles (Chapter 1.5.2.). The high viscosity and low thermostability of PLGA limit the use of manufacturing techniques that require a low melt viscosity, like spray-congealing (atomization of a lipid or polymer melt into droplets, solidified by spraying them into a cold air stream or cold non-solvent) [40,43,52]. In top-down granulation, also called melt-grinding method in this context, PLGA is first melted, extruded, or compressed together with the drug and then grinded [53–55]. If necessary, these granules are redispersed in a non-solvent and heated to achieve a rounded shape with a smooth surface [56]. Alternatively, in the melt emulsification method, also called melt

encapsulation, PLGA and drug are dispersed in a hot non-solvent without preprocessing. The temperature is chosen so that PLGA is sufficiently liquid to be emulsified into droplets, which are solidified into microparticles by cooling [57]. In particular, the high thermal stress on drugs and PLGA limits the use of these solvent-free methods [16].

1.4. Emulsification in the solvent extraction/evaporation method

Emulsification is a crucial step in the preparation of PLGA microparticles with the solvent extraction/evaporation method. The size of the droplets formed essentially determines the size and size distribution of the final microparticles. The microparticles are generally smaller than the droplets, as these shrink due to the removal of solvent. The extent of shrinkage depends mainly on the initial concentration of PLGA in the dispersed phase [58] and the solvent extraction rate (Chapter 1.5.1).

Emulsification for microparticle preparation can be performed with various techniques, whereby stirring (batch process) (Chapter 1.4.1) and microfluidic flow focusing (Chapter 1.4.2) are used in this dissertation and are therefore discussed in more detail in the following chapters. In addition, there are various other techniques, including e.g. static mixing, membrane emulsification, and step emulsification [41].

Static mixers are pipes equipped with built-in flow obstacles that break up and reunite the fluid flows, creating a homogeneous mixing field [41,59]. A static mixer has no moving parts, which reduces abrasion and maintenance. The droplet size is mainly determined by the geometry and number of mixing elements used, the flow velocities, viscosities, and the interfacial tension of the dispersed organic and continuous aqueous phase [41,59,60]. The effort of a classical scale-up can be reduced by producing continuously and minimizing downtimes. If this does not facilitate a sufficient production capacity, a numbering-up can be easily performed, where several mixers are connected in parallel, which leads to a considerable increase in throughput [41].

Emulsions can also be prepared by interfacial tension driven droplet formation. In this process, the organic PLGA solution is slowly introduced through microchannels [61,62] or porous membranes [63,64] into a slowly agitated continuous aqueous phase containing a surfactant. Droplets usually do not detach due to significant shear, but due to the instability resulting from the elongation of their surface and a drop of Laplace pressure [41,65]. For this reason, the droplets can be highly monodisperse and their size depends mainly on the geometry of the channel exits or pores. This passive droplet detachment is slow, but an acceptable throughput might be achieved by an easy numbering-up [41,65].

1.4.1. Droplet formation by the batch process

In the classical batch process, a continuous aqueous phase, usually containing a stabilizer, is stirred in a vessel with an impeller. The organic PLGA solution, containing the drug, is added slowly or all at once. Essentially, droplets of the forming emulsion can be split by drag and shear force induced by the impeller. This is counteracted by the Laplace pressure, i.e. pressure between the convex and concave side of the curved droplet interface, as a shape-retaining cohesion force [66]. This ratio between drag and cohesion force can be expressed by the Weber number:

$$We = \frac{\rho_c v^2 d}{\sigma} \quad \text{Equation 1}$$

ρ_c denotes the density of the continuous phase, v the velocity, d the droplet diameter, σ the interfacial tension between dispersed and continuous phase.

Increasing the shear forces by increasing size, number, agitation rate or changing impeller geometry decreases droplet size and possibly also polydispersity due to a homogeneous power input [41,67,68]. Vertical baffles in the vessel can increase the axial velocity and thus circulation and reduce the tangential and swirl velocity [69]. This results in a decreased and narrower size distribution of droplets, reduced air entrainment by preventing vortex formation and increased yield of solidified microparticles [70].

Formulation parameters that are relevant for the droplet size are the viscosity, interfacial tension and the phase ratio of the dispersed and the continuous phase [41]. The viscosity of the dispersed phase can be increased by a higher molecular weight of the PLGA grade used and a higher initial concentration. The viscosity of the continuous phase and the interfacial tension can be changed by adding surfactants/stabilizers. The most commonly used stabilizer PVA reduces particle size more efficiently than other surfactants/stabilizers [71], as it lowers the interfacial tension with increasing concentration to the critical micelle formation concentration (CMC), but also increases the viscosity of the continuous phase. With increasing PVA concentration, smaller droplets are formed and stabilized by reducing coalescence [41,72]. Since small satellite droplets that may form when larger droplets break up can

also be better stabilized, the particle size distribution can be broadened by increasing the stabilizer concentration.

In accordance with the relationships described above, various studies were carried out to calculate the droplet size of emulsions in general. However, due to the defined assumptions and limitations (e.g., viscosities) in the creation of many equations, these may not be applicable to microparticle preparation. An important mathematical correlation for O/W emulsions was developed by Calabrese [73]:

$$\frac{D_{32}}{L} = C \left(\frac{\rho_c}{\rho_d} \right)^{3/8} \left(\frac{\mu_d}{\mu_c} \right)^{3/4} Re^{-3/4} \quad \text{Equation 2}$$

D_{32} denotes the Sauter diameter, L the impeller diameter, C a dimensionless empirical constant, ρ_c and ρ_d are the densities and μ_c , and μ_d viscosities of the continuous and dispersed phases. Re , the Reynold number, describes the ratio of inertia forces to frictional forces and is defined as:

$$Re = \frac{\rho_c N L^2}{\mu_c} \quad \text{Equation 3}$$

Here N denotes the impeller speed. Calabrese points out that the influence of the viscosity of the continuous phase is cancelled out by inserting the Reynolds number, although this actually has an influence on the droplet size [73]. The effect of the phase ratio on the droplet size is also neglected in this correlation and might be described as follows [74]:

$$D_{32} L = (1 + b \varphi)^n We^{-0.6} \quad \text{Equation 4}$$

Here φ denotes the volume phase fraction and b and n are a numerical coefficient and exponent.

In principle, the correlations described for emulsions also reflect the influencing factors during microparticle production. However, predicting the size of microparticles is more complex. The described equations are based on an emulsion system in which an equilibrium is established between the droplet break-up and coalescence after some time. In microparticle preparation the formulation-dependent parameters, particularly

the viscosity of the dispersed phase, change significantly due to the solvent removal. The theoretical equilibrium of the droplet size distribution changes dynamically during the preparation process and may not be reached due to the solidification of PLGA. Therefore, opposite effects of the phase ratio on the microparticle size are described [41]. Theoretically, according to emulsion theory, an increasing volume of continuous phase reduces the final particle size. In practice, the particle size may not be affected by a change in the phase ratio [67,68] or even increases with an increasing proportion of continuous phase [75–77]. Increasing the solvent dissolving capacity of the continuous phase accelerates the solvent removal and solidification of PLGA and thus may prevent complete shrinkage of the droplets (Chapter 1.5.1).

1.4.2. Droplet formation by microfluidic flow focusing

Microfluidics describes the manipulation of small amounts of fluids through small channels ranging in size from ten to hundreds of micrometers [78]. At this microscale, interfacial and viscous effects dominate over bulk forces, enabling unique multiphase flow behavior [79]. A major advantage of this technique is the enormous control over the droplet size, as only one droplet is produced at a time. This allows, for example, the preparation of monodisperse droplets or the formation of multiple emulsions with a well-defined layer thickness [80]. A droplet generation frequency of hundreds to over ten thousand droplets per second can be achieved. However, this only corresponds to very small volumes, resulting in a low throughput, which might be seen as the biggest disadvantage of microfluidics. This challenge can be partially overcome by numbering up, i.e. the parallelization of different channels [81]. However, this may require complex geometries for distributing the fluids and a high level of manufacturing precision in order to achieve comparable hydrodynamic conditions in each channel. There are various microfluidic geometries for passive droplet generation (i.e. without moving parts or external actuation), the most common being coaxial, flow focusing and T-junction (Figure 2). These can be operated in different flow regimes, which determine whether, how and where (relative to the junction) droplets are formed, with the most common distinction between dripping, jetting and stable co-flow [78,79,81].

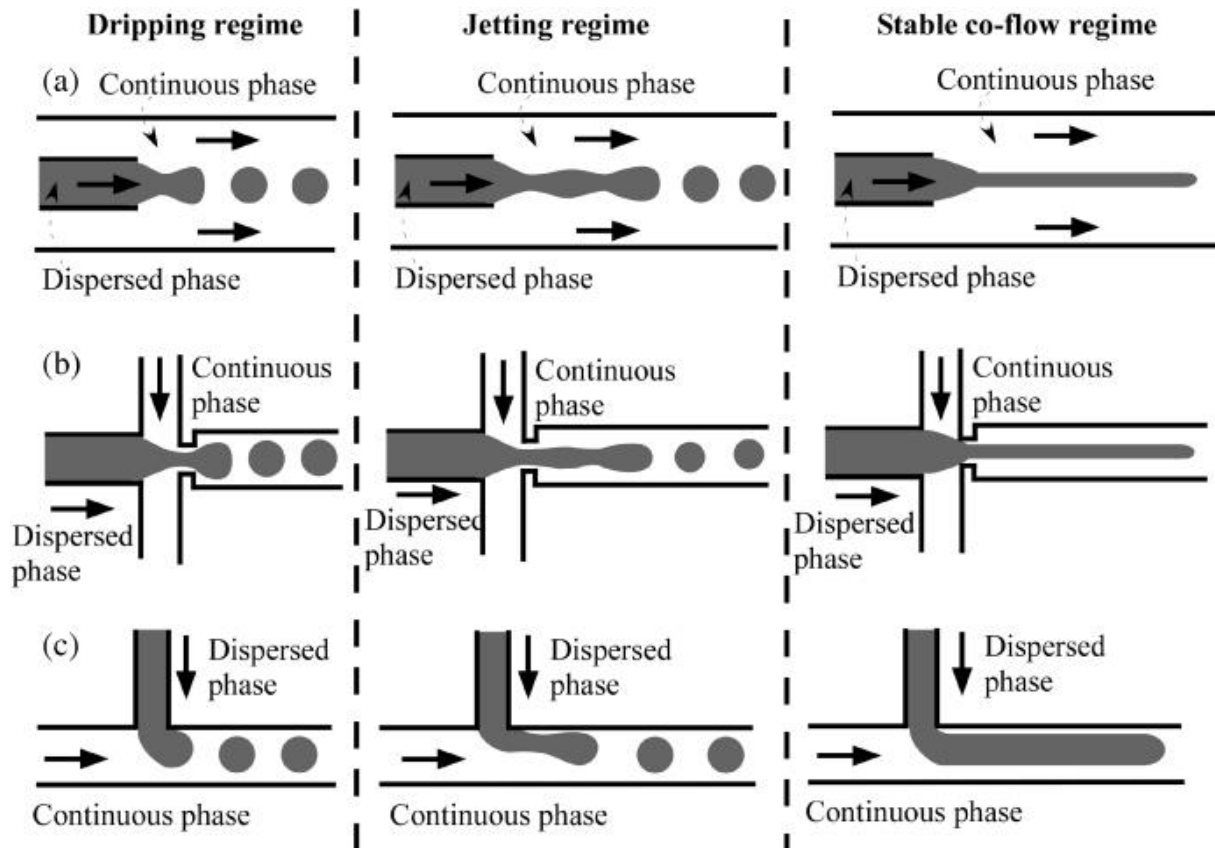


Figure 2: Schematic representation of different flow regimes in (a) coaxial, (b) flow focusing and (c) T-junction microfluidic devices [79]

In this study, only the flow focusing geometry was used, which has the advantage of avoiding contact of the dispersed phase with the channel walls downstream of the junction, which increases the process stability. In hydrodynamic flow focusing, the continuous phase flows on both sides of the dispersed phase to a junction/orifice, which is fabricated in a microfluidic device, usually a chip of glass, polydimethylsiloxane, silicon or polymethylmethacrylate [78,79,81]. At the junction, the continuous phase shears droplets of the dispersed phase when leaving the junction (dripping regime) or focusing it to a jet, which may break into droplets downstream of the junction due to shear induced elongation and undulation (jetting regime) [79]. Whether a droplet or a jet is formed depends on whether shear forces or capillary pressure predominate in the junction. This ratio can be expressed by the capillary number Ca :

$$Ca = \frac{\mu Q}{\sigma h^2} \quad \text{Equation 5}$$

1.4 Emulsification in the solvent extraction/evaporation method

Here μ , Q and σ indicate the viscosity, flow rate and interfacial tension of the described phase and h the channel height of the microfluidic device. The transition from dripping to jetting occurs, if the critical capillary number $Ca \approx 0.1 - 1$ of the dispersed or continuous phase is exceeded [80,82]. Near the critical capillary number, a viscous tail may form during droplet deposition, which can break into satellite droplets [82]. Jetting can also lead to a broader particle size distribution compared to dripping [83]. The dripping regime is sometimes subdivided depending on whether droplets are generated in the junction orifice (mode 1) or directly behind it (mode 2) [83]. In the dripping regime, droplets are formed by a combination of capillary instability and viscous drag [78]. With a fixed junction geometry and formulation, increasing the ratio of the continuous phase flow rate to the dispersed flow rate decreases the droplet size and increases the droplet generation frequency [83–85]. Increasing the flow rate of the continuous and the dispersed phase increases the droplet generation frequency while maintaining the droplet size until jetting occurs. As the viscosity of the dispersed phase increases, the droplet size increases and the dependency on the flow ratio becomes weaker [83].

The addition of water-soluble polymers, solvents or surfactants to the continuous phase may reduce the droplet size by reducing the interfacial tension and/or increasing the viscosity [86,87]. The effect of the interfacial tension seems to be predominant in some studies, since SDS reduced the droplet size more than PVA, although it increases the viscosity less, but significantly reduces the dynamic interfacial tension more [87]. Erb et al. observed no significant effect of the surfactant in the continuous phase on the droplet size in microfluidics. This is explained by the fact that the diffusion rate of surfactants at the interface (100 - 1000 ms) is usually much slower than droplet formation in microfluidics (often less than 1 ms) [80]. As a result, surfactants barely influence dripping, but can be decisive for the stability of the generated emulsion downstream of the junction.

1.5. Solvent removal in the solvent extraction/evaporation method

Most manufacturing methods for the preparation of microparticles require the dissolution of PLGA in an organic solvent (Chapter 1.3). The selection of a solvent for the solvent extraction/evaporation method primarily aims for a good solubility of PLGA, a limited miscibility with water to form an emulsion and often a high volatility to promote removal by solvent evaporation [12,88]. The solubility of PLGA in organic solvents depends on the molecular weight and especially on the lactide:glycolide ratio (Table 1), while the effect of end-capping is negligible [12].

Table 1: Dissolution of 2.5 % (w/V) PLGA in different solvents depending on the lactide:glycolide ratio at a constant molecular weight of around 80 kDa [12]

Solvent	PLGA L:G Ratio											
	50:50	55:45	60:40	65:35	70:30	75:25	80:20	85:15	90:10	95:5	100:0	
Dichloromethane												
Dimethyl sulfoxide												
Dimethyl formamide												
Ethyl acetate												
Methyl ethyl ketone												
Tetrahydrofuran												
Ethyl benzoate												
Chlorobenzene												
Benzyl alcohol												
Methyl n-propyl ketone												
n-Butyl acetate												
Trichloroethylene												
Ethyl-L-lactate												
2-Methyl tetrahydrofuran												
1,2-Dichlorobenzene												
Toluene												
Methyl isobutyl ketone												
Butyl lactate												
p-Xylene												

Other aspects, such as drug solubility or interfacial tension, may also be considered for solvent selection to control the encapsulation efficiency or distribution of the drug in the microparticle [89–91]. By far, the most common solvents are dichloromethane and ethyl acetate. Dichloromethane has a slightly better solubility for PLGA with less than 65 % lactide, a higher volatility, a lower interfacial tension to and solubility in water compared to ethyl acetate [12,89,90]. Mixtures of these solvents with other PLGA

solvents or non-solvents can also be used to modify the solubility of drugs and PLGA or the extraction rate and thus possibly morphology and drug release profile [88,91,92].

The removal of organic solvent is essential to transfer droplets into solidified microparticles and controlling the critical properties of the final product including drug release and storage stability [93]. Additionally, most of the organic solvents used have a certain toxicity and must therefore be removed to a minimum [93,94] (Chapter 1.5.4). The solvent removal process during microparticle manufacturing in the solvent extraction/evaporation method can be divided into a wet-processing step and a secondary drying step depending on whether the microparticles are dispersed in a liquid continuous phase or have been collected. In the following, wet processing is subdivided into rapid initial (Chapter 1.5.1) and slow final extraction (Chapter 1.5.2), since the latter is mechanistically comparable to secondary drying (Chapter 1.5.3) and can theoretically be skipped by early collection of the microparticles from the continuous phase.

1.5.1. Initial solvent extraction

When emulsification begins, the organic solvent is extracted from the dispersed droplets into the aqueous continuous phase by Fickian diffusion. This process is initially driven by the organic solvent concentration gradient between the dispersed drug:PLGA:solvent phase (O) and the continuous aqueous phase (W) [95,96]. The mass transfer follows Fick's second law:

$$\frac{\partial c}{\partial t} = D \frac{\partial^2 c}{\partial x^2} \quad \text{Equation 6}$$

Here c is the concentration of organic solvent, t the time, D the mutual diffusion coefficient and x the position. In parallel to the solvent extraction, various processes may take place including water influx, drug extraction, shrinkage of the droplet and thus shortening of the diffusion path and simultaneous increase in viscosity. Figure 3 summarizes the complex interplay of the main sub-processes around a single droplet during the initial extraction step, which are described in more detail below.

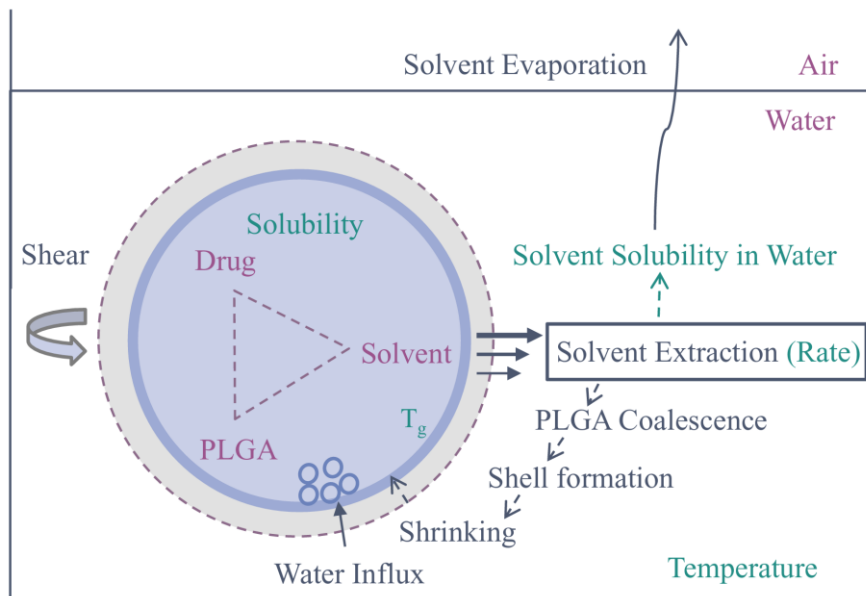


Figure 3: Initial sub-processes around a single droplet after emulsification during the solvent extraction/evaporation method [12]

Due to those various processes, the rate of solvent extraction is essential for the properties of the final microparticles. Generally summarized: Slow initial extraction of the organic solvent facilitates the formation of small microparticles, which tend to have pores and a low encapsulation efficiency due to an water influx [77,88,97,98]. Rapid initial extraction, by increasing the continuous phase volume initially or by fast dilution, facilitates fast solidification of the polymer. This may increase the encapsulation efficiency [99], but also the particle size, pore size, burst release and residual solvent content [75,100]. Moderate continuous extraction may allow particle shrinkage, thereby reducing the microparticle porosity and burst release of drugs [77,98].

Fast diffusion enables the extraction of the majority of the solvent volume within a few seconds from the dispersed phase, if the solvent dissolving capacity is unlimited [96]. The diffusion speed decreases with increasing droplet diameter and PLGA concentration [96]. Due to the limited aqueous solubility of the common organic solvents, the continuous phase is often saturated after a short time, terminating this first diffusion-controlled extraction step. The dissolution capacity for the organic solvent in the continuous phase, depends on the O/W phase ratio and the solubility of the organic solvent [38,97,101]. The solubilities of the organic solvents used differ, for example about 0.8 % chloroform, 1 - 2 % dichloromethane, 8 % ethyl acetate dissolve in pure water. The solubility might be increased by the addition of surfactants or by

1.5 Solvent removal in the solvent extraction/evaporation method

changing the temperature [38]. Dichloromethane, for example, shows better solubility at decreased temperature [97]. However, it should be noted that diffusion generally slows down when the temperature is decreased.

Rapid initial solvent extraction causes fast solidification of PLGA. If the extraction rate is faster than the diffusion within the droplet, a skin of solidified PLGA may form on the droplet surface. This skin can interrupt the emulsification process, leading to irregular precipitates or particles with a broad size distribution, slowing the further extraction of organic solvent and drug loss, preventing droplet shrinkage, favoring the influx of water, and thus increasing the porosity of the resulting microparticles [75,77,97,102]. Increased porosity may reduce drug encapsulation efficiency and increase burst release. The diffusion-controlled initial extraction can be reduced by pre-saturating the continuous phase with the organic solvent, which is for example commonly practiced if ethyl acetate is used due to its high aqueous solubility [103,104].

As soon as the continuous phase is saturated with organic solvent, the removal from the continuous phase limits further solvent extraction [96,104]. To prevent saturation, the continuous phase can be diluted incrementally or continuously [97,105] or be replaced by (membrane) separation techniques [102,106,107]. Classically, the volatile organic solvent evaporates from the continuous phase, allowing further organic solvent to be extracted from the dispersed phase. This manufacturing method is therefore often abbreviated as solvent evaporation method, without mentioning extraction. The evaporation rate depends on the volatility of the organic solvent, temperature, pressure, homogeneity of mixing in the continuous phase, volume-surface ratio of the continuous phase, and the removal of the evaporated organic solvent [95,108]. Fast solvent evaporation due to elevated temperature [98,100,105,109] and/or decreased pressure [42,110,111] may lead to the formation of a porous surface, inner, or a hollow core. At temperatures above almost 50 °C of the glass transition temperature of PLGA, very rapid solvent extraction and yet a dense microparticle structure can be achieved, because PLGA remains liquid or rubbery [109]. However, the resulting microparticles may have a smaller size and accelerated drug release.

1.5 Solvent removal in the solvent extraction/evaporation method

Based on the mass loss of a batch over time an evaporation constant can be determined. If the evaporation constant K is known for the given conditions, it can be used to calculate the evaporation rate and thus the solvent removal rate under saturation [108]:

$$V_{CP} \frac{\partial c}{\partial t} = -K c \quad \text{Equation 7}$$

V_{CP} is the volume of the continuous phase. The prediction of the evaporation constant after scale up might be performed by taking into account the changed surface to volume ratio of the continuous phase [108]:

$$K_2 = K_1 \frac{V_{CP1} A_{CP2}}{V_{CP2} A_{CP1}} \quad \text{Equation 8}$$

Here K_1 , V_{CP1} and A_{CP1} are the evaporation constant, the continuous phase volume and the surface area of the first batch. K_2 , V_{CP2} and A_{CP2} refer to the second batch for which the evaporation constant is calculated.

Continuous emulsification methods e.g. static mixers or microfluidic flow focusing may require a small phase ratio and processing in tubing prevents solvent evaporation. The variation of phase ratio in these processes is usually performed to control droplet size and not initial solvent extraction (Chapter 1.4.2). The subsequent solvent extraction after emulsification can be carried out continuously in tubing or discontinuously by introduction into an extraction vessel [102,112,113]. In continuous processing, extraction can be achieved by dilution or membrane separation techniques [102,113,114]. In the case of microfluidic, membrane-free extraction processes could also be possible, as two liquid streams can be brought into contact without mixing, flowing laminar next to each other and then be separated [115]. To achieve sufficient contact times in continuous processing for extraction, long lag-tubing or recirculation might be necessary. A distinction between complete or continuous/incremental dilution might be made. Gibson et al., for example, present a process in which a continuous phase is added downstream through several inlets to an emulsion created by a static mixer and a slower, but more complete solvent extraction is achieved by this incremental dilution because skin formation is avoided [102].

1.5 Solvent removal in the solvent extraction/evaporation method

The use of membrane separation techniques, e.g. tangential flow filtration, enables the controlled and sometimes selective removal of the organic solvent, stabilizers and unencapsulated drugs in batch or continuous processes [102,113,116–119]. Diafiltration, i.e. the simultaneous removal of continuous phase and addition of the same amount of volume of fresh extractant, makes it possible to keep the equipment volume small and reduce the total extraction volume used [117,119]. Perstraction refers to the diffusion of the organic solvent from the continuous phase through a membrane into an extraction phase and pervaporation to the evaporation of volatile organic solvent out of a membrane [114,118]. Both enable the selective and uniform removal of organic solvent without interrupting the fluid stream during continuous processing. The extraction rate might be slow, especially for semipermeable membranes, due to the low diffusivity, which is essentially changed only by changing the temperature or the membrane [114]. If necessary, the extraction can be accelerated by increasing the membrane surface area, for example by splitting the fluid stream into hollow fiber membrane contactors [117]. Regardless of whether components or the complete continuous phase are removed, the dispersed phase must usually be retained by membranes, filters, or sieves. Sufficient shear by flow viscosity might be required to avoid deposition of droplets or sticky particles on the membrane [114]. To reduce the risk of blockage, membrane separation is usually performed separated in place and time from emulsification, when parts of dichloromethane have already been extracted [114,117,119].

As extraction progresses, the proportion of organic solvent in the dispersed phase decreases and the proportion of PLGA increases. Therefore, the viscosity of the dispersed phase increases and the diffusivity decreases. When the solvent extraction rate from the dispersed phase becomes slower than the solvent evaporation rate from the continuous phase, the organic solvent content in the continuous phase decreases. Further solvent removal is diffusion controlled and limited by low diffusivity within the dispersed phase [96,120]. This phase of solvent removal is referred to as final solvent extraction and is described in the following chapter.

1.5.2. Final solvent extraction & free volume theory

The final extraction essentially depends on the diffusivity of the organic solvent in the dispersed phase, which decreases with decreasing organic solvent content and thus increasing viscosity and glass transition temperature and decreasing free volume [96,120]. The depression of the glass-transition temperature with increasing solvent content can be calculated with the Gordon-Taylor equation:

$$T_{g\text{System}} = \frac{w_P T_{gP} + k w_S T_{gS}}{w_P + k w_S} \quad \text{Equation 9}$$

Here, w_P and w_S are the weight fractions and T_{gP} and T_{gS} the glass transition temperatures of the polymer P and the solvent S. The constant k can be estimated with the corresponding densities ρ_P and ρ_S and the glass transition temperatures [121]:

$$k = \frac{\rho_S T_{gS}}{\rho_P T_{gP}} \quad \text{Equation 10}$$

Diffusion in rubbery polymers, such as PLGA, is described by the free volume theory, introduced by Vrentas and Duda [122,123]. The volume of the polymer is therefore divided in a proportion occupied by the polymer molecules (occupied volume), an interstitial free volume, which is the temperature dependent space occupied by the vibration of molecules and the remaining so-called hole free volume (Figure 4) [124,125]. The hole free volume refers to vacancies discontinuously distributed in the polymer matrix. Diffusion results from elementary jumps of small segments of the molecules, the so-called jumping units, between these holes. Increasing the hole free volume, facilitates diffusion of molecules, like solvents, through the polymer matrix [120,124–126]. As the temperature decreases, the free volume decreases. Below the glass transition temperature, the extra free volume describes vacancies formed by incomplete volume reduction due to solidification [124,125]. This extra free volume might also enhance the drug release from the final microparticles, but can be lost over time due to the so-called aging, caused by the relaxation of the PLGA chains [127,128].

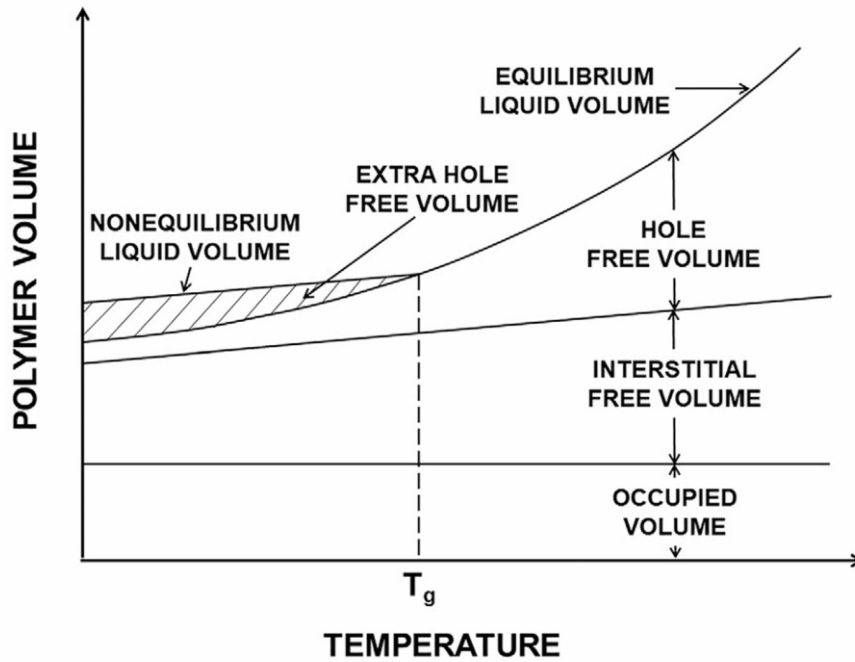


Figure 4: Schematic representation of the different contributions to the polymer volume as a function of temperature based on the free volume theory [124]

The free volume and thus the diffusivity in PLGA increases not only with increasing temperature, but also with increasing (residual) solvent content [125,126]. This dependency of the diffusion coefficient was described in the free volume theory [122,123]:

$$D_1 = D_0 \exp\left(\frac{-E}{RT}\right) \exp\left(-\frac{\omega_1 \hat{V}_1 + \xi \omega_2 \hat{V}_2}{\hat{V}_{FH1}/\gamma}\right) \quad \text{Equation 11}$$

Here, D_0 is a constant preexponential factor, E is the activation energy for a jumping unit making a jump into a hole of free-volume, R is the gas constant, T is the absolute temperature, ω and \hat{V} are the mass fraction and specific volume at 0 K of the organic solvent and PLGA, ξ is the ratio of the molar volume of the organic solvent and PLGA jumping units. \hat{V}_{FH1}/γ is the hole free volume of the dispersed phase, which is obtained by the addition of the free volumes of PLGA and organic solvent from the following expression:

$$\frac{\hat{V}_{FH1}}{\gamma} = \omega_1 \frac{K_{11}}{\gamma_1} [(K_{21} - T_{g1}) + T] + \omega_2 \frac{K_{12}}{\gamma_2} [(K_{22} - T_{g2}) + T] \quad \text{Equation 12}$$

Here, K_{11}/γ_1 and K_{21} are the free-volume parameters and T_{g1} the glass transition temperature of the pure solvent while K_{12}/γ_2 , K_{22} and T_{g2} are the values of pure PLGA. These were determined for PLGA 502H and dichloromethane, for example [120].

Particularly after solidification, when the glass transition temperature of the PLGA:solvent systems falls below the process temperature and thus the PLGA turns into the glassy state, the solvent extraction slows down [96,97,120]. To prevent the glass transition temperature from falling below and generally to accelerate diffusion during the final extraction, the process temperature can be increased.

The diffusivity in PLGA:solvent systems was only investigated above the glass transition temperature due to a high residual solvent content [96,97,108,120] or temperature [129]. The diffusion of organic solvents was not investigated in glassy PLGA, but in other amorphous polymers. Below the glass transition temperature, the dependency of volumetric dilations, contractions and thus the free-volume on the temperature becomes weaker [125,130–132]. Therefore, the diffusivity in a glassy polymer below the glass transition is greater than would be predicted with Equation 12 to calculate the free volume based on the original theory from Vrentas and Duda. Various approaches have attempted to achieve a better approximation of the free volume below the glass transition temperature. Inaccuracies arising from assumptions that, for example, the solvent content [130] or the temperature [132] no longer have any effect below the glass transition temperature. Sturm et al. established an equation for determining the free volume below the glass transition temperature, in which the effect of the residual solvent on the glass transition temperature is weighted, similar to the modification of the free volume theory by Vrentas and Vrentas [125,133]:

$$\frac{\hat{V}_{FH1}}{\gamma} = \omega_1 \frac{K_{11}}{\gamma_1} [(K_{21} - T_{g1}) + T] + \omega_2 \frac{K_{12}}{\gamma_2} [K_{22} - (1 - \lambda)f(\omega_1) + \lambda(T - T_{g2})]$$

Equation 13

Here λ describes the change in the volume contraction at the T_g , as established by Vrentas and Duda [130]. $f(\omega_1)$ is a function to model the effect of solvent content on the glass transition temperature and can be calculated by the difference of the glass transition temperature of the pure polymer and the polymer:solvent system [125]. The

latter can be predicted with the Gordon-Taylor equation (Equation 9). Sturm et al. successfully predicted the removal of water, acetone, methanol and tetrahydrofuran from spray dried hypromellose acetate succinate particles at different temperatures below the glass transition temperature by combining Equation 9, 11, and 13 [125].

The diffusivity of a solvent in a polymer does not depend exclusively on its concentration, but on the glass transition temperature and the free volume of the polymer:solvent system and can therefore also be influenced by other components, like solvents or drugs [134]. Schabel et al. showed that the diffusion coefficient of both solvents in a ternary polymer:solvent:solvent system is already increased by orders of magnitude at a low content of one of the solvents [135,136]. The plasticizing effect of different components does not necessarily add up, due to potential competing effects, known as antiplasticization [121,137]. Since even small amounts can have a major effect on the diffusivity, the third component does not have to be classified as a good solvent for the polymer, but only have to dissolve to a certain extent in the polymer. The solubility or miscibility of solvents and drugs in PLGA can be estimated using the Hansen solubility parameters (HSP) [138,139]. The partial solubility parameters, dispersive interactions δ_d , polar interactions δ_p and hydrogen bonding δ_h , are assigned to a substance so that it can be positioned in a three-dimensional coordinate system. The smaller the distance R_a of the coordinates between two substances, the higher their principal affinity and thus expected solubility in each other.

$$R_a = \sqrt{4(\delta_{d1} - \delta_{d2})^2 + (\delta_{p1} - \delta_{p2})^2 + (\delta_{h1} - \delta_{h2})^2} \quad \text{Equation 14}$$

Water, classified as non-solvent for PLGA, can migrate from the continuous phase to the dispersed phase during wet processing and plasticize PLGA [121,128]. Water may only hydrate the individual molecular chains of PLGA to a very limited extent and is rather present in pores or cavities, due to its low solubility in dichloromethane and PLGA [97]. Similarly, only the molecularly dissolved portion of encapsulated drug can decrease the glass transition temperature [140,141]. Thus, the effect of water and encapsulated drug on the free volume might be rather small.

1.5 Solvent removal in the solvent extraction/evaporation method

Organic non-solvents for PLGA can also be used for extraction of residual solvents from microparticles. This is commonly described for the organic phase separation technique, in which residual dichloromethane or ethyl acetate is extracted by e.g. octamethylcyclotetrasiloxane or alkanes after the phase separation has been caused by addition of silicon oil [109,142,143]. In the cryogenic solvent extraction of the ProLease[®] spray freeze drying process, dichloromethane is extracted from frozen PLGA:dichloromethane droplets by cooled ethanol and absorbed ethanol is removed by subsequent vacuum drying [47]. For the solvent extraction/evaporation method, the addition of alcohols, especially ethanol, to the continuous aqueous phase or post-processing with alcoholic media to remove the solvent was also investigated, but primarily as a modifier of the surface porosity of microparticles and thus a modifier of the drug release profile [144,145] or of the powder flow and the respirability [146].

Aqueous solutions of 10 - 30 % ethanol (mostly 25 %) were used to wash dried microparticles and extract residual dichloromethane, ethyl acetate or non-volatile benzyl alcohol [147–149]. The residual solvent content decreased with increasing process temperature [148]. Methanol and isopropanol were also used to extract dichloromethane from PLGA microparticles, but without investigating the effect on solvent residues [150,151]. Alonso et al. decreased time for wet processing before washing and freeze drying from 3 h to 30 min by the addition of 2 % isopropanol to the continuous phase [151]. Alcohol concentration, temperature and wet process time are limited by particle sticking, a reduction in encapsulation efficiency and altered drug release [144,145,148].

Increasing temperature during ethanolic washing increased extraction of encapsulated drugs, e.g. risperidone and naltrexone [145,148]. Alcohols might affect drug release profiles differently due to competitive effects: on the one hand, the closure of surface pores, the structural relaxation of PLGA and thus the reduction of the free volume can be caused by plasticization. Due to the reduced influx of water and reduced diffusivity, ethanol might decrease the initial burst release of drugs [144] and prolong [145] or avoid a potential lag phase [148]. On the other hand, increased molecular mobility due to plasticization by alcohols and increased process temperature can promote recrystallization of drugs and degradation of PLGA, leading to an increased burst release [145,148].

1.5 Solvent removal in the solvent extraction/evaporation method

In a process called supercritical fluid extraction of emulsions (SFEE), supercritical carbon dioxide (scCO₂) is mixed with the PLGA in Water emulsion or suspension for the final (and possibly also initial) extraction of organic solvent [152–154]. Above its critical point in terms of pressure and temperature, an extractant has liquid like density, solvating characteristics and gas-like diffusivity [154,155]. Supercritical carbon dioxide (scCO₂) is mostly used due its rather low critical pressure and temperature (7.38 MPa and 32.1 °C) and good solubility for various organic solvents. Due to the pressure needed, special equipment is required for the SFEE process. The solubility, density, viscosity, and tensile strength of scCO₂ change with variation of temperature and pressure, thus changing extraction rate of organic solvent [156]. PLGA is usually not dissolved by scCO₂, but both components have a high affinity for each other. Increasing the lactide content of PLGA increases absorption and thus plasticization and swelling of the PLGA matrix [157]. Pressure and temperature are limited in the SFEE process by the coalescence or aggregation of microparticles and drug loss [152]. Della Porta et al. shortened the time for ethyl acetate removal from small PLGA microparticles from 4 - 8 h in a conventional solvent evaporation process to 30 min by using a static SFEE and to 5 min by using continuous SFEE [152,153].

Microparticles can be collected from the continuous phase with a filter or sieve as soon as they are solidified, i.e. the glass transition temperature of the PLGA:solvent system has been reached. Early collection of microparticles might be advantageous to increase the manufacturing throughput, to prevent loss of encapsulated drug and to minimize the degradation of drug and PLGA. A high solvent content in the continuous phase can result in aggregation when the microparticles are collected [96]. Especially, if the wet extraction has been carried out with additional plasticizing solvents or at elevated temperature, their effect might be attenuated by dilution or cooling. Depending on the process temperature and the organic solvent used, solidified microparticles may still contain several percent of residual solvent. The residual solvent distribution in a microparticle can be very inhomogeneous, so that the outer skin of the apparently solidified microparticles is glassy, but the inside is still rubbery [97]. The remaining residual solvent and water are then removed by secondary drying, which is described in the next chapter.

1.5.3. Secondary drying

Secondary drying is usually performed after collecting the microparticles from the continuous phase to remove residual organic solvents and water to reach the ICH limits and produce storage-stable microparticles. The most common processes include vacuum drying and freeze drying, also called lyophilization [128]. Thomasin et al. showed that increasing the temperature during vacuum drying, limited by aggregation above the glass transition temperature of PLGA, increases the solvent removal rate from microparticles, while decreasing the pressure does not have a significant effect [142].

During freeze-drying, particles might still be suspended in water and are shock-frozen and then dried under vacuum [113,158,159]. This minimizes the crystallization of water, enables very gentle removal of water and residual organic solvents driven by the remaining vapor pressure in the frozen state. To prevent collapse of the sample, suitable cryo- and lyoprotectants such as sucrose, trehalose, mannitol or PVA might be added to the aqueous phase before freezing [113,159]. As diffusion in the PLGA is very slow at low temperatures, this process is usually less effective in solvent removal compared to conventional vacuum drying and energy intensive [160]. Freeze-drying might be used to ensure chemical and physical stability e.g. for PLGA nanoparticles, as they are difficult to separate completely from water without aggregation [113,159].

The choice of drying method not only affects the efficiency of the manufacturing process but can also change the properties of the microparticles. Although drug loading and particle size are usually not affected by secondary drying, the particle morphology and the drug release can be changed [77,158,160]. On the one hand, Yeo and Park stated that the removal of residual organic solvents and water by vacuum drying may cause migration of drug to the surface, increasing drug distribution inhomogeneity and burst release [77]. On the other hand Wu et al. showed that decreasing pressure during vacuum drying, increases shrinking and collapse of microparticles and thus delay drug release due to a denser structure [160]. During freeze drying, the microparticles are in the glassy state, independent of their residual solvent content, reducing drug migration and shrinkage. Freeze-dried microparticles may have a higher porosity and thus faster water uptake, which reduces the delay of drug release, but may cause an initial burst and accelerated PLGA degradation [158,160].

Residual organic solvents can also be extracted from collected microparticles with supercritical fluids, mostly scCO₂, similar to what has already been described for the final extraction (Chapter 1.5.2). The extraction rate is affected by temperature, pressure and contact time with the microparticles [156]. Kamali et al. achieved the best extraction rates of dichloromethane from PLGA at a temperature of approximately 45 °C and a pressure more than 15 MPa. With increasing static and dynamic extraction time, the residual solvent content decreases. Expansion of CO₂ during depressurization might lead to an increase of particle size, porosity, pore size of microparticles and thus increased water influx during drug release, resulting in an initial burst and accelerated PLGA degradation [155,156].

Organic non-solvents could theoretically also improve solvent removal during secondary drying in a similar way as described for the final extraction in wet processing (Chapter 1.5.2), e.g. by adding them as vapor. Kim et al. used ethanol vapor in a fluidized bed process to close surface-connected pores of PLGA microparticles, thereby reducing the burst release [161]. Aggregation of the microparticles caused by strong plasticization of PLGA limited the process time to 10 min. The absorption of ethanol and a potential effect on solvent residues were not investigated in alcohol vapor-assisted fluidized bed drying. Shepard et al. showed that water or methanol vapor-assisted nitrogen purge flow drying in an agitated vessel can improve the extraction of residual acetone or tetrahydrofuran from spray-dried particles, made of poly(methyl methacrylate-co-methacrylic acid) (Eudragit L100) and cellulose acetate phthalate compared to vacuum drying [162]. Methanol was more efficient compared to water as assisting solvent, as sufficient absorption was easier to achieve, due to its higher volatility and polymer affinity. Furthermore, methanol increased diffusivity stronger compared to water at an equal absorbed content, due to a greater contribution to the hole free volume [162]. The results were consistent with a model derived by Shepard et al. from the previously presented approaches of Vrentas and Duda [134], Sturm et al. [125] and Schabel et al. [135]. The polymers used by Shepard et al. have a significantly higher glass transition temperature than PLGA and are therefore easier to handle, as plasticization by the assisting solvent does not lead to sticking as fast. Compared to an agitated vessel, the use of a fluidized bed as used by Kim et al. offers the advantage that the particles have little contact with each other and are evenly

surrounded by the purge gas. This might reduce the risk of sticking, but (commercial) fluidized bed dryers are usually restricted to particles larger than 50 µm [163].

1.5.4. Solvent residues

Methods for final solvent removal mentioned above aiming for low residual solvent contents to assure storage stability and patient safety [93,94]. Acceptable limits for a permitted daily exposure (PDE) to residual solvents are recommended by the ICH Guideline Q3C, depending on the toxicity of the solvents [164]. Based on the dose [g/d] of a drug formulation administered daily and the PDE [mg/d] an acceptable residual solvent concentration can be calculated:

$$\text{Concentration [ppm]} = \frac{1000 \times \text{PDE}}{\text{dose}} \quad \text{Equation 15}$$

The solvents are categorized into three classes [164]: solvents to be avoided (class 1), solvents to be limited (class 2) and solvents with low toxic potential (class 3). For the latter PDEs of at least 50 mg/d are accepted. Some PLGA (Co-)Solvents or Non-solvents frequently used in the preparation of microparticles with the solvent extraction/evaporation method are listed below with their PDE limit (Table 2).

Table 2: Classification and permitted daily exposure (PDE) of organic solvents commonly used for preparation of PLGA microparticles by solvent extraction/evaporation method (adapted from [164])

Solvent	Class	PDE [mg/d]
Acetonitrile	2	4.1
Acetic acid	3	50
Acetone	3	50
Chloroform	2	0.6
Dichloromethane	2	6
Ethanol	3	50
Ethyl acetate	3	50
Isopropanol	3	50
Methanol	2	30

1.5 Solvent removal in the solvent extraction/evaporation method

The residual solvent content of microparticles can be determined with various analytical methods. Most commonly (static) headspace gas chromatography (hsGC) with a flame ionization detector (FID) is used. It offers the advantage of universal determination of the common volatile organic solvents with a high sensitivity sufficient regarding ICH limits. Headspace analysis instead of direct injection prevents contamination of the GC column with PLGA and drug [94]. Other GC detectors may have advantages such as a significantly higher sensitivity (mass spectrometer) or enable the parallel determination of residual water (thermal conductivity detector) [94,165]. Usually, residual water is determined with Karl Fischer analysis. Although water is toxicologically harmless, it must be removed to prevent the degradation of PLGA and thus achieve storage stability. Alternative methods for residual solvent analysis include simple loss of drying (LOD) or the more sensitive thermogravimetric analyses (TGA) [94]. The disadvantage of these two methods is the lack of identification and differentiation of solvents. Identification and quantification can be facilitated by evolved gas analysis, in which TGA is coupled with other analysis techniques such as Fourier transform infrared spectroscopy (FTIR) or mass spectrometry (MS) [166]. Derivative thermogravimetry (DTG) is a type of thermal analysis in which the rate of mass change is determined in dependency of temperature, so that not only different solvents can be distinguished, but also information about PLGA and the drug substance can be obtained [166]. Another method that can be used to determine various also non-volatile solvents in parallel is nuclear magnetic resonance spectroscopy (NMR) [94,109,142].

1.6. Research objectives

The purpose of this dissertation was to investigate and optimize the solvent removal from biodegradable microparticles prepared by solvent extraction/evaporation methods to increase the efficiency of manufacturing. The specific objectives were:

- Investigation of a diafiltration-driven solvent removal process and its effect on the properties of PLGA microparticles
- Investigation of the effect of temperature- and alcohol-assisted final extraction of residual solvents and its effect on the properties of PLGA microparticles
- Development and investigation of an alcohol vapor-assisted fluidized bed drying process for residual solvent removal from microparticles
- Evaluation of the effect of PLGA grade and drug loading on initial and final solvent removal from microparticles
- Preparation of microparticles with microfluidic flow focusing, comparison with the classical batch process and optimization of drug encapsulation and solvent removal

2. Materials and Methods

2.1. Materials

2.1.1. Drugs

Micronized dexamethasone (DEX) (Caesar & Loretz GmbH, Hilden, Germany); risperidone (RIS) (RPG Life Sciences limited, Navi Mumbai, India)

2.1.2. Biodegradable polymers

Poly(lactide-co-glycolide) (PLGA) RG 502H, RG 503, RG 503H, RG 504H, RG 752S, RG 753S (Resomer[®], Evonik Industries AG, Darmstadt, Germany)

2.1.3. Solvents and others

Acetonitrile (HPLC grade), ethyl acetate (EtAc) (chemical pure grade), glycerol, isopropanol (IPA) (technical grade), methanol (MeOH) (HPLC grade) (VWR International GmbH, Darmstadt, Germany); dichloromethane (DCM) (HPLC grade), dimethyl sulfoxide (DMSO) (headspace grade), propylene glycol (PG) (Carl Roth GmbH + Co. KG, Karlsruhe, Germany); ethanol absolute (EtOH), polyvinyl alcohol 4–88 (PVA) (Merck KGaA, Darmstadt, Germany)

2.2. Methods

2.2.1. Preparation of microparticles and films

2.2.1.1. Preparation of microparticles with diafiltration-driven extraction

Microparticles were prepared in two different batch sizes. The organic phase was prepared by dispersing or dissolving 0 - 40 % (w/w) dexamethasone or risperidone (based on polymer weight) in a 10 % (w/w) PLGA in dichloromethane solution for 1 min (VF2, IKA-Werke GmbH & Co. KG, Staufen im Breisgau, Germany). 2.5 or 10.0 mL of the organic phase was emulsified in 50 or 200 ml aqueous continuous phase containing 0.25 % (w/V) PVA using a propeller stirrer (d = 3.5 cm, 800 rpm or d = 5.0 cm, 500 rpm). The 50 mL batches were prepared in a stirred cell (Millipore Corporation, Bedford, USA) equipped with a 10 μ m stainless-steel sieve at the bottom to retain the dispersed phase. The 200 mL batches were prepared in a filter funnel with an integrated sintered glass filter (VitraPOR[®] Filter-Funnel 250 ml Por. 4, ROBU Glasfilter-Geräte GmbH, Hattert, Germany), equipped with two probes for in-process video microscopy (PVM) and focused beam reflectance measurement (FBRM) (PVM V819 and Lasentec FBRM D600T, Mettler Toledo AutoChem Inc., Redmond, USA) (Figure 5). To control solvent extraction by diafiltration, the aqueous phase was continuously exchanged for 60 min, by removing it through a bottom outlet and replacing the same amount of volume with fresh PVA solution from above with a double-head peristaltic pump (323S, Watson-Marlow Limited, Falmouth, England).

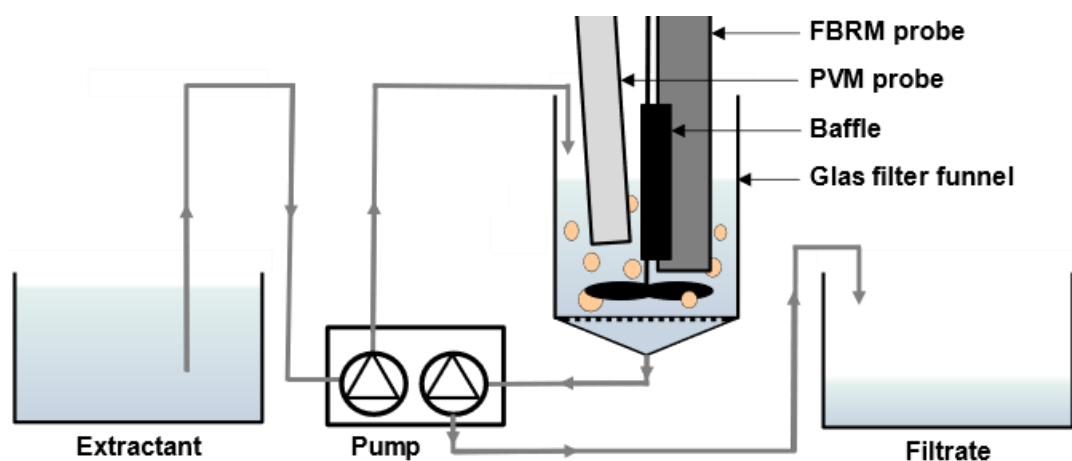


Figure 5: Schematic setup for diafiltration-controlled extraction for microparticle preparation, equipped with probes for in-process video microscopy (PVM) and focused beam reflectance measurement (FBRM)

If a one-step dilution was carried out instead of continuous diafiltration, the entire batch was transferred into a ten times larger volume of continuous phase 15 min after the start of emulsification and stirred with a magnetic stirrer. The microparticles were collected 24 h after emulsification by vacuum filtration with a 10 μm stainless-steel sieve, washed three times with 250 mL deionized water and dried under vacuum at 35 °C for 72 h. Dried microparticles were stored in a desiccator at 7 °C.

2.2.1.2. Preparation of microparticles for final extraction and secondary drying

PLGA microparticles were prepared by the solvent extraction/evaporation method. The organic phase was prepared by dispersing or dissolving 0 - 40 % dexamethasone or risperidone (based on polymer weight) in a 10 % (w/w) solution of PLGA in dichloromethane or ethyl acetate for 1 min (VF2, IKA-Werke GmbH & Co. KG, Staufen im Breisgau, Germany). 2.5 mL of drug:PLGA:dichloromethane phase was emulsified with a propeller stirrer (d = 3.5 cm, 800 rpm) in 50 mL of 0.25 % (w/V) PVA solution. If the organic phase contained ethyl acetate, 50 mL of 0.25 - 1 % (w/V) PVA solution containing 0 - 4 g ethyl acetate was used as continuous phase. Drug-loaded microparticles were transferred into 450 mL 0.25 % (w/V) PVA solution 15 min after the start of emulsification, stirred with a magnetic stirrer and collected after further 15 min. Blank microparticles were collected after 2.5 h without previous dilution. Separation and washing of the microparticles was performed by vacuum filtration with a 10 μm stainless-steel sieve and rinsing them three-times with 250 mL deionized water. Subsequently they were analyzed for solvent content, dried (hood, vacuum oven or fluidized bed), or redispersed in 50 mL aqueous extraction phase containing 0 - 50 % (w/w) non-solvent. This extraction phase was sampled over time and microparticles were separated, washed, and analyzed in the same way as untreated samples. Microparticles were dried under vacuum at 35 °C for determination of encapsulation efficiency and stored in a desiccator at 7 °C.

2.2.1.3. Preparation of films

PLGA films were prepared by evaporating a solution of 10 % (w/w) PLGA in DCM containing 2 % (w/w) dexamethasone or 10 % (w/w) risperidone based on the polymer weight. 1.0 mL of this solution was dosed in a petri dish (d = 3.5 cm) and placed for 24 h under a hood to form a film. Within the first hour petri dishes were covered with paper to slow down evaporation

2.2.1.4. Preparation of microparticles with microfluidic flow focusing

PLGA microparticles were prepared by a modified solvent extraction/evaporation method. The organic phase was prepared by dissolving 0 - 30 % risperidone (based on polymer weight) in a 10 % (w/w) solution of PLGA in dichloromethane for 1 min (VF2, IKA-Werke GmbH & Co. KG, Staufen im Breisgau, Germany). This organic phase and an aqueous 0.25 - 2 % (w/V) PVA solution were each placed in the pressure chamber of a pressure pump (Mitos P-Pump, The Dolomite Centre Ltd., Royston, UK) with a connected flow sensor. The pumps are connected with tubing (0.8 mm inner diameter) to a 7-channel junction microfluidic flow focusing chip made of glass (Telos 1 Reagent 3D Flow Focusing Chip Surface Connection (100 μm etch depth) Hydrophilic, The Dolomite Centre Ltd., Royston, UK), assembled in the corresponding manifold device to divide both fluids evenly into 7 channels each. In the 7 junctions of the chip, an O/W-emulsion was formed. The pressure and flow rates were controlled by the corresponding software (Flow Control Centre, The Dolomite Centre Ltd., Royston, UK). The resulting emulsion was introduced downstream of the chip by tubing into a stirred aqueous phase or processed continuously by dilution and tangential flow filtration. For continuous processing the emulsion was diluted by the addition of 0 - 35 ml/min aqueous extraction medium in a cross fitting with a peristaltic pump (323S, Watson-Marlow Limited, Falmouth, England) and forwarded in a 150 cm or 450 cm long lag tubing with an inner diameter of 1.6 mm, at the end of which there was a planar flow cell in which microscopic images were taken (Figure 6). Solidified microparticles were filtered, washed, dried and stored as described for the batch process.

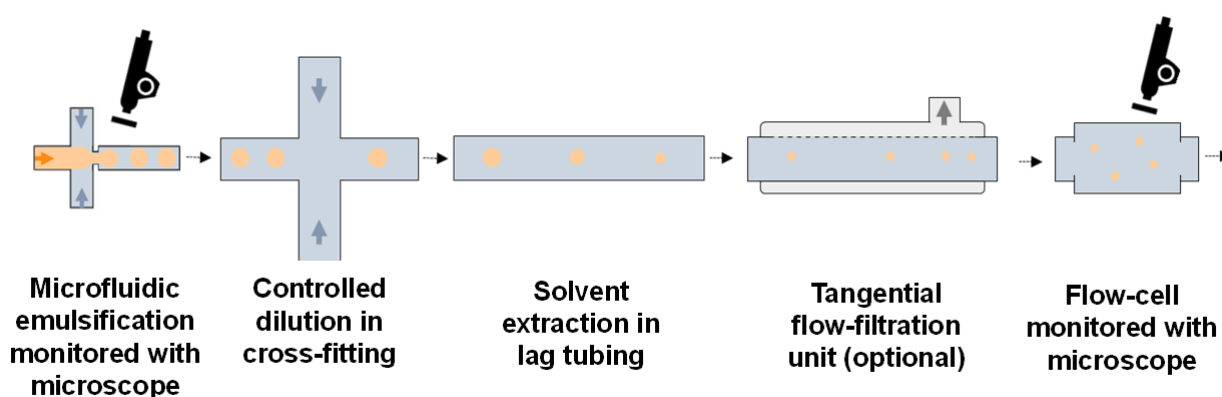


Figure 6: Schematic setup for continuous solvent extraction downstream to microfluidic emulsification

2.2.2. In-process monitoring with focused beam reflectance measurement and video microscopy

The probes for focused beam reflectance measurement (FBRM) and in-process video microscopy (PVM) (Lasentec FBRM D600T and PVM V819, Mettler Toledo AutoChem Inc., Redmond, USA) were positioned in the emulsification vessel (Figure 5) using the FBRM fixed beaker stand and additional clamps for the PVM. The FBRM online measurements were performed every 10 s, with a scan speed of 2 m/s and the coarse electronic discrimination setting. The data were processed with the iC FBRM 4.0 and iC PVM 7.0 software (Mettler Toledo AutoChem Inc., Redmond, USA). The resulting chord lengths from the FBRM were expressed as squared weighted median to obtain the best estimate of particle size [167].

2.2.3. Alcohol vapor-assisted fluidized bed drying

PLGA microparticles were dried in a self-constructed fluidized bed dryer, in which purge gas (compressed air) could be heated and enriched with alcohol vapor (Figure 7). The volume flow was regulated by a valve and tempered with an air heater. The purge gas was passed through a three-way valve into the fluidized bed chamber or previously into a bubbler. The latter was a tightly sealed vessel in which the purge gas was enriched with alcohol. For this purpose, the pressurized air was introduced into alcohol via a sintered metal filter. It could only escape from the container at one exit up towards the fluidized bed dryer. The bubbler was tempered by a heating jacket and the temperature inside was monitored with a sensor.

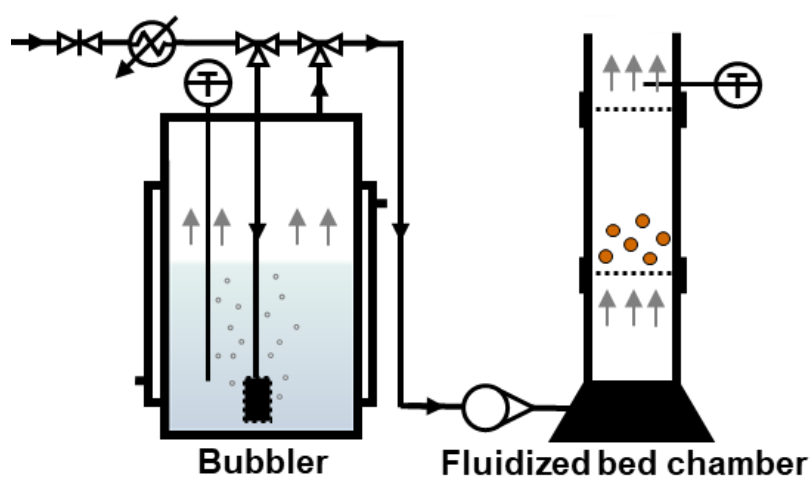


Figure 7: Schematic setup for alcohol vapor-assisted fluidized bed drying of microparticles

The evaporation rate of the alcohols in the bubbler was determined by the weight loss of the filled bubbler over time. Before the purge gas reached the fluidized bed dryer, the volume flow was determined with a rotameter. The fluidized bed dryer was constructed from a sintered metal filter on the bottom and three glass cylinders above connected with polytetrafluoroethylene seals. The cylinders had an inner diameter of 2.5 cm and a height of 5 cm (bottom and top) and 8 cm (middle). The purge gas flow was directed from bottom to top. There were 10 μm stainless-steel sieves between the cylinders, which retained the microparticles in the middle segment. A sensor was placed in the upper segment to determine the temperature of the purge gas escaping.

If the microparticles were dried without alcohol vapor, the bubbler was bypassed, and 10 L/min of pressurized air were used at different temperatures for 24 h. To determine the solvent content in the microparticles during the process, the purge flow was briefly interrupted, the fluidized bed chamber was opened, and a sample was taken. For drying with alcohol vapor, pressurized air at ambient temperature was directed through the bubbler, filled with methanol or ethanol, for 6 h. The evaporation rate was controlled by purge flow rate and bubbler temperature. The concentration of alcohol in the purge gas was calculated based on the evaporation rate divided by the flow rate. After 6 h the bubbler was bypassed, and purging was performed for 18 h with 20 L/min of dry pressurized air heated to 35 °C. In some reported cases, pre-drying was carried out for 1 h before adding alcohol vapor. Pre-drying was performed with 10 L/min dry pressurized air at ambient temperature.

The described setup was modified for the alcohol vapor-assisted drying of PLGA films. The fluidized bed chamber was replaced with a desiccator having a purge inlet and outlet. The films were purged with 1 L/min alcohol vapor at ambient temperature for 24 h. Alternatively, the inlet and outlet of the desiccator containing alcohol were sealed airtight to investigate the effect of an atmosphere saturated with alcohol. The alcohol was removed from the PLGA films by storing under a fume hood for a further 24 h.

2.2.4. Residual Solvent content

2.2.4.1. Coulometric Karl Fischer titration

The water content of microparticles was determined according to the method for coulometric Karl-Fischer determination (Ph. Eur. 2.5.32). 10 - 20 mg microparticles were accurately weighed and dissolved in 1.0 mL acetonitrile. About 250 mg of this

solution, accurately weighed, was analyzed in triplicate for the water content with a coulometric Karl Fischer titrator (831 KF Coulometer, Metrohm AG, Herisau, Switzerland) using HYDRANDAL Coulomat AD (Honeywell Specialty Chemicals Seelze GmbH, Seelze, Germany). The water content based on total weight was calculated after correction for the water content of a blank.

2.2.4.2. Headspace Gas Chromatography

The content of the organic solvents dichloromethane, ethyl acetate, methanol, ethanol and isopropanol was quantified with headspace gas chromatography (GC-2014, Shimadzu Corp., Kyoto, Japan) with a method adapted from USP monograph for residual solvents using a capillary column equivalent to USP G43 phase (Rtx-1301, Restek Corp., Bellefonte, USA). 5.0 mL continuous phase or 10.0 - 50.0 mg microparticles, dissolved in 5.0 mL dimethyl sulfoxide, were sealed in a 20 mL headspace GC vial with an aluminum screw cap with PTFE septum. Samples were equilibrated automatically under shaking by an autosampler (AOC-6000, Shimadzu Corp., Kyoto, Japan) for 60 min at 80 °C (water) or 45 min at 105 °C (DMSO). 1.0 mL of the gas phase was sampled automatically, with a needle temperature 5 °C above previous equilibration temperature and injected at 140 °C with a subsequent split ratio of 5. The column oven temperature was maintained at 80 °C (water) or 40 °C (DMSO) and increased after 7 min to 160 °C (water) or 120 °C (DMSO) with a heating rate of 30 K/min. The carrier gas was nitrogen. Samples were detected with a flame ionization detector (FID) set to 250.0 °C. Evaluation of the spectra was performed with LabSolutions 5.98 (Shimadzu Corp., Kyoto, Japan). The solvent content in the samples was calculated from peak area using linear calibration curves obtained by dilution series. For filtered wet microparticles, the water content was deducted from the sample weight to calculate their dichloromethane content.

2.2.5. Solubility

The solubility of dichloromethane in aqueous mixtures of 0 - 50 % (w/w) of various alcoholic non-solvents was investigated. 15 g of non-solvent:water mixture were added into a 20 mL vial, filled up with 3 - 5 mL dichloromethane, sealed and shaken at room temperature for 24 h. The vial was then left for another 24 h to allow the two phases to separate. 0.5 mL was sampled from the aqueous supernatant, diluted, and examined using headspace GC. For this purpose, the previously mentioned method was adapted

as follows: 5 mL sample were incubated in a 20 mL GC vial for 60 min at 80 °C. The column oven temperature was maintained at 80 °C and heated to 160 °C after 7 min. The dichloromethane content in the samples was calculated from peak area with a linear calibration curve obtained by dilution series.

The solubility of risperidone in aqueous media was investigated by adding an overage amount of the drug to the medium to be tested and shaken 24 h at 180 rpm with a horizontal shaker. The dissolved amount in the aqueous media was determined by measuring the UV absorbance of the centrifuged supernatant.

2.2.6. Optical Microscopy

For microscopic images of microparticles, samples were observed on a glass slide under polarized light microscope (Axioscope) equipped with an AxioCam 105 color camera (Carl Zeiss Microscopy GmbH, Jena, Germany) and images were processed by the software Zen 3.2 (Carl Zeiss Microscopy GmbH, Jena, Germany).

Microscopic images of emulsification on microfluidic chips and subsequent downstream processing were observed with a high-speed microscope camera (Meros High Speed Digital Microscope, The Dolomite Centre Ltd., Royston, UK).

2.2.7. Droplet and particle size analysis

2.2.7.1. Laser diffraction

The particle size and size distribution of microparticles prepared by the batch process were measured with laser diffraction (HELOS BF and CUVETTE, Sympatec GmbH, Clausthal-Zellerfeld, Germany) after redispersing the microparticles in deionized water. Particle size distributions were analyzed with Sympatec WINDOX 5.4.1.0 software using the LD evaluation mode and expressed as volumetric density distribution (q3lg).

2.2.7.2. Microscopic image analysis

The droplet and particle size of microparticles prepared by microfluidic was measured with the software Zen 3.2 (Carl Zeiss Microscopy GmbH, Jena, Germany) based on microscopic images taken with AxioCam 105 color camera (Carl Zeiss Microscopy GmbH, Jena, Germany) or Meros High Speed Digital Microscope (The Dolomite Centre Ltd., Royston, UK). Since the latter does not allow automatic calibration of

the scaling, this was carried out manually based on the manufacturer's information on the channel width of the microfluidic chips.

2.2.8. Drug loading and encapsulation efficiency

The actual drug loading was determined by dissolving 10 - 20 mg microparticles in acetonitrile and diluting 1:1 (V/V) with deionized water. The absorbance of the solution was then measured by UV-Vis spectroscopy (UV-1900i, Shimadzu Corp., Kyoto, Japan) at 242 nm (dexamethasone) or 276 nm (risperidone). Concentrations were calculated with previously established standard curves. The encapsulation efficiency (%) was calculated as the ratio of actual drug loading to the theoretical drug loading.

2.2.9. In-vitro release

Approximately 10 mg of microparticles, accurately weighed, were immersed in 100 mL of phosphate-buffered saline pH 7.4 (PBS), when loaded with risperidone, or in 100 mL of 0.9 % (w/V) sodium chloride solution adjusted to pH 7.4, when loaded with dexamethasone, and stored in an incubation shaker (37 °C and 80 rpm). At designated time points, 10.0 mL of release medium was removed and replaced. Sink conditions were maintained throughout. The concentration of the drug in each sample was determined with the spectroscopic method described above. In-vitro release was performed in triplicate and results were depicted only as the mean value when the standard deviation was below 5 %.

2.2.10. Morphology

Scanning electron microscopy (SEM) (SU8030, Hitachi High-Technologies Europe GmbH, Krefeld, Germany) was used to image the surface and internal morphology of the microparticles. To investigate the inner structure, the microparticles were dispersed in a solvent-free glue (UHU GmbH & Co. KG, Baden, Germany) and the hardened matrix was cut with a razor blade. Samples were sputtered under an argon atmosphere with gold (CCU-010 HV, Safematic GmbH, Zizers, Switzerland) and then observed.

2.2.11. Viscosity

1.0 mL sample was analyzed with a rotational rheometer (MCR 302e, Anton Paar GmbH, Graz, Austria) using a double gap Couette geometry (Anton Paar,

DG27/T200/SS). The viscosity was determined at 25 °C as the average of the shear rate range of 10 - 100 s⁻¹.

2.2.12. Surface tension

Surface tension was determined with a dynamic contact angle meter and tensiometer (DCAT 21, DataPhysics Instruments GmbH, Filderstadt, Germany). 1.5 mL of sample was transferred to a measuring plate. The cylindrical plate probe PT10 was automatically immersed in the sample where exerted tensile force that was captured by the integrated weighing system. Measurement was completed when standard deviation was below 0.03 mN/m for at least 5 consecutive data points.

2.2.13. Differential scanning calorimetry (DSC)

Thermograms were recorded with DSC 6000 (PerkinElmer Inc., Waltham, USA). Therefor 5 - 10 mg sample were accurately weighed into 50 µL aluminum pans with a pierced aluminum lid. The samples were heated twice from -20 °C to 200 °C with a heating and cooling rate of 10 K/min. To evaluate the glass transition temperature, the second heating cycle is shown after normalization.

3. Results

3.1. Initial removal in the solvent extraction/evaporation method

Microparticle preparation with the solvent extraction/evaporation method starts with dissolving PLGA in an organic solvent and emulsifying it subsequently in an aqueous stabilizer solution to obtain an O/W-emulsion (Chapter 1.4). As soon as the two phases are in contact, the organic solvent begins to diffuse from the dispersed into the continuous phase and evaporates from there (Chapter 1.5.1). This solvent removal process is essential to obtain solidified microparticles from the initial droplets and thus affect the final microparticle properties. The initial solvent removal in a conventional process, limited by the O/W phase ratio and dichloromethane evaporation rate, was investigated in Chapter 3.1.1, a diafiltration-driven process was developed to accelerate solvent extraction in Chapter 3.1.2 and the effect of the co-solvent methanol was studied in Chapter 3.1.3.

3.1.1. Phase-ratio limited solvent extraction and drug encapsulation

The amount of organic solvent extracted at the beginning of emulsification depended on its solubility in the aqueous phase and the O/W phase ratio. At a phase ratio of 1:20 and a temperature-dependent solubility of dichloromethane of 10 - 20 mg/mL, about 15 - 30 % of dichloromethane was rapidly extracted into the continuous phase until saturation. As long as saturation persisted, the evaporation rate from the continuous phase determined the further extraction [95]. The evaporation rate was about 70 mg/min for a 50 mL batch size. In the first 45 min, more than 98 % of the dichloromethane was removed from the dispersed phase by rapid initial extraction followed by slow evaporation (Figure 8). The viscosity of the droplets increased with time and the diffusivity of the solvent slowly decreased due to an increase in PLGA concentration. When the glass transition temperature of the PLGA:solvent mixture in the dispersed phase exceeded ambient temperature, the droplets solidified into microparticles, resulting in a sharp decline in the extraction rate of residual dichloromethane.

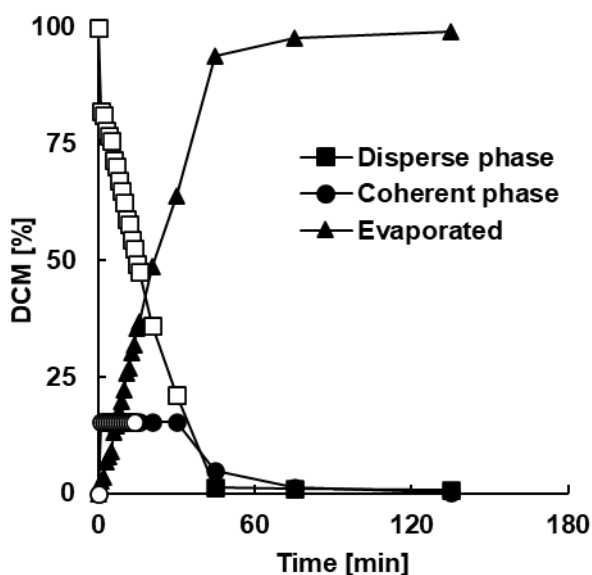


Figure 8: Distribution of dichloromethane during the solvent evaporation controlled microparticle preparation with an initial phase ratio of 1:20 (50 mL batch size). Closed symbols represent values determined by gas chromatography (dispersed and continuous phase) or mass loss (evaporated), while open symbols are calculated

Depending on the solvent dissolving capacity of the continuous aqueous phase and the solvent evaporation from it, the droplets remained in a liquid, viscous or rubbery state for several minutes before finally solidifying. During this time, drug was able to partition from the dispersed to the continuous phase [88]. This resulted in an encapsulation efficiency of about 70 % risperidone and 90 % dexamethasone with a phase ratio of 1:20 and a theoretical drug loading of 30 %. Risperidone has lower encapsulation efficiency than dexamethasone for two reasons. First, risperidone has a higher solubility in the continuous aqueous phase ($S_{RIS} = 0.17 \text{ mg/mL}$, $S_{DEX} = 0.075 \text{ mg/mL}$). In addition, risperidone was dissolved in the PLGA solution, while dexamethasone was dispersed. The dissolved risperidone can therefore better partition into and be lost to the continuous phase than dispersed dexamethasone [168]. Although an initially larger volume of the continuous phase would lead to faster solidification of microparticles, it also influenced the emulsification process. A higher initial phase ratio of 1:200 resulted in larger, porous particles with a broader particle size distribution (Figure 9) and a slightly decreased encapsulation efficiency of risperidone of only 66 % due to the sudden extraction. In order to achieve rapid solidification without interruption of the emulsification process and to achieve a certain droplet shrinkage before solidification, a one-step dilution was carried out after 15 min. This resulted in a similar final microparticle size distribution.

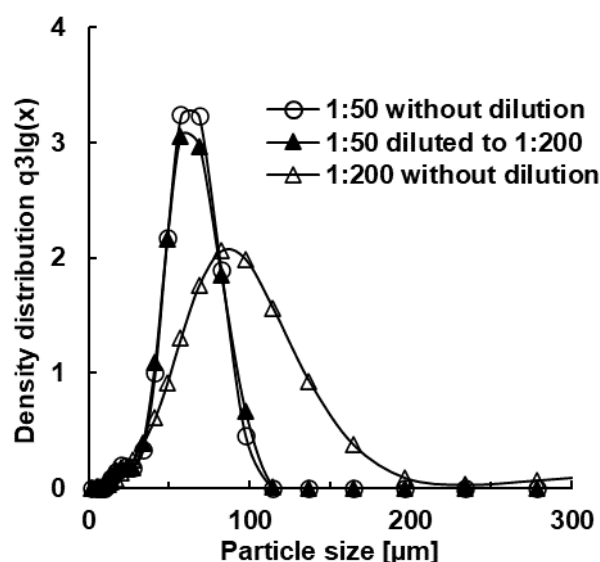


Figure 9: Effect of initial phase ratio and dilution after 15 min on the particles size distribution

Next, the effect of dilution and pH of the continuous phase on risperidone encapsulation was investigated. The continuous phase was buffered to pH 4 with 0.04 mol/L acetate/acetic acid buffer or to pH 10 with 0.04 mol/L sodium carbonate/sodium bicarbonate buffer. The batches were divided into four aliquots 15 min after emulsification, subsequently one aliquot remained undiluted or three were diluted to 2.5, 5 or 10 times their volume with continuous phase. From a dilution factor of 5 on, a maximum encapsulation efficiency of around 90 % was achieved in unbuffered and alkaline-buffered batches. The solubility of risperidone in 0.25 % PVA was increased from 0.17 mg/mL to 12.25 mg/mL by decreasing the pH to pH 4, due to protonation of risperidone. Therefore, the encapsulation efficiency was reduced to less than 7 % independent of dilution. The increased dissolution capacity of the continuous phase favored almost complete extraction of risperidone before dilution. At pH 10, the solubility of risperidone decreased to 0.07 mg/L. Without further dilution, the encapsulation efficiency was increased to more than 80 %, due to decreased dissolution capacity in continuous phase. A smaller dilution factor of 2.5 reduced the encapsulation efficiency again. The solubility of risperidone was increased, while at the same time the solidification of PLGA was not as fast as with higher dilution factors.

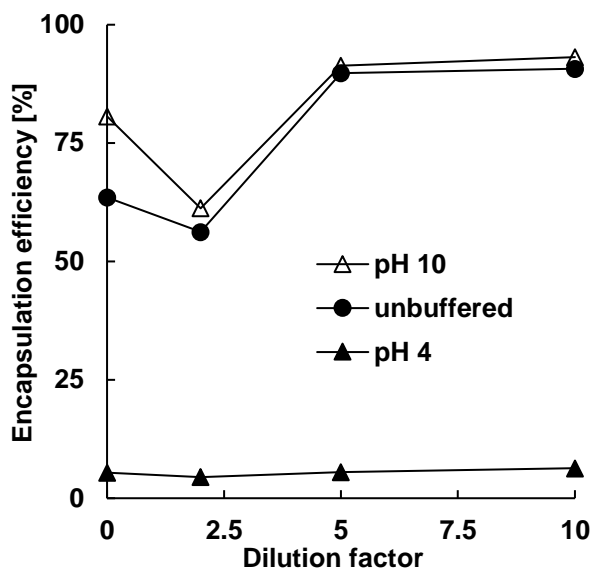


Figure 10: Effect of one-step dilution, 15 min after emulsification and buffering of the continuous phase, on the encapsulation efficiency of risperidone

3.1.2. Diafiltration-driven solvent extraction

As shown above, drugs like risperidone being soluble in both the continuous and the dispersed PLGA:solvent phase are encapsulated better, if the droplets solidify into microparticles early in the process through rapid solvent extraction. The disadvantage of a one-step dilution process is the need for large-volume manufacturing equipment and emulsion transfer with a potential risk to the emulsion stability (e.g., droplet coalescence). As an alternative, a diafiltration-driven extraction process was investigated, where the continuous phase, enriched with dichloromethane, was continuously removed and replaced with fresh aqueous phase. A solvent saturation of the continuous phase is avoided and thus not limiting to solvent extraction, and dichloromethane was removed faster from the dispersed phase. Faster solidification of the microparticles enabled earlier subsequent processing steps, e.g. collection of the microparticles without sticking or aggregation. Once the glass transition temperature of the dispersed PLGA phase exceeded ambient temperature, further diafiltration had little effect on the residual solvent content because diffusion was limited by the smaller solvent diffusion coefficient and not by the concentration gradient. This behavior was independent of the type of drug encapsulated (Figure 11).

3.1. Initial removal in the solvent extraction/evaporation method

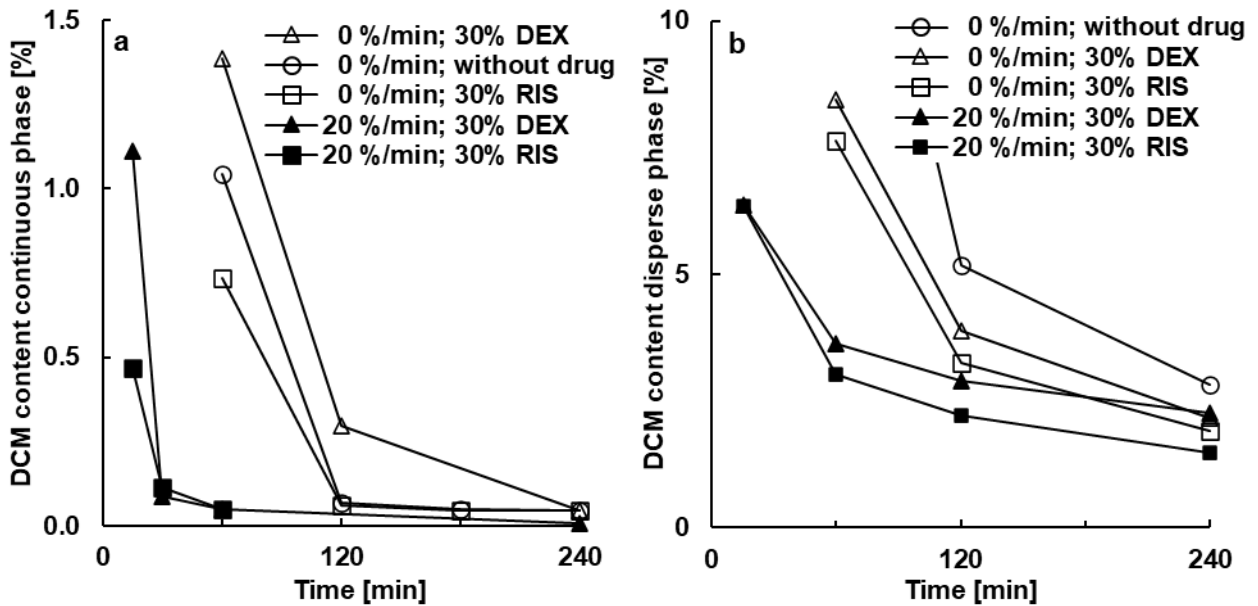


Figure 11: Effect of relative diafiltration rate and drug loading on the dichloromethane content in (a) the continuous phase and (b) the dispersed phase (200 mL batch size)

When diafiltration was combined with a slightly elevated temperature (35 °C), lower residual solvent contents were achieved faster (Figure 12). At 35°C, the process temperature remained longer above the glass transition temperature, thus the dispersed phase remained longer in a liquid or viscous state which favored solvent removal.

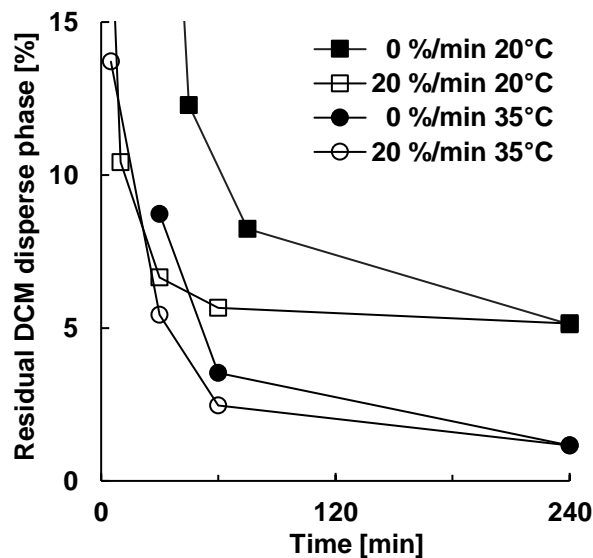


Figure 12: Effect of diafiltration and temperature on the dichloromethane content in the dispersed phase (50 mL batch size)

3.1. Initial removal in the solvent extraction/evaporation method

Focus Beam Reflectance Measurement (FBRM) can be used to monitor the preparation of microparticles by solvent evaporation process online [169,170]. The data obtained with FBRM, not only depend on size and geometry, but also strongly on the optical properties of the dispersed PLGA phase [167]. A decrease in chord length may initially be noticeable due to emulsification and shrinkage. Another transitionally increase in the FBRM signal can be caused by occurrence of subsurface scattering in addition to specular reflection, due the onset of phase separation during PLGA solidification. When solidification progresses, a smooth surface forms and the opacity increases. This means that specular reflection is almost exclusively present, which again results in a decreased FBRM signal. The following stagnation of the FBRM signal indicates that the particles are solidified, at least near the surface [167].

Encapsulation of drugs affected the FBRM signal in different ways. In particular, the initial subsurface scattering was enhanced by the presence of dexamethasone crystals in the PLGA phase (Figure 13). In contrast, dissolved risperidone did not affect the initial chord length. It caused a delayed transient increase of chord length as it was completely dissolved and only precipitated in the dispersed phase after most of the dichloromethane was extracted. The media chord length increased slightly further between 60 and 65 min, if 30 % risperidone was encapsulated without diafiltration.

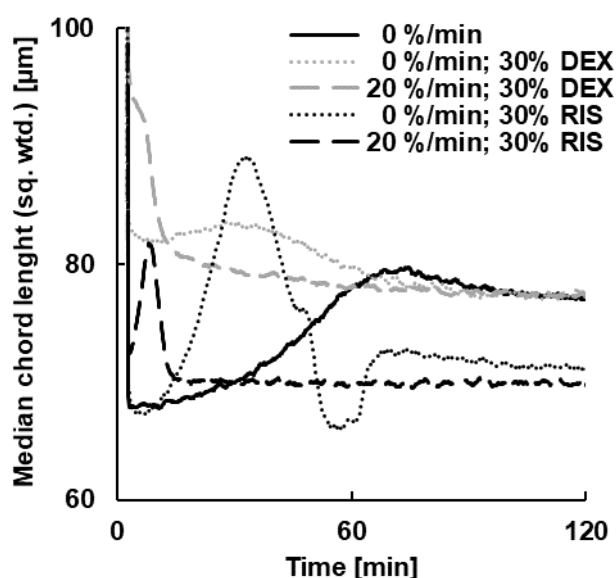


Figure 13: Effect of relative diafiltration rate and drug loading on square weighted media chord length (200 mL batch size)

3.1. Initial removal in the solvent extraction/evaporation method

Splitting the FBRM signal into size classes resulted in an increase in the number of particles counted, which occurred primarily in the particle size fraction $< 25 \mu\text{m}$, consisting mainly of risperidone crystals (Figure 14).

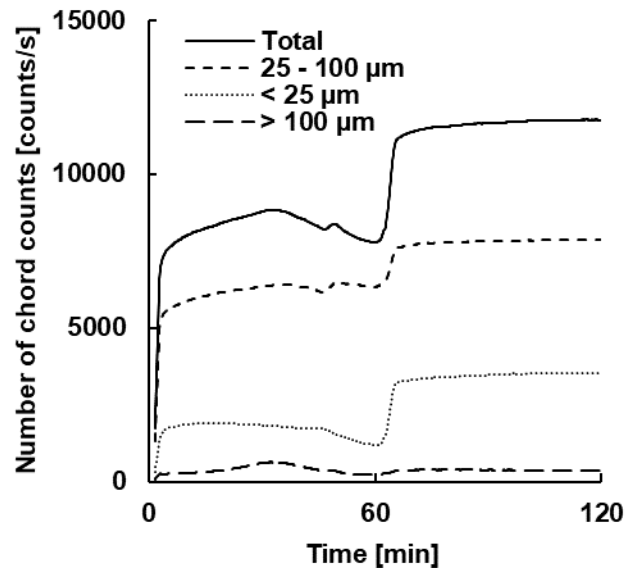


Figure 14: Number of chord counts of size fractions during encapsulation of 30 % risperidone with the solvent evaporation method (200 mL batch size)

The formation of needle-shaped crystals was also confirmed by in-situ microscopy (Figure 15). Risperidone was extracted with dichloromethane from the dispersed PLGA phase and precipitated in the continuous aqueous phase when the extraction rate became slower than the evaporation rate. The risperidone solubility then decreased with decreasing dichloromethane content in the aqueous phase and the drug precipitated.

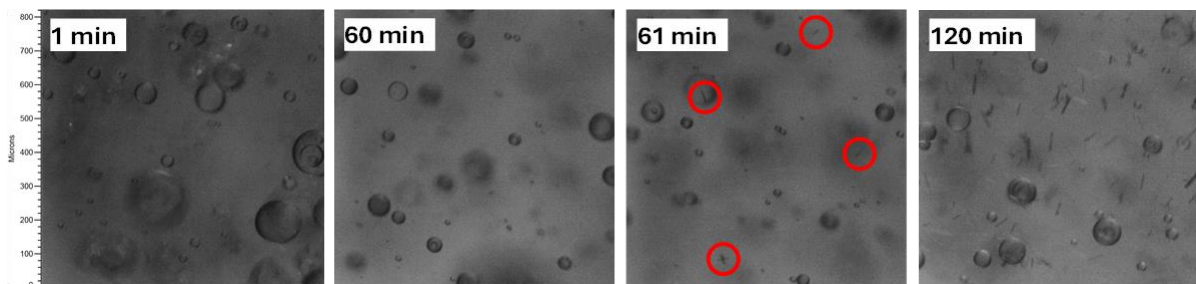


Figure 15: Microscopic appearance (in-situ) during encapsulation of risperidone in PLGA 503H (circles mark first appearance of needle-shaped risperidone crystals)

If dichloromethane extraction was accelerated by diafiltration, an earlier increase, decrease and stagnation of chord length was observed, indicating a faster solidification of the microparticles. The lack of increase in chord length after solidification also showed that unencapsulated risperidone did not crystallize, because of removal by diafiltration (Figure 13). With increasing diafiltration rate, the average particle size of microparticles loaded with 30 % drug increased (Figure 16).

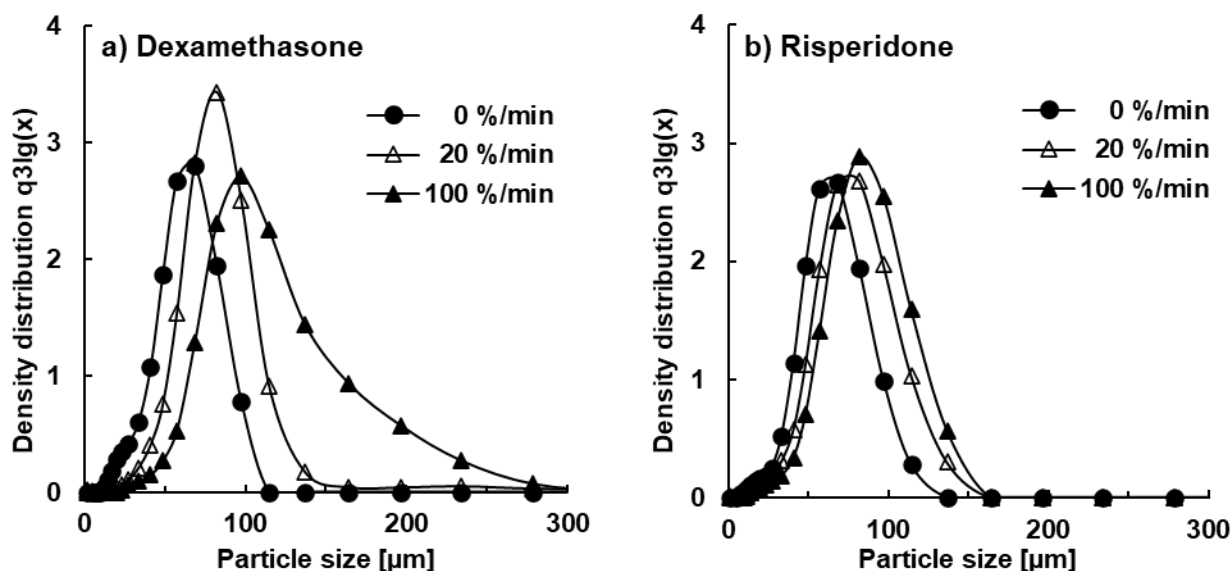


Figure 16: Effect of relative diafiltration rate and drug loading on the particle size distribution of microparticles loaded with (a) 30 % dexamethasone and (b) 30 % risperidone

Due to the faster extraction, a skin of PLGA could have been formed on the droplet surface. This could have prevented shrinkage of the droplets during further extraction of dichloromethane, resulting in larger, more porous particles [77]. The increase in particle size was greater with dexamethasone. Dexamethasone was encapsulated in the form of dispersed drug crystals, this increased the viscosity of the dispersed PLGA phase and further impeded uniform shrinkage. Moderate diafiltration rates ($\leq 20\%/min$) did not change the homogeneous dense morphology of blank PLGA microparticles. At high relative diafiltration rate (100 %/min), numerous slightly deformed microparticles, with a large hollow core were formed (Figure 17).

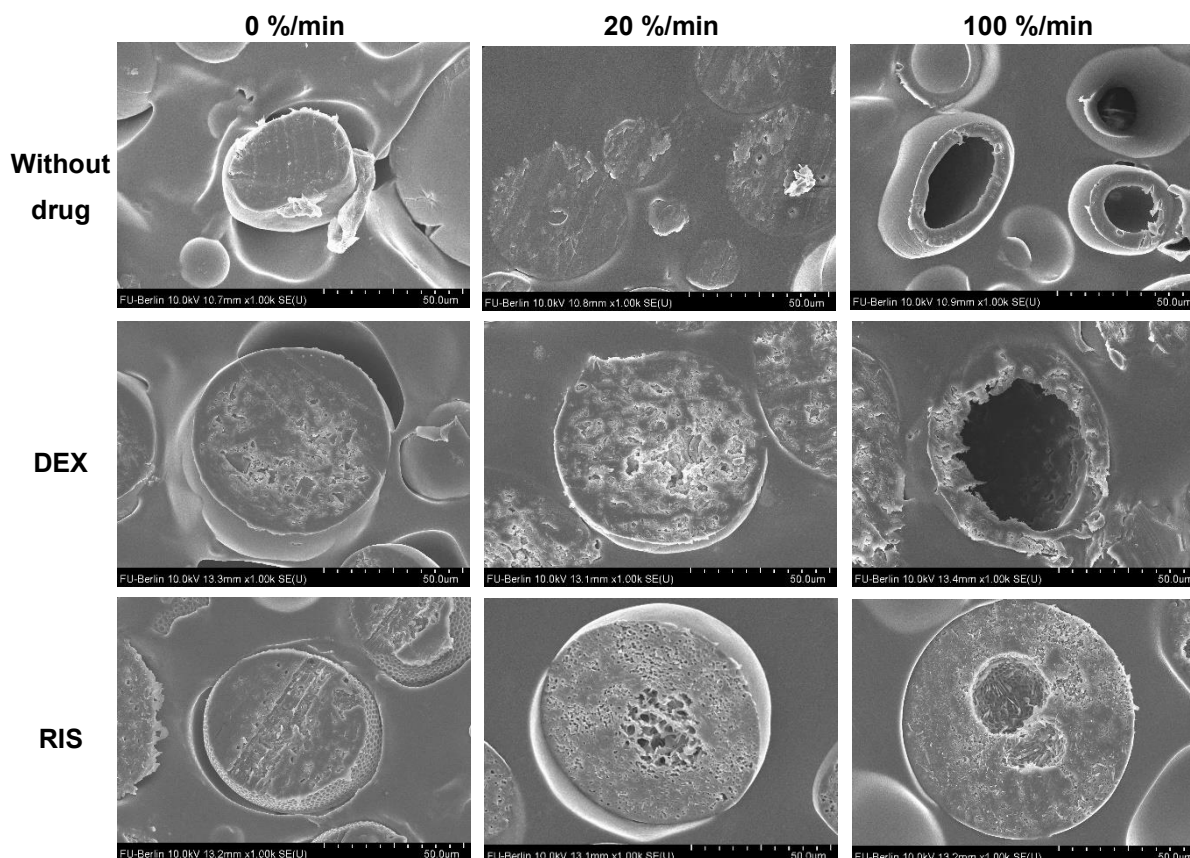


Figure 17: Effect of relative diafiltration rate and drug loading on the morphology of microparticle cross-sections

The formation of a robust, solidified polymer skin probably almost completely prevented the shrinkage in this case. As the extraction progresses, PLGA completely precipitated under the existing skin. Water, which may have entered by rapid extraction, coalesced inside and filled a large cavity. The formation of such large hollow cores was previously observed due to rapid solvent extraction by gradually increasing temperature [100,105] or entrapment of water by $W_1/O/W_2$ double emulsion method with low O/W_2 phase ratio [98]. The encapsulation of 30 % dexamethasone generally led to a more inhomogeneous and porous morphology (Figure 17). Dexamethasone crystals in the dispersed phase hindered shrinkage during extraction. In comparison, microparticles loaded with risperidone had a dimpled surface and the inner pores had a smaller, more regular size. The hollow core structure, formed at high a diafiltration rate (100 %/min), was less pronounced with risperidone, partially, drug crystals had grown in the cavity.

3.1. Initial removal in the solvent extraction/evaporation method

At a high diafiltration rate, diffusion of drug from the dispersed to the continuous phase was prevented earlier because of a faster droplet solidification. This was particularly the case for risperidone again, because of its greater solubility in the PLGA phase and the aqueous phase compared to dexamethasone. Increasing the relative diafiltration rate from 0 to 100 %/min increased the encapsulation efficiency from 62 to 78 % or 69 to 80 % at a theoretical drug loading of 10 % or 30 % (Figure 18). The encapsulation efficiency has been increased more at the lower 10 % theoretical drug loading because the amount of drug extracted up to the solubility limit in the continuous phase corresponded to a larger percentage of the theoretical drug loading.

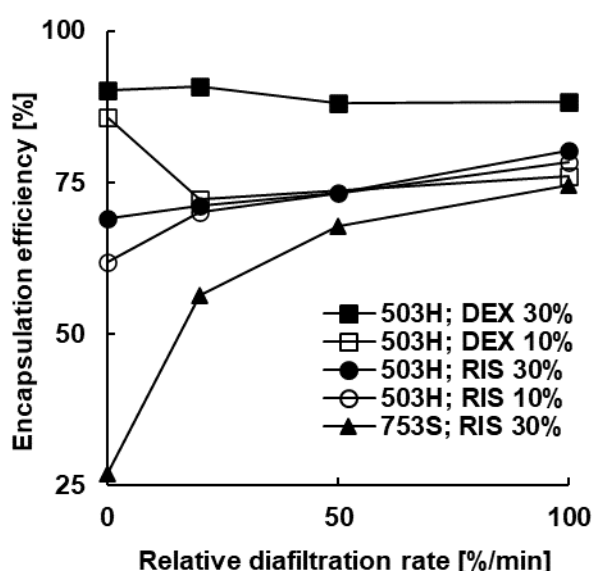


Figure 18: Effect of relative diafiltration rate, drug loading and PLGA grade on the encapsulation efficiency

The positive effect of accelerated solvent removal by diafiltration on the encapsulation efficiency was particularly evident with the more hydrophobic PLGA grade 753S. In general, it is assumed that the solubility of hydrophobic drugs within a PLGA matrix increases with increasing hydrophobicity of PLGA at the same molecular weight [171]. The encapsulation efficiency of risperidone in 753S, which has a similar molecular weight to 503H but an increased lactide content and end-capping, was only 27 %. The FBRM signal of 753S microparticles stagnated later with and without risperidone compared to 503H (Figure 19).

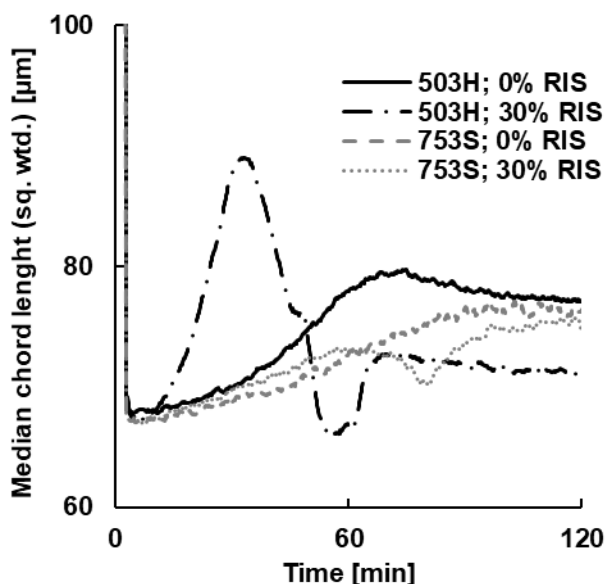


Figure 19: Effect of PLGA grade and risperidone loading on the square weighted media chord length during the solvent evaporation process (200 mL batch size)

The signal without drug increased only slowly without a subsequently decrease, indicating a more uniform solidification without rapid phase separation in the dispersed phase. The slower extraction of dichloromethane in the continuous phase was also reflected by the later crystallization of unencapsulated risperidone in the continuous phase (approx. 10 min later) (Figure 20). The slower solidification of 753S favored the loss of risperidone. Diafiltration increased the encapsulation efficiency from 27 % to about 75 % (Figure 18).

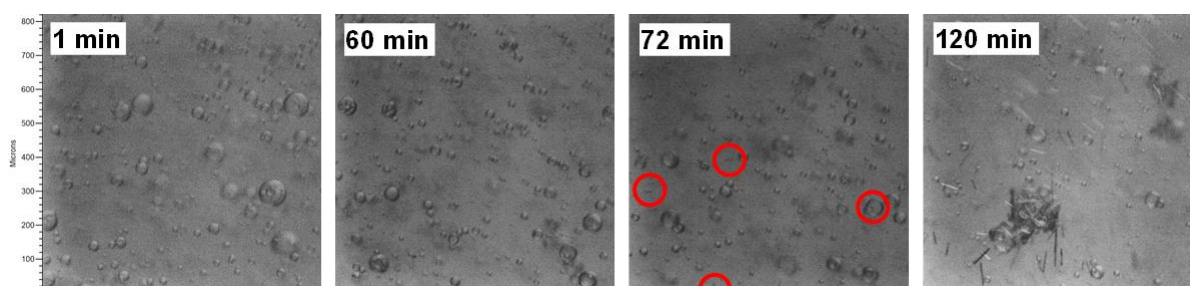


Figure 20: Microscopic appearance (in-situ) during encapsulation of risperidone in PLGA RG 753S (circles mark first appearance of needle-shaped risperidone crystals)

Dexamethasone, which is poorly soluble in dichloromethane and water, resulted in microparticles with good encapsulation efficiency without diafiltration. At a theoretical loading of 10 %, diafiltration decreased the encapsulation efficiency (Figure 18), which was caused by increasing dissolution capacity not only for dichloromethane but also

for dexamethasone. At a low drug loading and low diafiltration rate, the faster drug extraction outweighed the more rapid PLGA solidification due to the opposing effect of improved dichloromethane and drug dissolution capacity on the encapsulation efficiency.

The in-vitro release of dexamethasone from PLGA 503H was investigated at theoretical loadings of 10 % and 30 %, which corresponded to an actual drug loading of 8 ± 1 % and 26 ± 0.7 %, respectively. The release of risperidone from PLGA 503H was also examined at a theoretical drug loading of 30, corresponding to an actual drug loading of 22.5 ± 1.5 %. For the release from PLGA 753S, the theoretical drug loading was varied between 30 - 40 % to compensate the strong effect of diafiltration, an actual drug loading of 27 ± 3 % was achieved. Since no comparable encapsulation in PLGA 753S was achieved for a process without modification of the extraction, a one-step dilution was carried out 15 min after emulsification as a comparison. This resulted in a particle size distribution comparable to the microparticles without modified extraction and a high encapsulation efficiency of 85 %.

An increasing diafiltration rate did not affect the in-vitro release of risperidone from PLGA 503H or 753S and 10 % dexamethasone from 503H (Figure 21). The release was completely controlled by the PLGA matrix, independent of morphological changes (Figure 17).

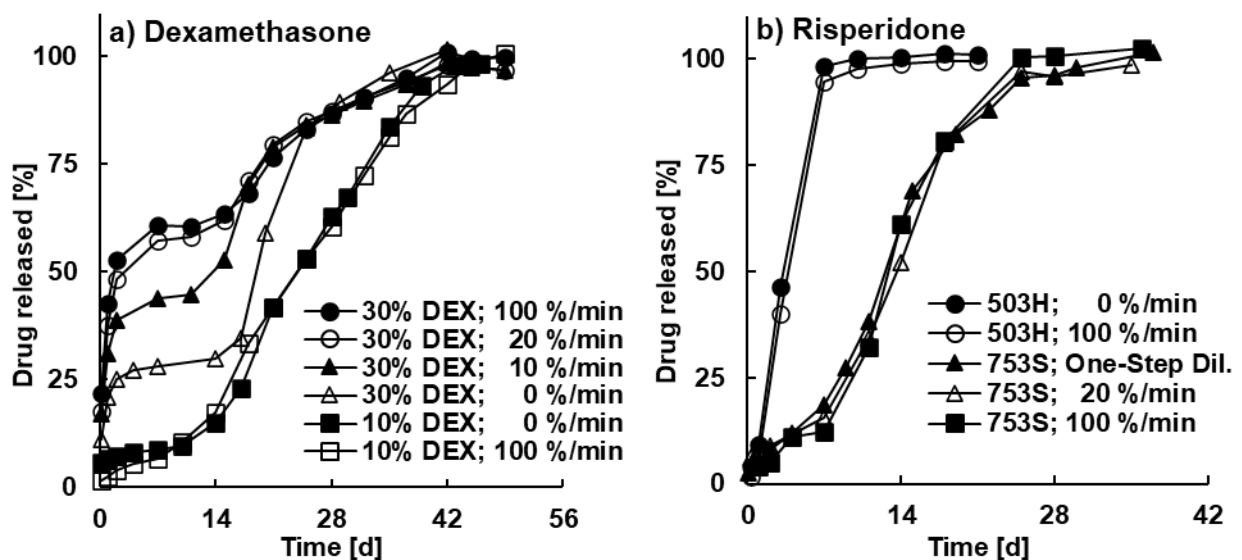


Figure 21: Effect of relative diafiltration rate on the in-vitro release of (a) dexamethasone as a function of the theoretical drug loading and (b) risperidone as a function of the PLGA grade

3.1. Initial removal in the solvent extraction/evaporation method

Compared to dexamethasone, risperidone showed a significantly faster diffusional release, due to its higher solubility in the matrix and the release medium. This increased further after a few days, as the polymer began to degrade, the micro-pH dropped, and risperidone became protonated and more soluble [172]. Dexamethasone was almost completely undissolved in the PLGA matrix. Microparticles with a drug loading of 30 % had a burst release of more than 25 % within 48 h. This burst was followed by a plateau phase lasting for about two weeks with a third rapid release phase due to the beginning of microparticle erosion. The initial burst was caused by percolation, which occurs at high loadings (above the percolation threshold) with dispersed drug particles [39]. Increasing the diafiltration rate increased the initial burst release from 30 % dexamethasone to more than 50 % in 48 h as the percolation network was expanded through pre-existing pores and cavities created by fast solvent extraction (Figure 21). An increase in initial release was also observed due to higher porosity microparticles created by other means, e.g. by the W/O/W double emulsion process or the use of porogens [173,174].

When diafiltration-controlled extraction was performed at elevated temperature, the inhomogeneous matrix structure of the microparticles hardly changed at 35 °C, but it became significantly denser at 45 °C (Figure 22). Being close to the glass transition temperature of pure 503H of 44 - 48 °C, the microparticles remained deformable and shrinkable for a longer time. According to the visual appearance of the cross-sections, 20 %/min diafiltration increased the residual water content from 2.2 to 10.6 %, reinforcing the assumption that pores and cavities were filled with water during manufacturing. Increasing additionally the process temperature increased the water content first to 12.7 % (35 °C) and then reduced it to 6.8 % (45 °C).

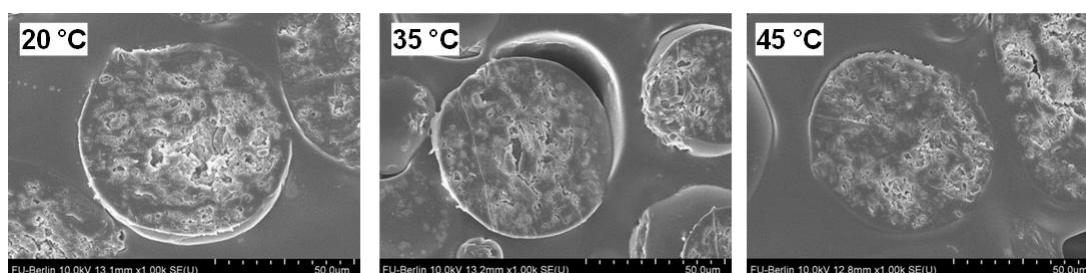


Figure 22: Effect of temperature during diafiltration-assisted preparation of dexamethasone-loaded microparticles (30 % theoretical drug loading) on the morphology of microparticle cross-sections

3.1. Initial removal in the solvent extraction/evaporation method

For 30 % dexamethasone microparticles, the encapsulation efficiency decreased from 90 % to 81 % (35 °C) and to 77 % (45 °C). At 35 °C, the initial burst release was slightly increased further due to the increased porosity caused by the faster dichloromethane extraction (Figure 23a). At 45 °C the burst decreased due to the denser morphology, although not to the level of microparticles prepared without diafiltration. The subsequent plateau phase was significantly shortened. Such an earlier erosion-controlled final release was facilitated by an increased hydrolysis of PLGA during manufacturing. This might be caused by a longer surpassing of the glass transition temperature of the polymer-solvent system at higher process temperatures [145]. The initial burst release within the first 48 h correlated directly with the residual water content before drying, as an indicator of the porosity, confirming percolation theory for high dexamethasone loadings (Figure 23b).

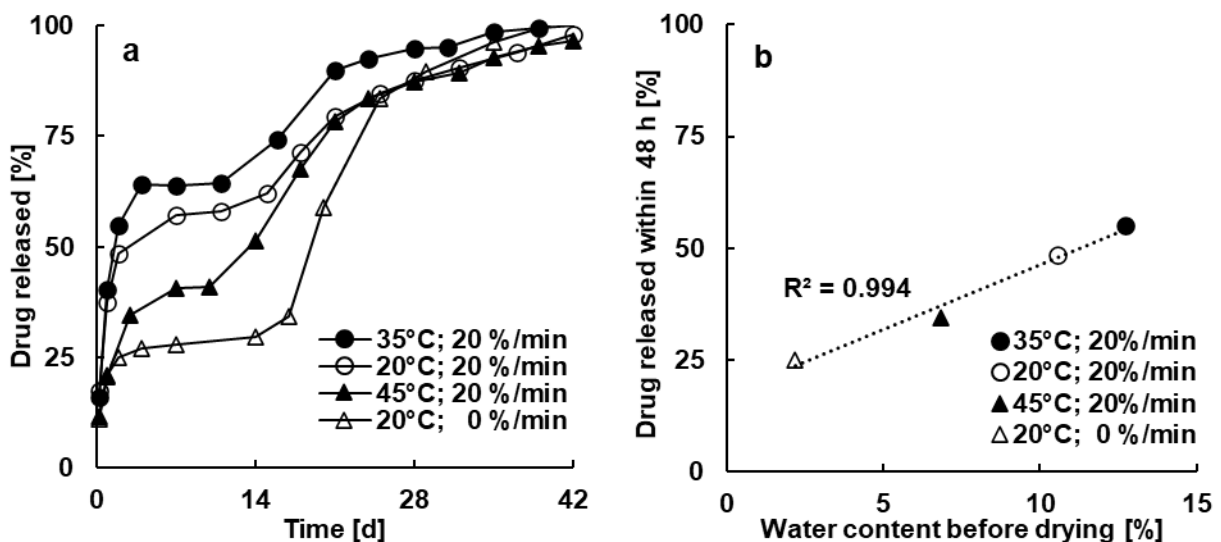


Figure 23: Effect of temperature during diafiltration assisted preparation of dexamethasone-loaded microparticles (30 % theoretical drug loading) (a) on the in-vitro drug release and (b) on the correlation of the water content before drying and the burst release within 48 h

3.1.3. Effect of co-solvent methanol on the initial extraction

In microparticle manufacturing by the solvent extraction/evaporation method, co-solvents, especially alcohols, are sometimes used in addition to the main solvent for PLGA, for example to improve the solubility of drugs [88,91,92]. In the following, the effect of methanol on the solvent removal process and the microparticle properties was investigated. Replacing parts of dichloromethane in the dispersed PLGA phase by methanol affected the initial and final solvent extraction. Methanol itself was removed almost completely in the beginning, due to its complete miscibility with water. The residual methanol content was about 0.3 % (w/w) after 1 h, independent of the initial content in the dispersed phase. The content of residual dichloromethane was slightly increased by the presence of methanol after 1 h (Figure 24).

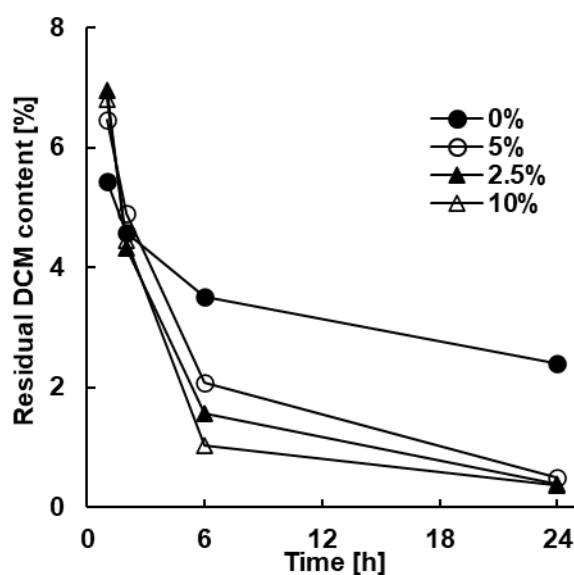


Figure 24: Effect of the methanol content in the dispersed phase on the residual dichloromethane content of dexamethasone-loaded microparticles

This might be caused by a diffusion-slowing skin of precipitated PLGA that has formed on the surface of the dispersed phase due to the accelerated influx of water [97]. The extraction rate of dichloromethane was faster after 2 h when methanol was initially in the formulation, resulting in lower residual solvent contents. After 24 h, less than 0.5 % (w/w) instead of 2.4 % (w/w) residual DCM was present in the microparticles.

Increasing the methanol content increased the porosity due to an increasing proportion of dispersed phase rapidly extracted in the beginning (Figure 25). 5 % (w/w) methanol resulted in clearly visible pores on the surface and within the microparticles.

3.1. Initial removal in the solvent extraction/evaporation method

At 10 % (w/w) methanol, the microparticles became increasingly irregular-shaped and highly porous. The resulting increase of the outer surface area and shortened diffusion paths may have slightly accelerated the extraction. However, since increased porosity caused by diafiltration had no significant effect on the residual dichloromethane content, other reasons had to be considered. Methanol, which evaporates very slowly from the continuous phase, could have acted as a plasticizer for PLGA during final extraction.

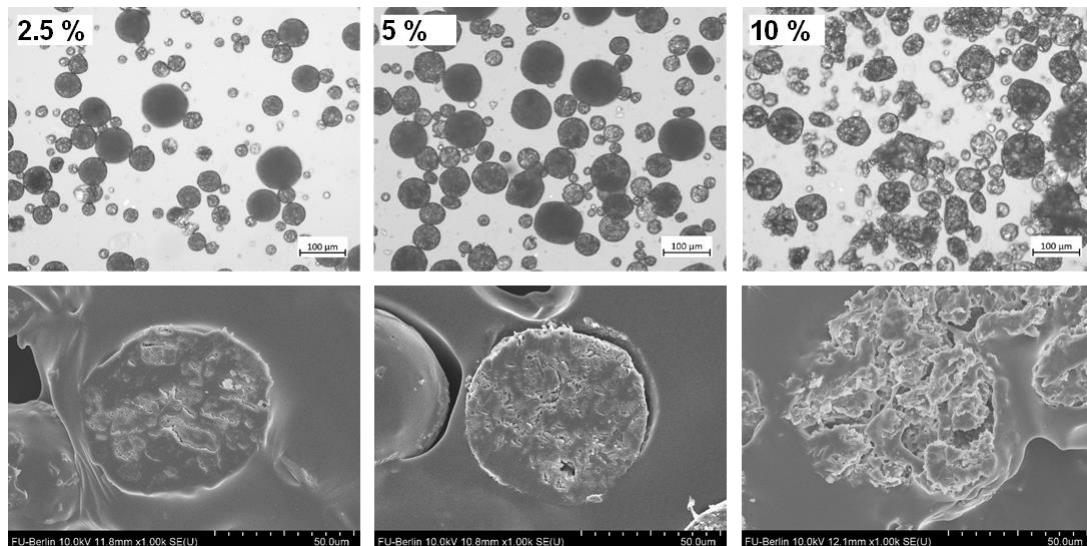


Figure 25: Effect of the methanol content in the dispersed phase on the microscopic appearance (top) and the morphology of cross-sections (bottom) of microparticles with 30 % dexamethasone

Increasing the methanol content in the dispersed phase above 2.5 % (w/w) decreased the encapsulation efficiency of dexamethasone (Figure 26) and increased the burst release (Figure 27). This was independent of the theoretical loading being above or below the percolation threshold because of the greatly increased porosity. Processing a theoretical drug loading of 30 % dexamethasone with 10 % (w/w) methanol reduced the encapsulation efficiency from 92 % to 62 % and increased the initial release within 48 h from 25 % to 63 %.

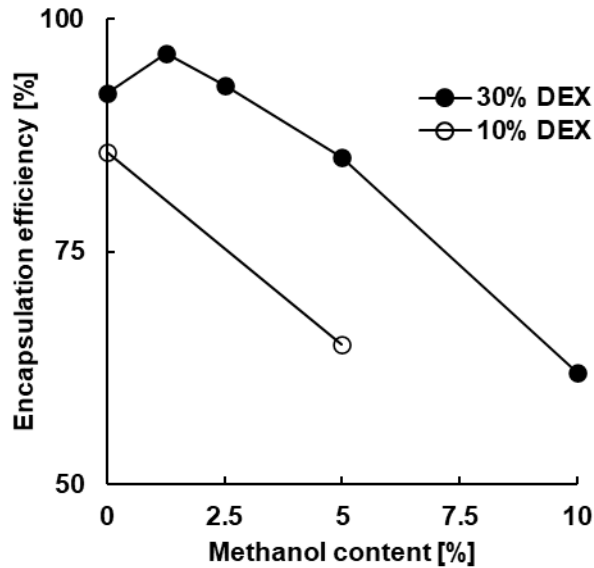


Figure 26: Effect of the theoretical dexamethasone loading and the methanol content in the dispersed phase on the encapsulation efficiency of microparticles

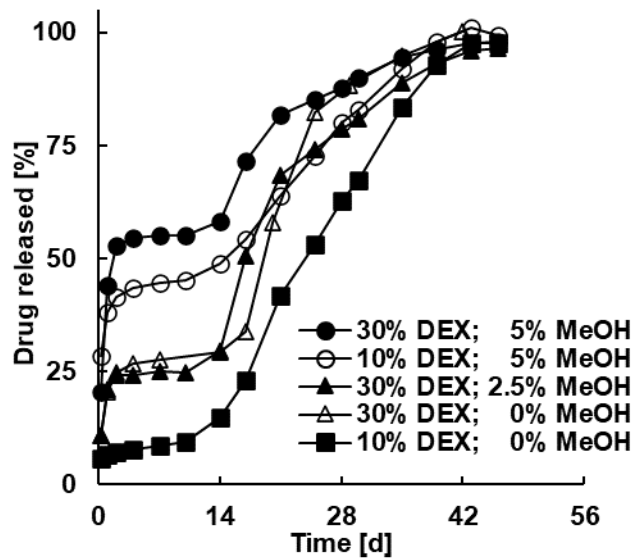


Figure 27: Effect of the theoretical dexamethasone loading and the methanol content in the dispersed phase on the in-vitro release of microparticles

In summary, the initial removal of the organic solvent dichloromethane has a great impact on the properties of the microparticles. Drugs like risperidone, which are soluble in both the continuous and dispersed PLGA phase are better encapsulated if the microparticles solidify early through rapid solvent extraction. Microparticle solidification was accelerated by a one-step dilution of the continuous phase or diafiltration. Diafiltration could eliminate the need for large-volume manufacturing equipment and emulsion transfer. Diafiltration-driven solvent extraction shortened the process time by

3.1. Initial removal in the solvent extraction/evaporation method

accelerating solidification of the microparticles but reduced the residual dichloromethane content only in combination with increased temperature. Increasing the diafiltration rate increased particle size, porosity, and the encapsulation efficiency of risperidone. The latter effect was particularly evident with increasing lipophilicity of PLGA due to its slower solidification without diafiltration. Accelerated solvent extraction by diafiltration did not affect the in-vitro release of risperidone. The initial burst release of dexamethasone was increased by diafiltration when encapsulated at drug loadings above the percolation threshold. Both porosity and burst release could be reduced by increasing the process temperature during diafiltration.

Methanol, as a co-solvent, was extracted significantly faster than dichloromethane because of its complete water miscibility. This rapid extraction resulted in an increased porosity, decreasing dexamethasone loading and a significant increase in the burst release of the final microparticles. The final dichloromethane extraction was faster, although methanol had already been completely extracted. The resulting porosity cannot adequately explain this because, if caused by diafiltration, it had no effect on the residual solvent content. Therefore, the effect of alcohols in the continuous phase is examined below (Chapter 3.2.2).

3.2. Final solvent removal in the solvent extraction/evaporation method

As shown above, it is essential to control the initial solvent extraction during microparticle production in order to control the final microparticle properties. Process modifications, which efficiently control the initial solvent removal and thus increase drug encapsulation, may not influence the residual solvent content because the diffusivity in the polymer decreases with residual solvent content (Chapter 1.5.2). Since the solvent content of the final microparticles has to be reduced to a certain minimum to facilitate storage stability and assure patient safety (Chapter 1.5.4), the final solvent removal step in wet processing is examined below. In particular, the effect of temperature and PLGA grade were studied in Chapter 3.2.1, as well as the effect of the alcohol content in the continuous phase in Chapter 3.2.2, which, as seen in the previous chapter, may affect the residual solvent removal.

3.2.1. Effect of temperature and PLGA grade on the final solvent extraction

PLGA 503H microparticles prepared by the solvent extraction/evaporation method solidified at a residual dichloromethane content of 5 - 10 % (w/w). Based on the Gordon-Taylor equation (Equation 9) and the physical properties of both excipients (Table 3), the glass transition temperature of a PLGA 503H:dichloromethane system would only increase above ambient temperature (approx. 20 °C) at about 3.5 % (w/w) residual dichloromethane. However, residual solvents are not necessarily homogeneously distributed within microparticles and an outer skin may solidify completely with higher solvent content towards the center of the microparticles [97].

3.2. Final solvent removal in the solvent extraction/evaporation method

Table 3: Density and glass transition temperature of excipients (references in parenthesis) used to calculate the glass transition temperature of binary systems with the Gordon-Taylor equation

Excipients	ρ at 25 °C (g/cm ³)	T _G (K)
PLGA 503H	1.580 [121]	319 [121]
DCM	1.326 [175]	100 [145]
Water	0.997 [175]	138 [121]
MeOH	0.786 [175]	103 [176]
EtOH	0.785 [175]	97 [177]
IPA	0.781 [175]	115 [178]
PG	1.033 [175]	167 [179]
Glycerol	1.258 [175]	191 [179]

The extraction of the last 5 % (w/w) residual dichloromethane was slow (Figure 28). After 24 h stirring in continuous phase, the microparticles still contained 2.4 % (w/w) residual dichloromethane, due to the slow final extraction (Figure 28). If the solidified microparticles were filtered after 6 h with a residual dichloromethane content of around 5 % (w/w), the dichloromethane removal slowed down even more compared to microparticles dispersed in the continuous phase. Water acted as a plasticizer in the wet extraction process and thus improved the diffusion of dichloromethane out of the PLGA matrix [121].

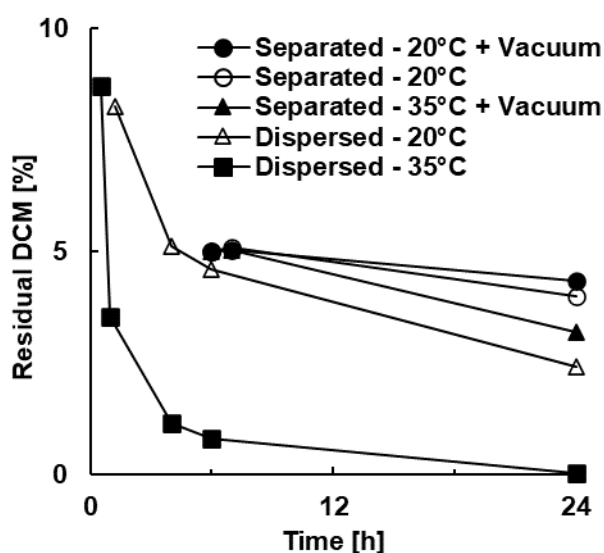


Figure 28: Effect of extraction conditions on the residual dichloromethane content of blank PLGA 503H microparticles

3.2. Final solvent removal in the solvent extraction/evaporation method

Vacuum drying hardly improved the solvent removal from filtered microparticles, since it was not the evaporation of the highly volatile dichloromethane that limited the final extraction, but rather the low diffusivity within the PLGA matrix [120]. A parallel increase of temperature to 35 °C only slightly reduced the solvent content, 3.2 % (w/w) dichloromethane remained after a total process time of 24 h. Due to the low glass transition temperature of PLGA, a further increase in temperature was not possible without agglomeration/aggregation of the microparticles. Increasing the temperature in the wet extraction process, i.e. in combination with the plasticizing effect of water, resulted in a significantly improved solvent extraction. A residual dichloromethane content of 0.8 % (w/w) after 6 h and 0.03 % (w/w) after 24 h was achieved.

Increasing the temperature of the continuous phase during solvent extraction may affect the stability of both PLGA and the encapsulated drugs and promote drug loss to the continuous phase, resulting in lower encapsulation efficiencies [145]. Nucleophilic drugs such as risperidone catalyze the degradation of PLGA, especially at temperatures above the glass transition temperature of the system [32,145,180]. Stirring risperidone-loaded 503H microparticles at ambient temperature did not result in drug loss. The encapsulation efficiency decreased only from 88 % to 86 % within 24 h. Increasing the temperature to 35 °C decreased the encapsulation efficiency to 75 % within 4 h. Between 4h and 24h, swelling and partial erosion of microparticles was visible due hydrolysis of PLGA, caused by risperidone and the increased temperature (Figure 29). This significantly decreased the risperidone loading to approx. 3 %, i.e. an encapsulation efficiency of only 7 %.

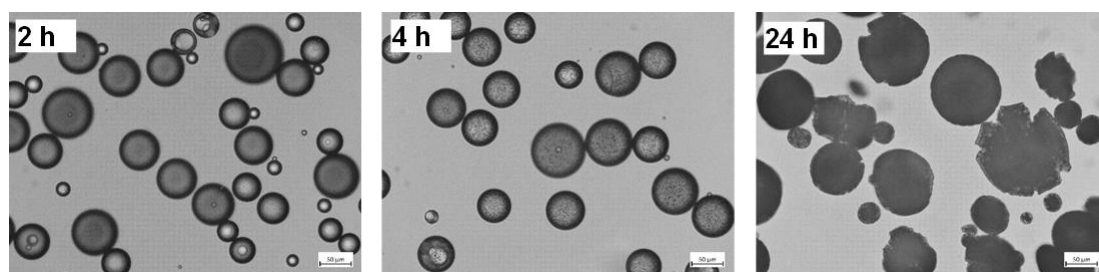


Figure 29: Effect of the extraction time at 35 °C on the microscopic appearance of risperidone-loaded 503H microparticles

3.2. Final solvent removal in the solvent extraction/evaporation method

The PLGA grade affected not only the solidification speed and encapsulation efficiency (Chapter 3.1), but also the residual solvent content. To eliminate the effect of solidification speed, a 1:9 one-step dilution was performed 15 min after the start of emulsification. After stirring in the aqueous phase for 24 h, a decreasing water content and an increasing residual dichloromethane and risperidone content was obtained with higher molecular weight (502H < 503H < 504H; 752S < 753S) or end-capped PLGA (503)(Table 4). An increased lipophilicity and decreased molecular mobility of the polymer chains increased the affinity for dichloromethane, reduced the affinity for water and reduced the diffusivity for both. A higher lactide content (752S and 753S), although it increased the lipophilicity of the PLGA, did not increase the residual solvent content. The slower initial solvent extraction and microparticle solidification shown above for 753S (Figure 19) may have prevented the formation of a diffusion-limiting PLGA skin on the droplet/microparticle surface and resulted in better final solvent extraction.

Table 4: Effect of PLGA grade and extraction temperature on the encapsulation efficiency (EE) of 35 % risperidone and residual water and solvent content

PLGA grade	24 h 20 °C			1 h 20 °C + 3 h 35 °C		
	EE %	Water %	DCM %	EE %	Water %	DCM %
502H	64	32	0.0	72	75	0.0
503H	86	17	1.6	94	22	0.8
503	92	24	2.1	90	27	1.1
504H	91	21	2.0	95	31	0.9
752s	74	38	0.1	66	32	1.8
753s	87	28	0.7	93	23	1.2

3.2. Final solvent removal in the solvent extraction/evaporation method

Furthermore, increasing molecular weight of PLGA increased the viscosity of the polymer solution and thus the particle size (Figure 30). Increased diffusion pathways and decreased total surface area of the microparticles reduced the extraction rate.

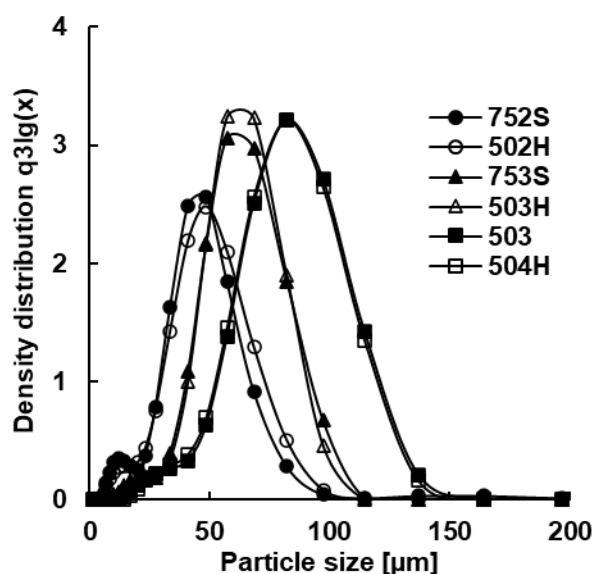


Figure 30: Effect of PLGA grade on the particle size distribution of risperidone-loaded microparticles

Increasing the temperature to 35 °C 1 h after emulsification and shortening extraction to 4 h (to limit PLGA degradation) decreased the residual dichloromethane content of all PLGA grades except those with higher lactide content. The encapsulation efficiency was not significantly affected, except for a decrease from 74 % to 66 % for 752S. Only the microscopic appearance of 502H microparticles changed significantly with the use of short-term heating (Figure 31). The visible swelling and erosion of the microparticles due to PLGA degradation also led to a strong increase in the residual water content. Therefore, an increase in temperature was particularly critical for PLGA grades with low molecular weight, as they had the lowest glass transition temperature. In addition, the critical chain length at which PLGA oligomers became soluble in water, resulting in erosion of the microparticles, was most likely reached.

3.2. Final solvent removal in the solvent extraction/evaporation method

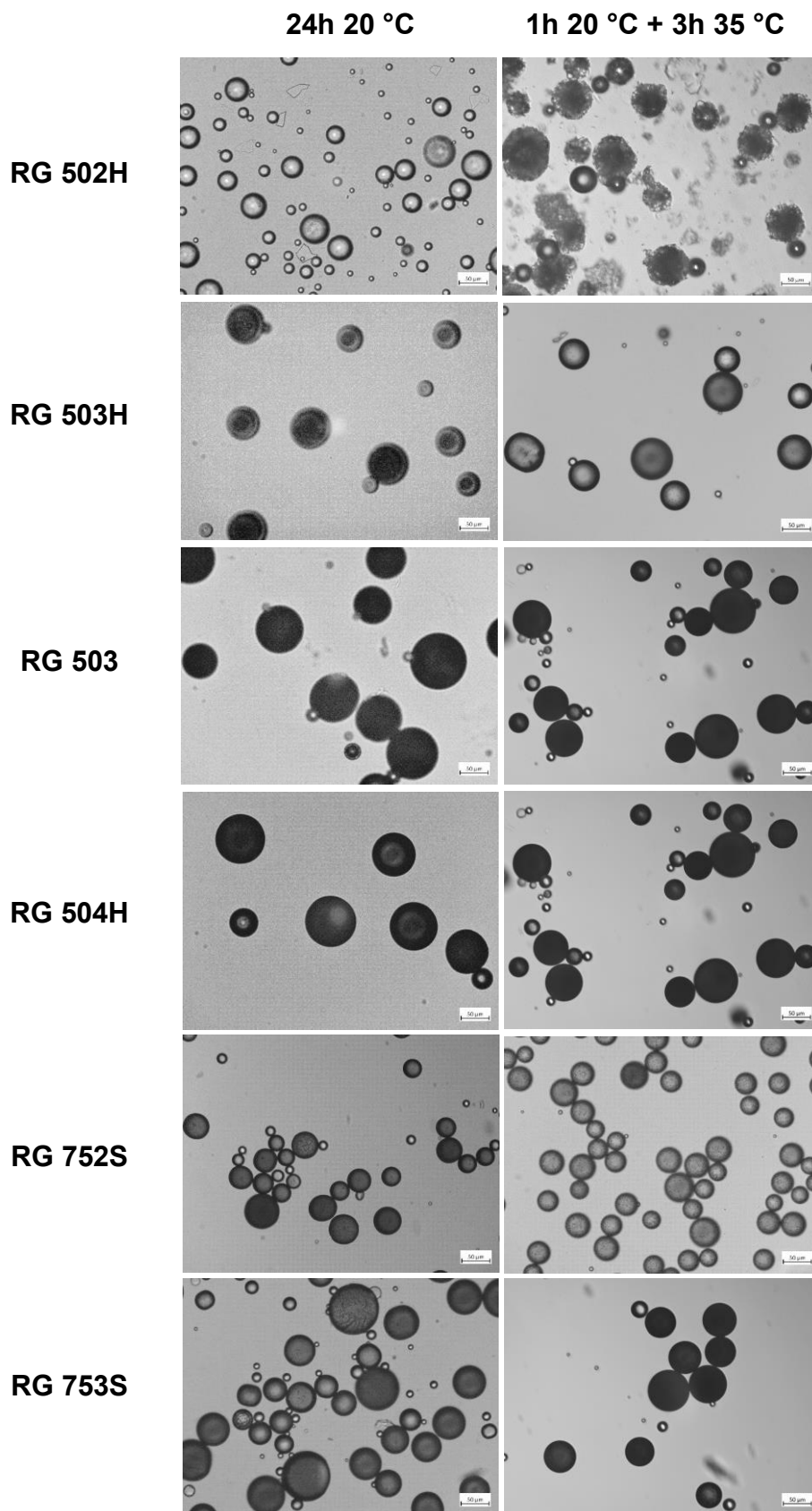


Figure 31: Effect of PLGA grade and the extraction temperature on the microscopic appearance of risperidone-loaded microparticles

3.2. Final solvent removal in the solvent extraction/evaporation method

In accordance with the literature [181] the in-vitro release of risperidone was slightly sustained and delayed by an increased molecular weight, end-capping and especially increased lactide content (Figure 32). Increasing the lipophilicity of PLGA in general led to slower water influx and swelling at the beginning of release [30–33]. Furthermore, the diffusivity was decreased by a slightly decreased solubility in PLGA [168] and a reduction in the free volume between the longer, less mobile polymer chains [182].

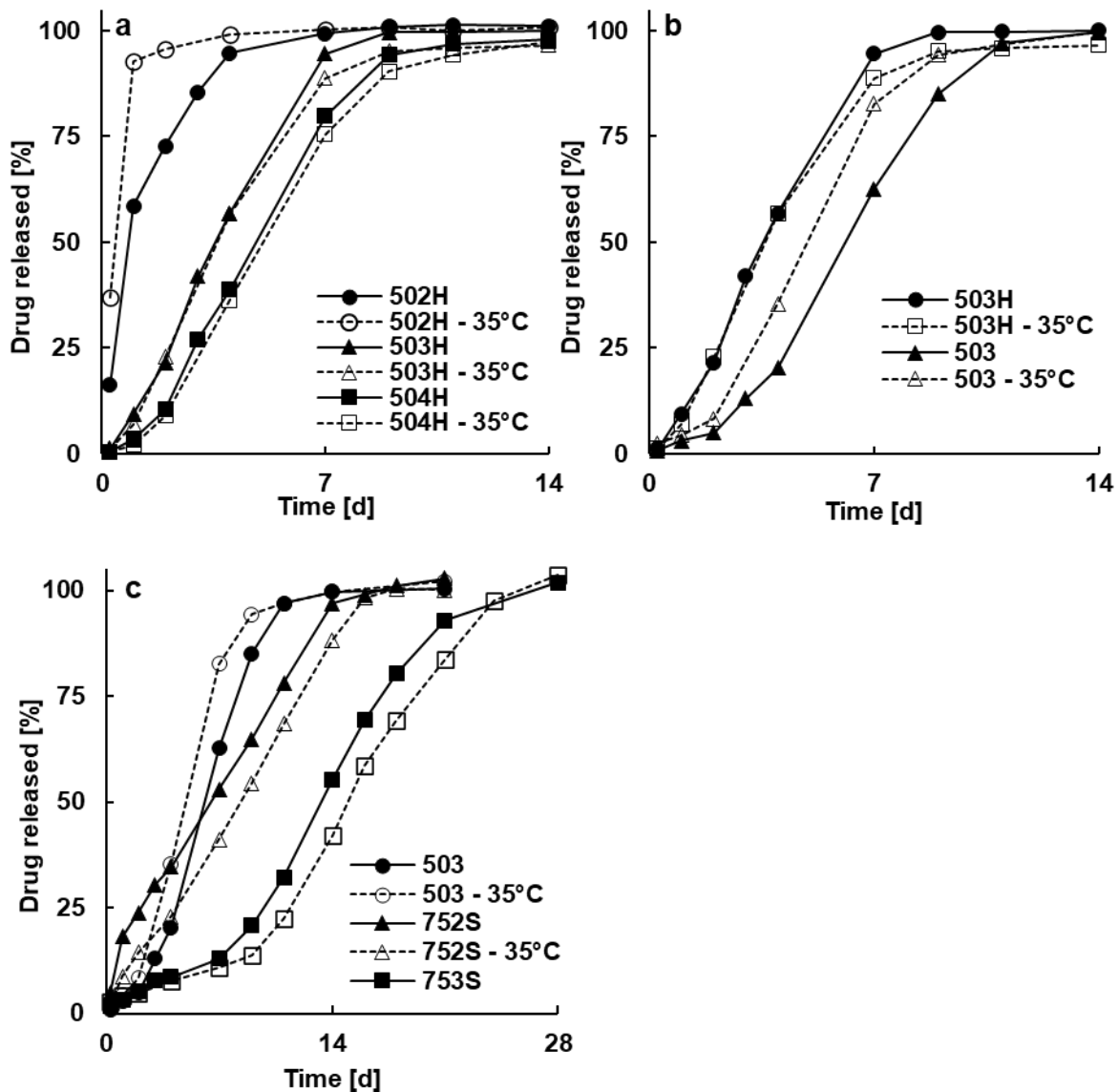


Figure 32: Effect of increased extraction temperature and modification of PLGA grade, i.e. (a) molecular weight, (b) end-capping and (c) lactide content on the in-vitro release of 30 % risperidone (n=1)

3.2. Final solvent removal in the solvent extraction/evaporation method

PLGA degradation during extraction at 35 °C was only reflected by an accelerated in-vitro release of risperidone from 503 and especially 502H microparticles (Figure 32). The in-vitro release for 503H and 504H microparticles was not affected and slightly delayed for 752S and 753S microparticles. The latter could have been caused by an increased microparticle density, as previously obtained by increased process temperature (Figure 22 and 23), which slows down the water influx and initial risperidone diffusion.

3.2.2. Effect of alcohols in the continuous phase on the final solvent extraction

A modification in the composition of the continuous aqueous phase was investigated as an alternative to elevated temperature. To evaluate the potential of various alcoholic PLGA non-solvents having at least one hydroxyl group, solidified PLGA microparticles with a residual dichloromethane content of 5 - 6 % (w/w) were filtered, washed, and redispersed in water containing different alcohols and amounts. The residual dichloromethane content of blank microparticles after 6 h decreased even less with 50 % (w/w) Glycerol (3.6 % (w/w) DCM) or Propylene glycol (PG) (4.4 % (w/w) DCM) compared to pure water (3.2 % (w/w) DCM). The addition of the monohydric alcohols methanol (MeOH), ethanol (EtOH) and isopropanol (IPA) reduced the residual dichloromethane content significantly, these were further investigated. A potential explanation was a lower solubility of dichloromethane in the aqueous continuous phase containing polyhydric alcohols when compared to monohydric alcohols (especially ethanol) (Table 5).

Table 5: Effect of the type and amount of alcohol in the continuous phase on the dichloromethane solubility

Alcohol content [% (w/w)]	S_{DCM} [mg/mL] in water:alcohol mixtures		
	0	20	50
MeOH	11	19	73
EtOH	11	14	147
IPA	11	11	27
PG	11	14	20
Glycerol	11	8	13

3.2. Final solvent removal in the solvent extraction/evaporation method

The diffusivity in the PLGA matrix was ranked as more important for the final extraction from solidified microparticles than the solution capacity in the continuous phase [97]. The HSP distance R_a (Equation 14) between the monohydric alcohols and PLGA is smaller compared to the one of polyhydric alcohols and PLGA, showing the higher affinity and solubility of the first, although their distance appears still large compared to dichloromethane and PLGA (Table 6).

Table 6: Hansen solubility parameters of the investigated drugs and excipients (references in parenthesis) and their HSP distance R_a to PLGA

Excipients	δ_d	δ_p	δ_h	Method	R_a PLGA
PLGA 50:50	16.4	8.7	3.6	Solubility testing by turbidity [134]	-
DEX	20.5	15.4	8	Group contribution by Hoftyzer and van Krevelen [177]	11.5
RIS	18.5	8.4	8.1	Molecular dynamic simulation [178]	6.2
DCM	17	7.3	7.1	Group contribution by Barton [175]	4.0
Water	15.5	16	42.3	Group contribution by Barton [175]	39.4
MeOH	14.7	12.3	22.3	Group contribution by Barton [175]	19.3
EtOH	15.8	8.8	19.4	Group contribution by Barton [175]	15.8
IPA	15.8	6.1	16.4	Group contribution by Barton [175]	13.1
PG	16.8	9.4	23.3	Group contribution by Barton [175]	19.7
Glycerol	9.3	15.4	31.4	Group contribution by Barton [175]	31.9

Because of the increased affinity to PLGA and their smaller molecule size, monohydric alcohols diffused better into the matrix resulting in an increased free volume and lower glass transition temperature. Although the removal of absorbed alcohols was not examined in this study, their permissible limits in the final product, 30 mg/d methanol, 50 mg/d ethanol and 50 mg/d isopropanol, are significantly higher than for dichloromethane (6 mg/d), due to their lower toxicity [164]. In general, increasing the alcohol content in the continuous phase, increased the content of absorbed alcohol in the microparticles (Figure 33).

3.2. Final solvent removal in the solvent extraction/evaporation method

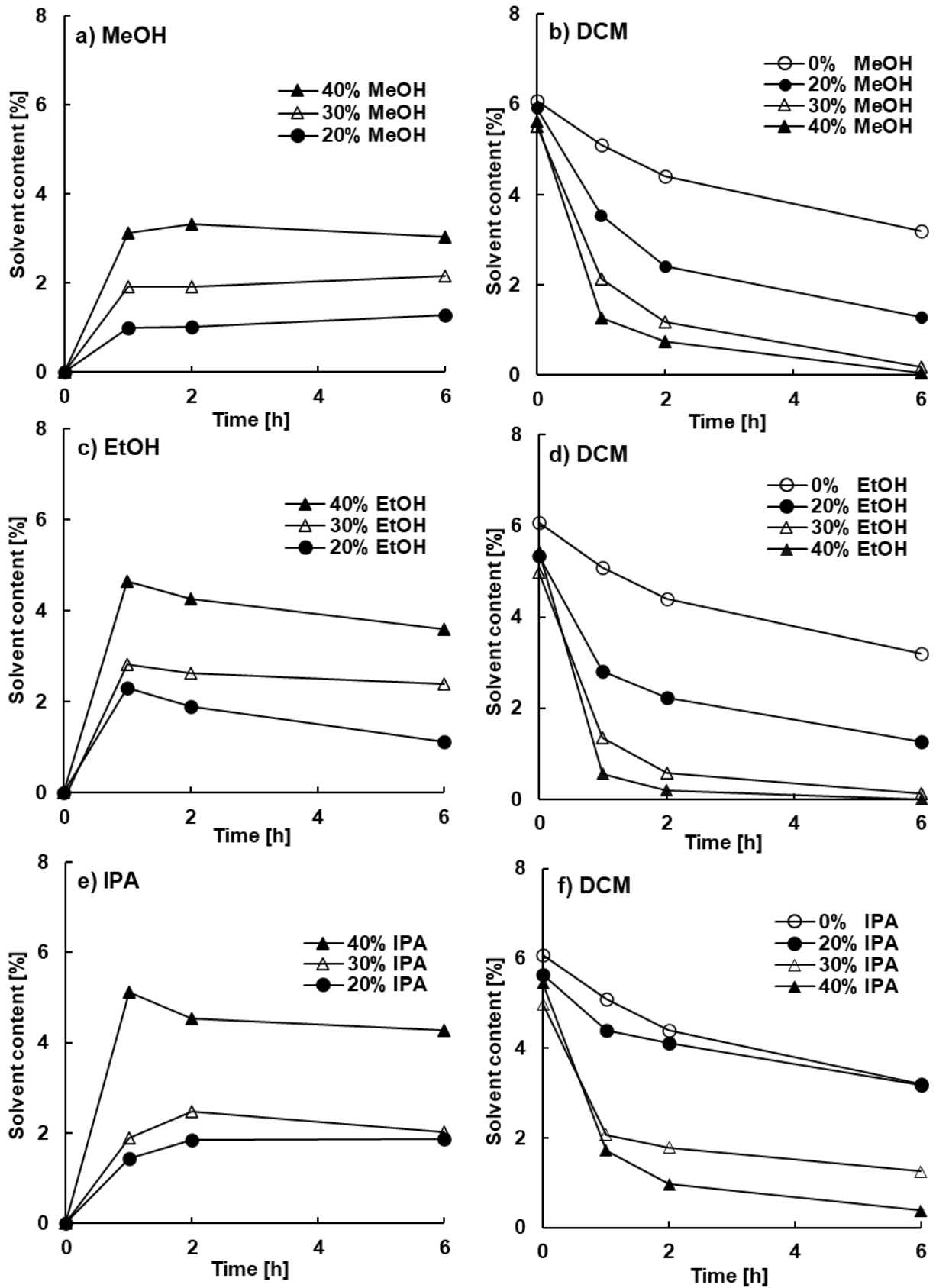


Figure 33: Effect of the amount of methanol (a, b), ethanol (c, d) or isopropanol (e, f) in the continuous phase on the content of absorbed alcohol (a, c, e) and residual dichloromethane (b, d, f) in blank microparticles

3.2. Final solvent removal in the solvent extraction/evaporation method

As the chain length of the monohydric alcohols increased, the HSP distance to PLGA decreased. Accordingly, the order of alcohol absorption was isopropanol > ethanol > methanol, despite a decrease in molecule size (4.3 % (w/w) isopropanol, 3.6 % (w/w) ethanol or 3.0 % (w/w) methanol after 6 h in 40 % (w/w) non-solvent). However, the residual dichloromethane content did not correspond to this trend and was lowest in ethanol, followed by methanol and isopropanol (Figure 33). Not only the content of the absorbed non-solvent but also its plasticizing potency was crucial for the extraction of residual dichloromethane. The effect of (non-)solvents on the glass transition temperature of the polymer was estimated with the Gordon-Taylor equation (Equation 9). According to the density and especially to the glass transition temperature of the different excipients (Table 3), the plasticizing effect was in order of ethanol > methanol > isopropanol > dichloromethane (Figure 34).

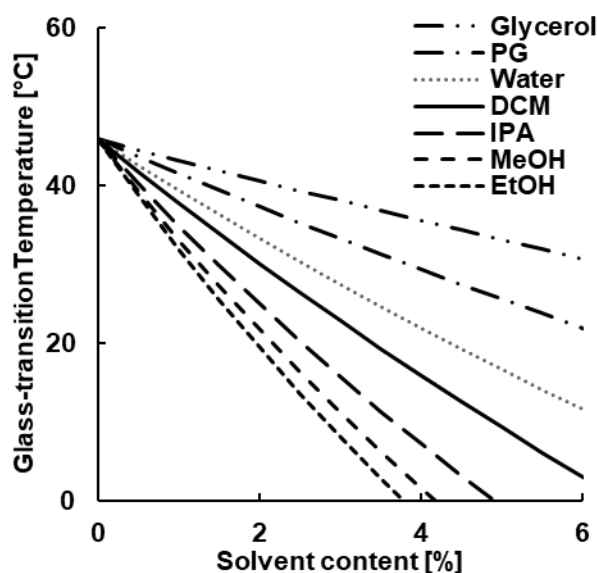


Figure 34: Effect of the type and amount of absorbed (non-)solvent on the glass-transition temperature of PLGA, calculated with the Gordon Taylor equation

Microparticles that were redispersed in up to 50 % (w/w) propylene glycol or glycerol did not agglomerate and had no optical changes compared to microparticles redispersed in water. With higher molecular weight of monohydric alcohols, the microparticles agglomerated and stuck together at a lower content of absorbed alcohol (Figure 35). The dispersibility of the microparticles was only retained up to 40 % (w/w) methanol, 30 % (w/w) ethanol or 20 % (w/w) isopropanol. This trend contradicted the calculated plasticizing effects, according to which ethanol reduced the glass transition

3.2. Final solvent removal in the solvent extraction/evaporation method

temperature of PLGA the most and was therefore the most likely to cause stickiness. Rather, the trend of HSP distances was reflected here (Table 6). Although isopropanol is a poor solvent for PLGA, it had the shortest HSP distance among the alcohols examined. As isopropanol was perhaps the best solvent to dissolve the surface of the microparticles, the microparticles agglomerated at the lowest content of 30% (w/w). Since isopropanol addition caused stickiness and had the least effect on the residual dichloromethane content, further work focused on methanol and ethanol.

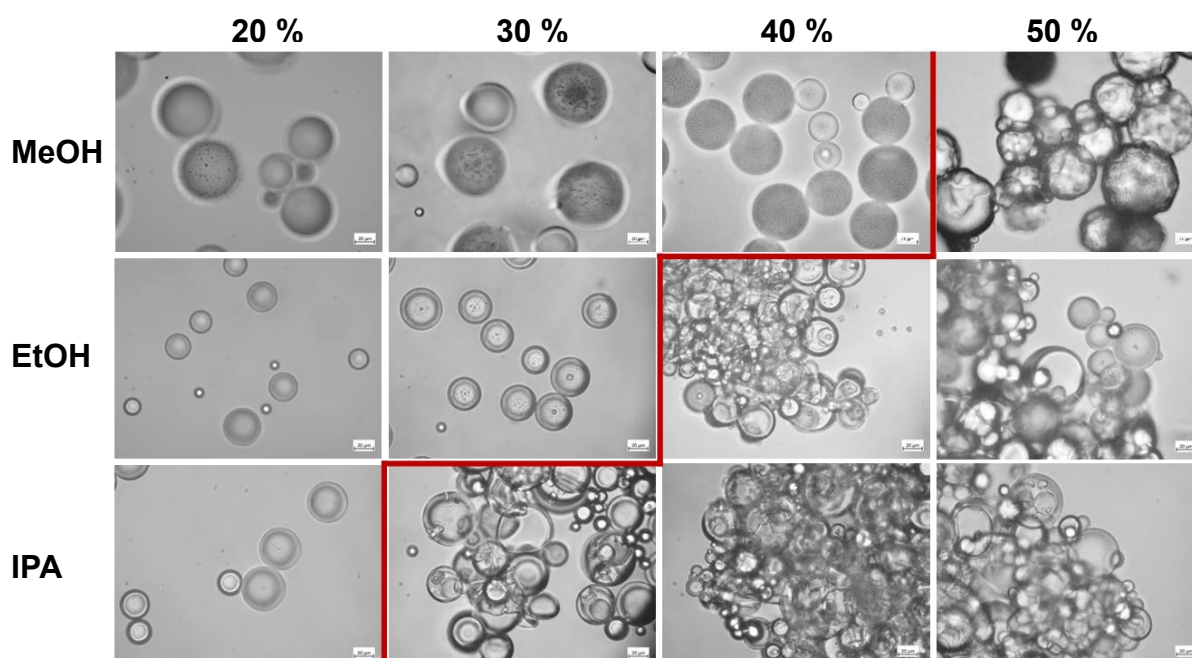


Figure 35: Effect of the type and amount of alcohol in the continuous phase on the microscopic appearance of blank microparticles after 6h (the red line marks the limit when sticking occurred)

Microparticles loaded with dexamethasone absorbed less methanol or ethanol than blank microparticles (Figure 36a). They only contained 0.6 % (w/w) or 0.7 % (w/w) compared of 2.4 % (w/w) or 2.2 % (w/w) of methanol or ethanol after 6 h in 30 % (w/w) non-solvent. Despite the lower content of absorbed alcohol, dichloromethane was removed efficiently. A residual dichloromethane content below 0.1 % (w/w) was achieved with both alcohols within 6 h (Figure 36b). Due to its low solubility in PLGA [172], dexamethasone was present almost entirely as dispersed crystals in the microparticles. These absorbed neither dichloromethane nor alcohols but contributed to the mass of the microparticles and thereby reduced the calculated solvent contents.

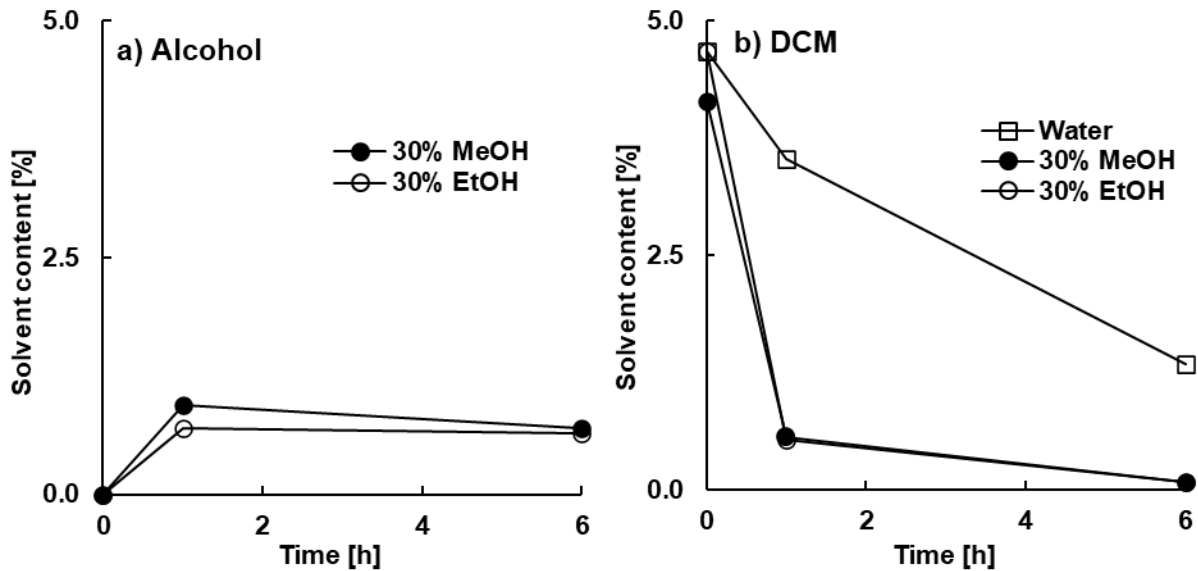


Figure 36: Effect of the type and amount of alcohol in the continuous phase on the content of (a) absorbed alcohol and (b) residual dichloromethane in microparticles (30 % theoretical dexamethasone loading)

The encapsulation efficiency of dexamethasone was significantly reduced by methanol and ethanol (Figure 37). While the encapsulation efficiency of the microparticles with a theoretical drug loading of 30 % remained unchanged at around 85 % during extraction in water, it decreased to 42 % in methanol and 37 % in ethanol after 6 h.

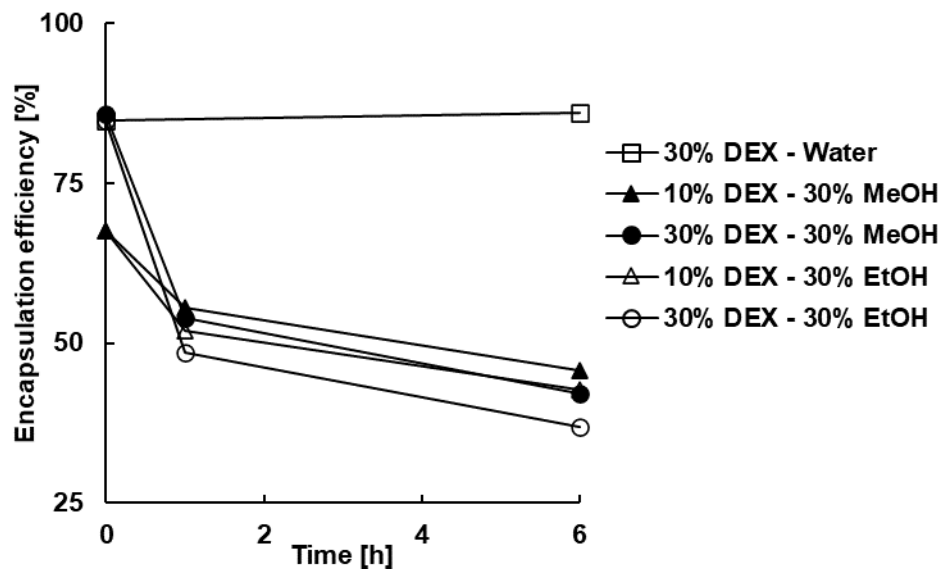


Figure 37: Effect of the theoretical dexamethasone loading and type and amount of alcohol in the continuous phase on the encapsulation efficiency

3.2. Final solvent removal in the solvent extraction/evaporation method

As a result of extraction, some microparticles apparently no longer contained crystalline drug on the surface or even none at all (Figure 38). Both alcohols increased the solubility of dexamethasone in the continuous phase as well as in PLGA, increasing the concentration gradient and thus the diffusion of drug out of the microparticles. In addition, microparticles with a high loading of dispersed drug tend to percolate during the in-vitro release, which means that drug crystals close to the surface dissolve, creating pores that allow media access to further drug crystals. The result is a pore network that results in the rapid initial burst release [39]. Extraction with alcohol in the continuous phase also resulted in pores of the rectangular shape and size corresponding to dissolved dexamethasone crystals on the surface of microparticles with 30 % dexamethasone loading indicating percolation (Figure 38). However, microparticles with only 10 % theoretical dexamethasone loading, i.e. presumably far below the percolation threshold, also showed a reduction in encapsulation efficiency from 68 % to 45 % or 43 % after 6 h in 30 % (w/w) methanol or ethanol.

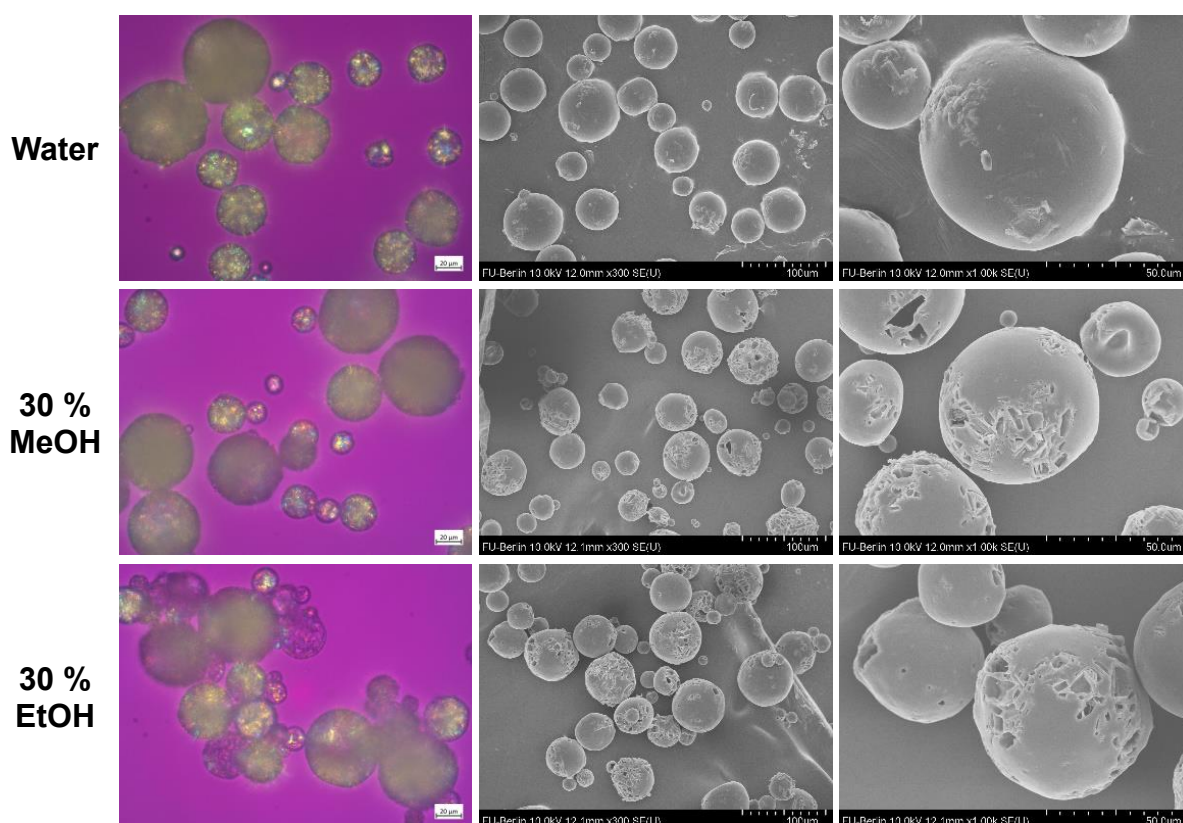


Figure 38: Effect of the type and amount of alcohol in the continuous phase on the appearance of microparticles (30 % theoretical dexamethasone loading) after 6 h extraction under polarized light microscope (left) and scanning electron microscope (mid and right)

3.2. Final solvent removal in the solvent extraction/evaporation method

Encapsulated risperidone resulted in an increased absorption of the alcohols, especially methanol when compared to blank microparticles (Figure 39a). After 6 h in 30 % (w/w) methanol, the microparticles contained 4.6 % (w/w) methanol. Despite the increased alcohol absorption, dichloromethane was removed less efficient compared to the blank or dexamethasone-loaded microparticles (Figure 39b). 30 % (w/w) ethanol in particular accelerated the dichloromethane extraction within the first hour due to its potent plasticizing effect. However, the residual dichloromethane content of 2.4 % (w/w) after 6 h in 30 % (w/w) methanol or ethanol was comparable to 2.7 % (w/w) in water.

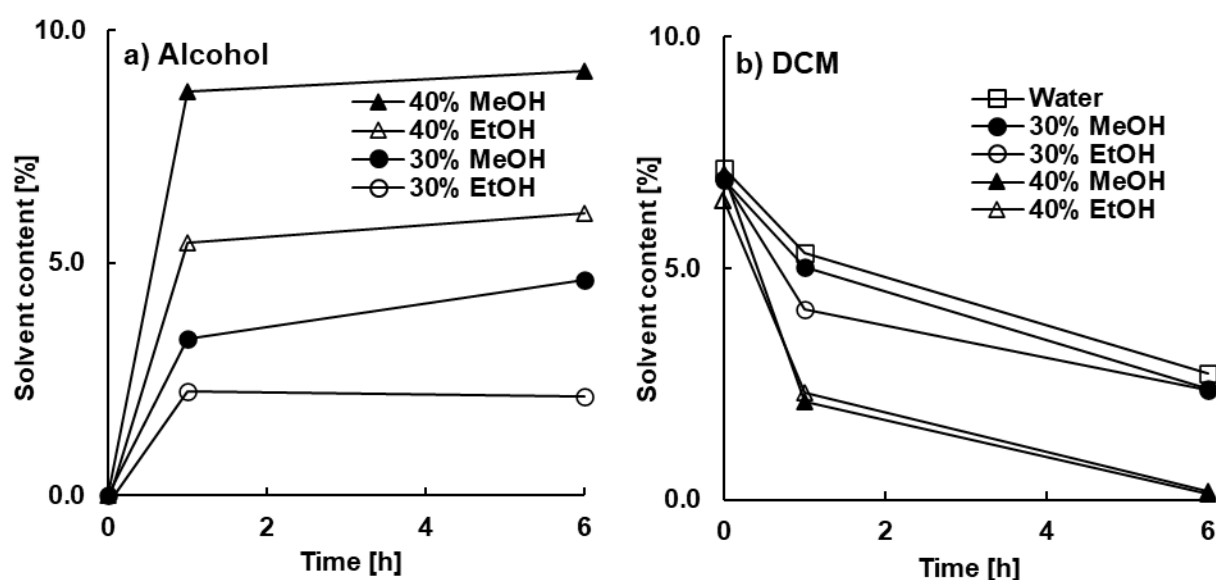


Figure 39: Effect of the type and amount of alcohol in the continuous phase on the content of (a) alcohol and (b) dichloromethane in microparticles (30 % theoretical risperidone loading)

The plasticizing effect of both alcohols was evident from visible changes of the microparticle surface (Figure 40). Extraction in both alcohols caused small dents, possibly due to the polymer skin collapsing because of underlying cavities. Additionally, ethanol resulted in a wrinkled surface, due to its greater plasticization effect. In contrast to dexamethasone, risperidone was mainly dissolved in the PLGA matrix, as observed under polarized light microscope. Only the molecularly dissolved fraction of encapsulated drug affected the mobility of polymeric chains and therefore the glass transition temperature, solubility and diffusivity [140,141]. Thus, risperidone was able to increase the affinity of dichloromethane and alcohols to PLGA.

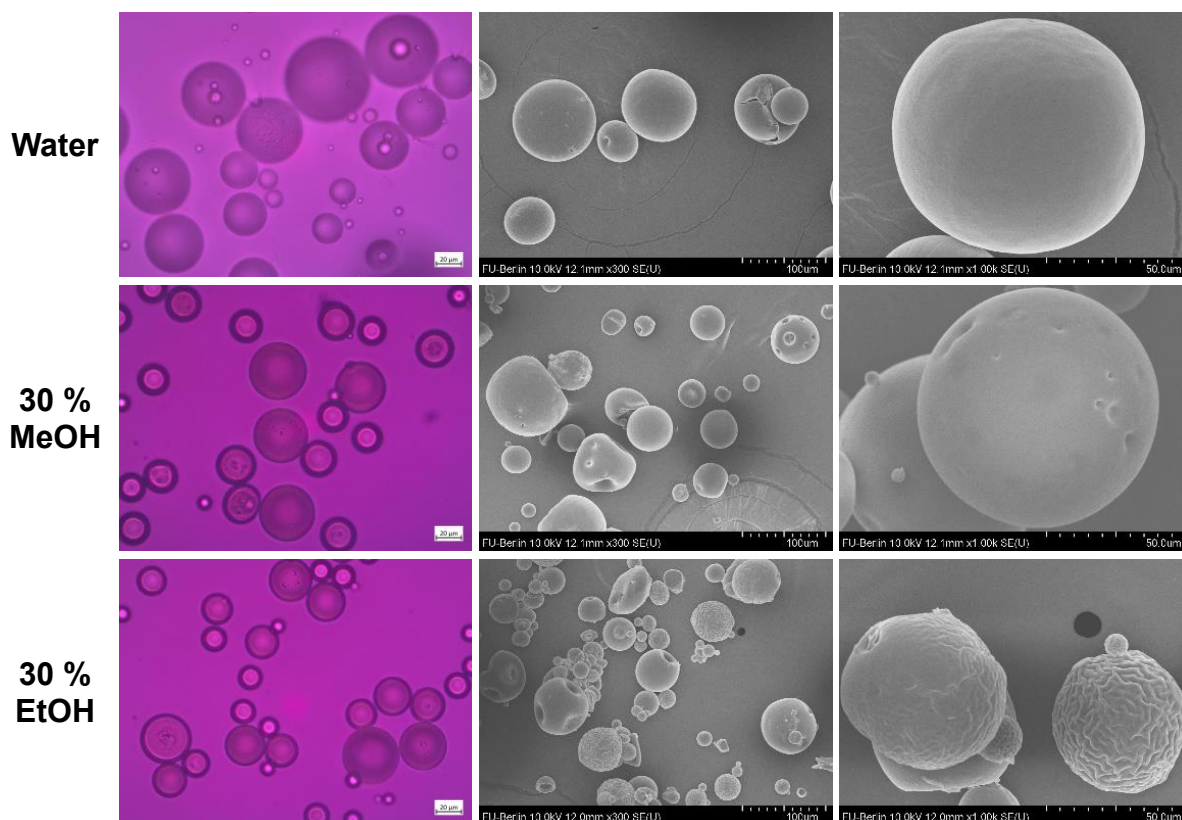


Figure 40: Effect of the type and amount of alcohol in the continuous phase on the appearance of microparticles (30 % theoretical risperidone loading) after 6 h extraction under polarized light microscope (left) and scanning electron microscope (mid and right)

Risperidone was barely extracted in 30 % (w/w) alcohol (Figure 41), although it was dissolved and therefore diffusible, due to its significantly higher affinity for PLGA ($R_a = 6.2$) and residual dichloromethane ($R_a = 3.3$) compared to methanol ($R_a = 16.6$) and ethanol ($R_a = 12.5$). Within 6 h, the encapsulation efficiency decreased only slightly from 92 % to 87 % or 85 % in 30 % (w/w) methanol or ethanol. Increasing the content of methanol or ethanol in the continuous phase to 40 % (w/w) reduced the residual dichloromethane content to below 0.2 % (w/w) after 6h (Figure 39b). However, the encapsulation efficiency was also reduced significantly to 36 % by methanol or to 72 % by ethanol and the microparticles stuck together due to the strong plasticizing effect.

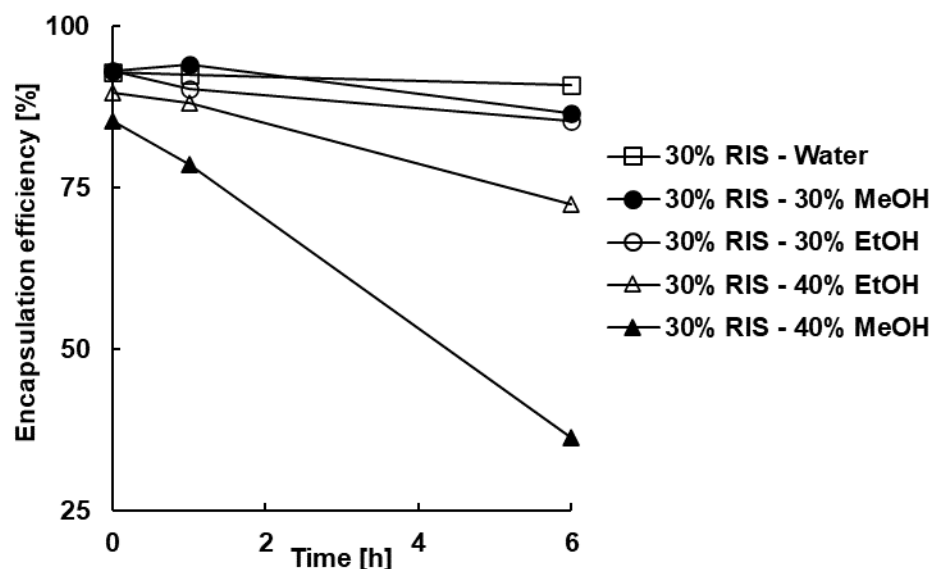


Figure 41: Effect of the type and amount of alcohol in the continuous phase on the encapsulation efficiency of 30 % risperidone

In summary, the final removal of residual dichloromethane from microparticles was investigated. The removal rate decreased with decreasing dichloromethane content due to the decreasing plasticizing effect. Microparticles of higher molecular weight or end-capped PLGA had a higher residual solvent content, due to the higher polymer-solvent affinity, viscosity and droplet/microparticle size. Removal of residual dichloromethane was most efficient with alcoholic wet extraction, followed by aqueous wet extraction and vacuum drying of the microparticles. The aqueous wet extraction was more efficient at 35 °C compared to 20 °C, but caused, depending on the PLGA grade, drug loss (752S), microparticle erosion (502H) and a change of the in-vitro release profile (502H, 503, 752S, 753S) even after a short time (3 h) at elevated temperature. Redispersing filtered, wet microparticles in alcoholic media significantly improved residual dichloromethane extraction due to the good plasticizing effect of alcohols. Short-chain monohydric alcohols decreased the glass transition temperature of PLGA more than polyhydric alcohols, water, or dichloromethane. Ethanol had the strongest plasticizing effect of all the tested (non-)solvents. As the chain length of the monohydric alcohols increased, the affinity for PLGA increased and thus the absorption and aggregation tendency of the microparticles. Extraction in methanol or ethanol:water mixtures efficiently decreased the residual dichloromethane content, but also caused drug loss.

3.3. Secondary drying in an alcohol vapor-assisted fluidized bed

As shown above, the final solvent removal from microparticles is challenging due to the decreasing diffusivity with decreasing residual solvent content. Increasing the process temperature or decreasing the glass transition temperature of the PLGA:solvent system with the plasticizing effect of alcohols or water improved the solvent removal, but also caused degradation of PLGA and loss of encapsulated drug. To prevent this and utilize the full potential of alcoholic extraction of residual solvents, an alcohol vapor-assisted fluidized bed drying process was developed for secondary drying of filtered microparticles.

Blank PLGA 503H microparticles with a high residual dichloromethane content of about 7 % (w/w) were dried at different temperatures in a fluidized bed. At ambient temperature (18 °C) the dichloromethane content decreased only to 6.4 % (w/w) within 24 h due to the low diffusivity in the glassy PLGA microparticle matrix. Increasing the temperature of the purge gas accelerated dichloromethane removal, especially within the first hours (Figure 42).

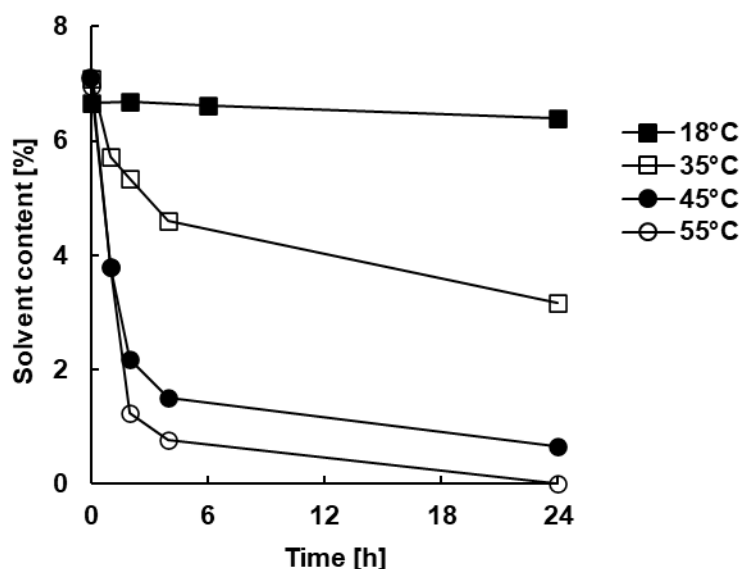


Figure 42: Effect of the purge gas temperature on the residual dichloromethane content of blank PLGA 503H microparticles during fluidized bed drying

As the residual dichloromethane content decreased, PLGA was less plasticized, and the removal rate decreased. A higher temperature resulted in a lower residual dichloromethane content, at which the removal rate decreased. At 45 °C, i.e. at the glass transition temperature of PLGA 503H ($T_G = 44 - 48$ °C), a residual

3.3. Secondary drying in an alcohol vapor-assisted fluidized bed

dichloromethane content of 0.7 % (w/w) was achieved after 24 h, but the microparticles had some dents (Figure 43). Only at 55 °C dichloromethane was removed completely within 24 h. However, the glass transition temperature of PLGA was significantly exceeded and microparticles aggregated.

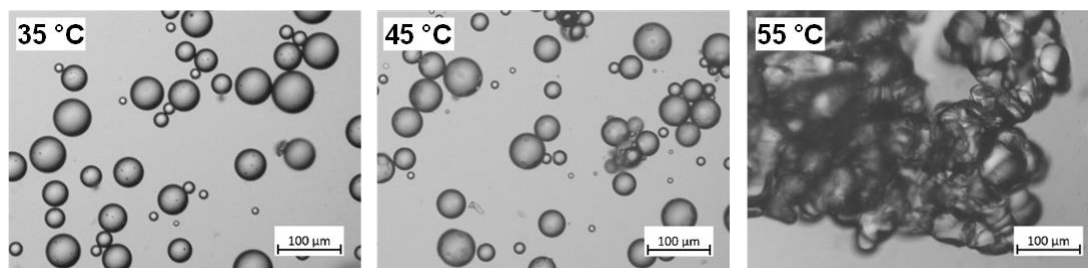


Figure 43: Effect of the purge gas temperature on the microscopic appearance of blank PLGA 503H microparticles during fluidized bed drying

Next, the purge gas was enriched with alcohol by passing it through a bubbler. After 6 h of alcohol vapor-assisted purge, the bubbler was bypassed and dry warm air (35 °C, 20 L/min) was used for another 18 h to remove the absorbed alcohol. The alcohol evaporation rate in the bubbler was increased by increasing bubbler temperature and purge flow rate (Table 7). Increasing the bubbler temperature from 10 °C to 16 °C at a constant flow rate of 10 L/min increased the evaporation rate of methanol from 998 mg/min to 1401 mg/min. Increasing the purge flow rate from 1 L/min to 30 L/min increased the evaporation rate of methanol from 157 mg/min to 3098 mg/min. Since the evaporation rate did not increase at the same rate as the flow rate, the calculated methanol concentration in the purge gas decreased from 157 mg/L to 103 mg/L. Ethanol evaporates more slowly than methanol under the same conditions due to its lower vapor pressure. To achieve a comparable concentration of around 100 mg/L in the purge gas, a bubbler temperature of 20 °C for ethanol was required compared to 10 °C for methanol. 20 °C was the limit at which condensation could still be avoided in the unheated setup downstream of the bubbler.

Table 7: Effect of the purge flow rate and bubbler temperature on the concentration of methanol and ethanol in the purge gas

Alcohol	Flow rate [L/min]	Temperature [°C]	Evaporation rate [mg/min]	Concentration in purge gas [mg/L]
MeOH	1	16	157	157
	10	16	1401	140
	20	16	2227	111
	30	16	3098	103
	10	10	998	100
EtOH	10	10	553	55
	10	16	829	83
	10	20	1010	101

The absorption of alcohol into the microparticles depended only on the type and concentration of the alcohol in the purge gas and not on the purge flow rate (Figure 44a). At an alcohol concentration of 100 mg/L, the microparticles absorbed 2.2 - 2.5 % (w/w) methanol, but only up to 1 % (w/w) ethanol. However, ethanol was as effective as methanol in removing dichloromethane, despite a lower absorption (Figure 44b). Ethanol has a lower glass transition temperature than methanol and therefore plasticized PLGA to a greater extent (Figure 34). Since the ethanol concentration could not be increased above 100 mg/L without condensation in the unheated setup, methanol was used for further experiments. Increasing the methanol absorption into the microparticles decreased the residual dichloromethane content (Figure 44b). At a concentration of 140 mg/L in the purge gas, about 4.2 % (w/w) methanol was absorbed and the residual dichloromethane content was reduced to 0.1 % (w/w) within 2 h and completely removed within 6 h.

Methanol and ethanol could be effectively removed at 35 °C under vacuum (data not shown) or in a fluidized bed (Figure 44a). The dichloromethane content was not affected by this alcohol-free drying (Figure 44b). Compared to dichloromethane, both alcohols had a lower affinity to PLGA and a higher molecular mobility within the free volume of the polymer, due to their lower molecular weight. In addition, higher residual alcohol contents in the final product are permitted compared to dichloromethane (Chapter 1.5.4).

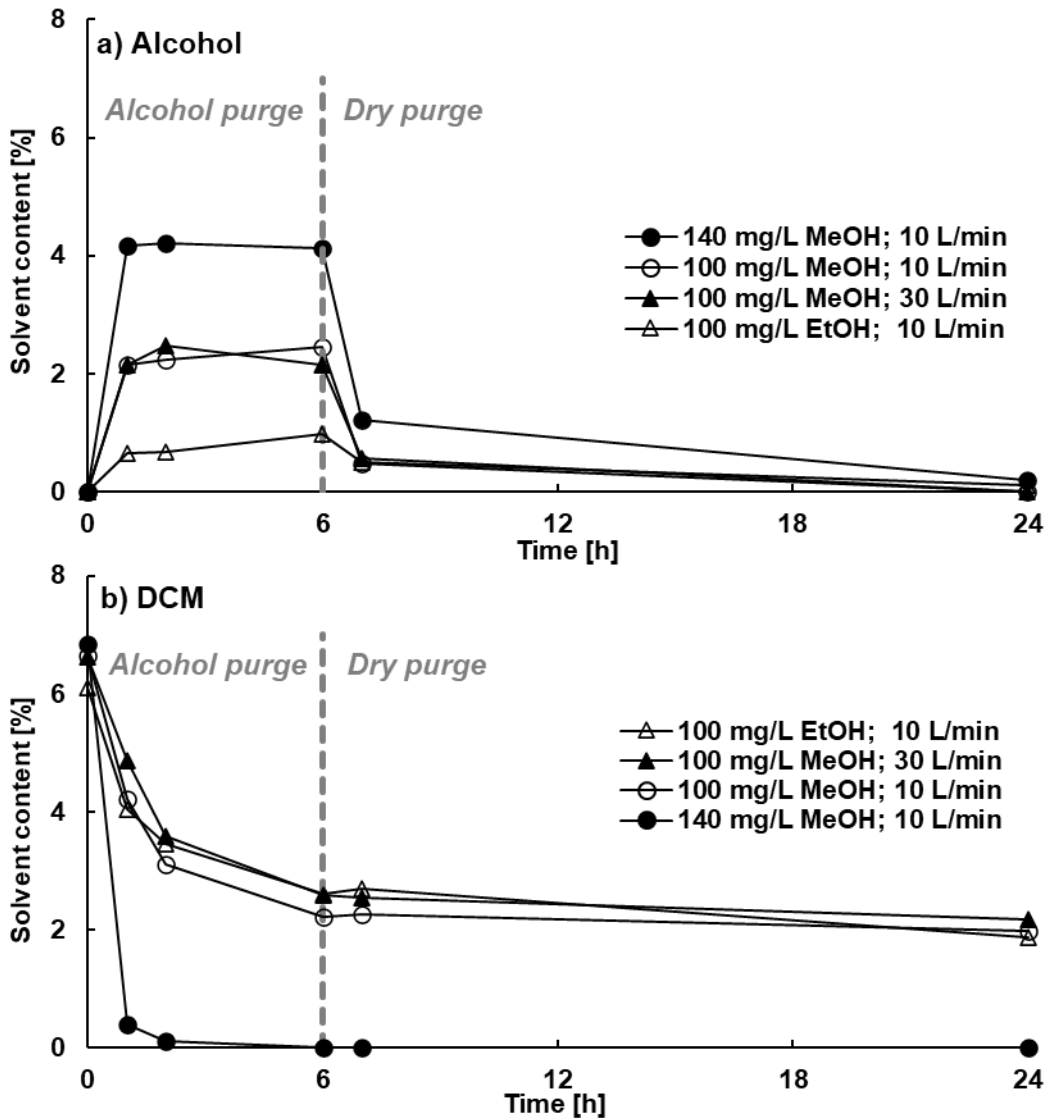


Figure 44: Effect of the alcohol concentration and flow rate during fluidized bed drying, on the content of (a) absorbed alcohol and (b) residual dichloromethane of blank 503H microparticles (6 h alcohol purge, followed by 18 h dry purge (20 L/min, 35 °C))

The use of alcohol vapor-assisted fluidized bed drying was not limited to the removal of dichloromethane. As proof of concept, PLGA microparticles were prepared with ethyl acetate as a common less toxic alternative to dichloromethane. To investigate the removal of residual ethyl acetate, the preparation method had to be adapted to obtain comparable microparticles [75]. Replacing dichloromethane by ethyl acetate without process modifications resulted in increased porosity and particle size (Figure 45).

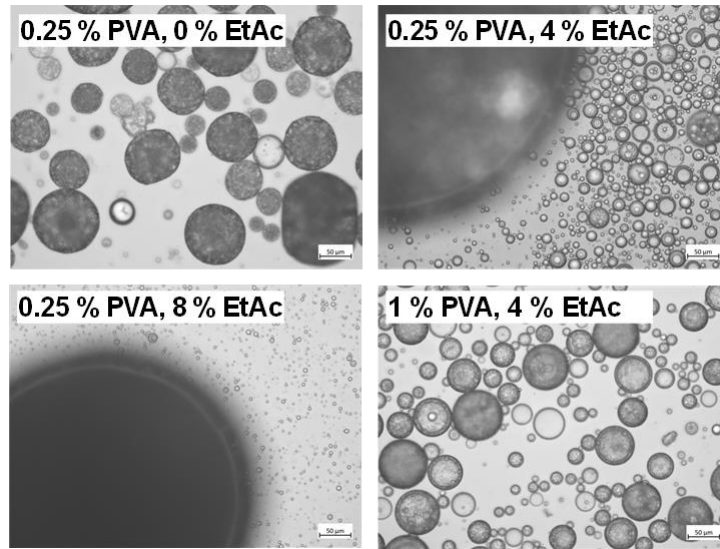


Figure 45: Effect of the stabilizer and ethyl acetate content in the continuous phase on the microscopic appearance of blank 503H microparticles

Since ethyl acetate has about eight times greater solubility in water, it was initially almost completely extracted. The addition of ethyl acetate to the continuous phase before emulsification to reduce the initial extraction significantly reduced the droplet size (Figure 46). After a short time, however, some very large drops were formed by coalescence, which led to a bimodal particle size distribution. Increasing the PVA concentration to 1 % (w/V) and decreasing the ethyl acetate content to 4 % (w/w) (= 50 % saturation) resulted in microscopic similar microparticles to those produced with dichloromethane.

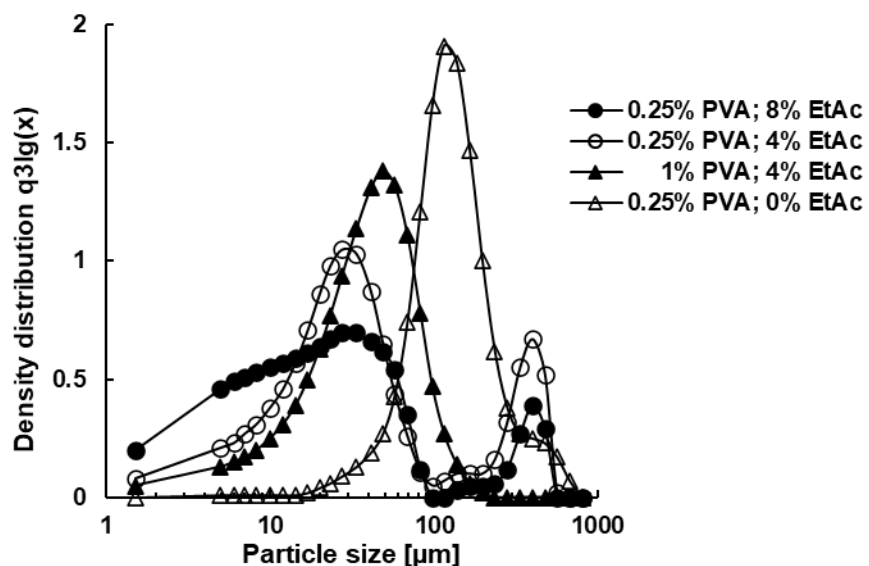


Figure 46: Effect of the stabilizer and ethyl acetate content in the continuous phase on the particle size distribution of blank 503H microparticles

3.3. Secondary drying in an alcohol vapor-assisted fluidized bed

The residual ethyl acetate content of 0.8 % (w/w) was lower compared to the residual dichloromethane contents obtained above because of a smaller particle size ($d_{50} = 38 \mu\text{m}$ instead of $61 \mu\text{m}$), a lower affinity of ethyl acetate for PLGA and a higher solubility in water. 6 h of methanol vapor-assisted fluidized bed drying at 100 mg/L reduced the residual ethyl acetate content to 0.4 % (w/w) and at 140 mg/L to 0.1 % (w/w) (Figure 47).

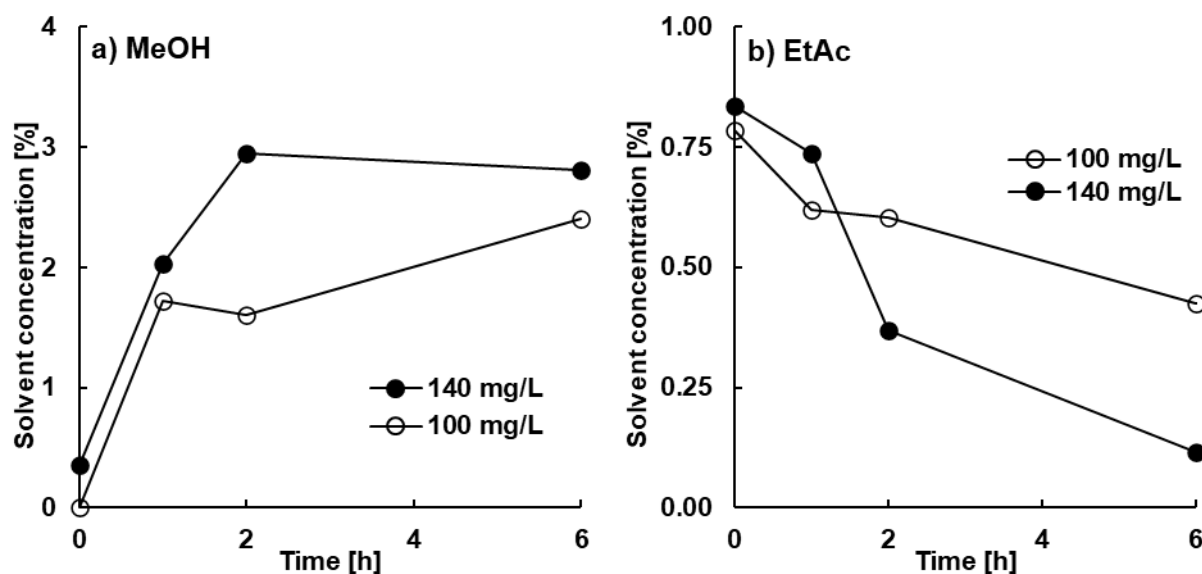


Figure 47: Effect of the methanol concentration in the purge gas during fluidized bed drying, on the content of (a) absorbed methanol and (b) residual ethyl acetate of blank PLGA 503H microparticles

100 mg/L methanol in the purge gas reduced the residual dichloromethane content of risperidone-loaded microparticles from 3.0 - 3.5 % (w/w) to below 0.06 % (w/w) within 6 h (Figure 48b). Microparticles prepared with the more lipophilic PLGA 753S absorbed slightly less methanol than those with 503H (Figure 48a).

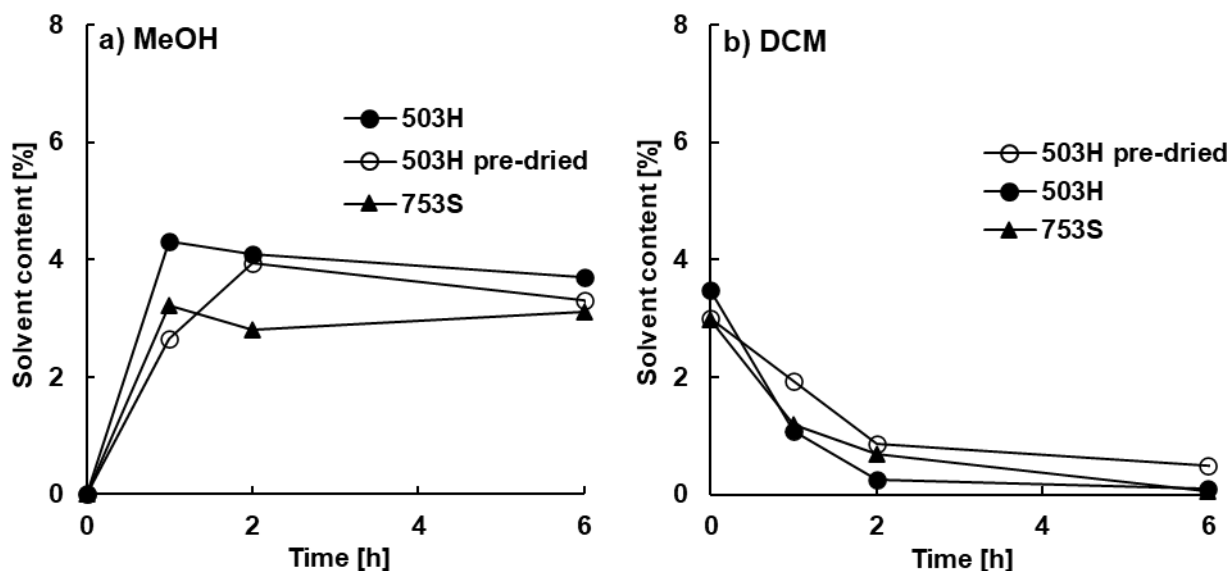


Figure 48: Effect of PLGA grade and pre-drying during fluidized bed drying (100 mg/L methanol; 10 L/min) on the content of (a) absorbed methanol and (b) residual dichloromethane of risperidone-loaded microparticles

While the 753S microparticles only formed a few agglomerates that could be easily separated again, the 503H microparticles partially aggregated and formed larger lumps (Figure 49).

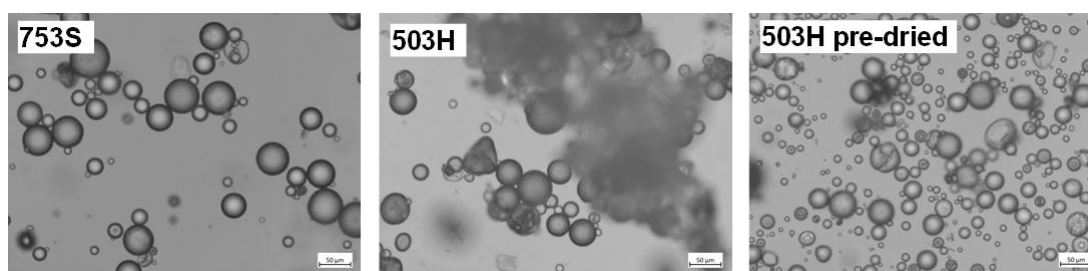


Figure 49: Effect of PLGA grade and pre-drying during fluidized bed drying (100 mg/L methanol; 10 L/min) on the microscopic appearance of risperidone-loaded microparticles

The glass transition temperature range of the two PLGA grades was approximately the same ($\approx 44 - 50$ °C) (Figure 50). Despite the good solubility of risperidone in the PLGA matrix, 30 % drug loading did not significantly reduce the glass transition temperature by plasticization. The pronounced sticking of risperidone-loaded 503H microparticles was probably due to the slightly increased content of residual solvent and absorbed methanol, possibly in interaction with risperidone.

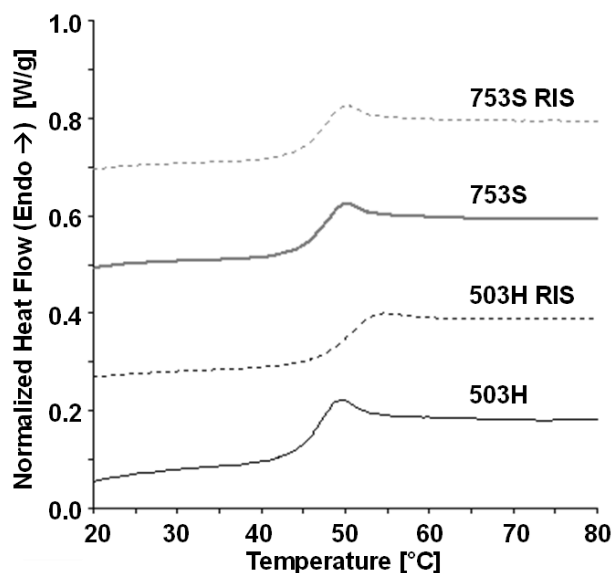


Figure 50: Effect of PLGA grade and 30 % risperidone loading on the DSC thermogram of microparticles

Sticking of microparticles could be prevented by completely removing water from the microparticles. Immediately after collection from the continuous phase, the risperidone-loaded microparticles had a high water content of about 35 % (w/w). Due to the low affinity of water to PLGA, it was assumed that this was mostly on the surface and in pores than dissolved in the polymer matrix. 5 min vacuum drying, performed before fluidized bed drying, reduced this content to about 25 % (w/w) and the first hour of methanol purge removed it completely. Increased initial water content led to an increased methanol absorption and thus aggregation. Water itself could have served as an additional plasticizer and therefore facilitated the absorption of methanol. Furthermore, methanol could have accumulated in water-filled pores and then diffused into the polymer.

An additional unheated dry purging step in the fluidized bed, prior to the methanol purge, reduced the water content to 1 % (w/w) within 30 min and to 0 % (w/w) within 60 min. Meanwhile residual dichloromethane was not removed. Complete water removal reduced the subsequent methanol uptake and the dichloromethane removal slightly (Figure 48) and prevented the aggregation of the microparticles (Figure 49).

The pre-dried risperidone-loaded microparticles could also be purged with 140 mg/L methanol without aggregating, which reduced residual dichloromethane content to 0.04 % (w/w) within 2 h (Figure 51b). The type of encapsulated drug affected both the

3.3. Secondary drying in an alcohol vapor-assisted fluidized bed

initial residual dichloromethane content and the amount of absorbed methanol. At 140 mg/L methanol in the purge gas microparticles with 30 % dexamethasone absorbed up to 3.2 % (w/w), without drug 4.2 % (w/w), and with risperidone (after pre-drying) 5.5 % (w/w) (Figure 51a).

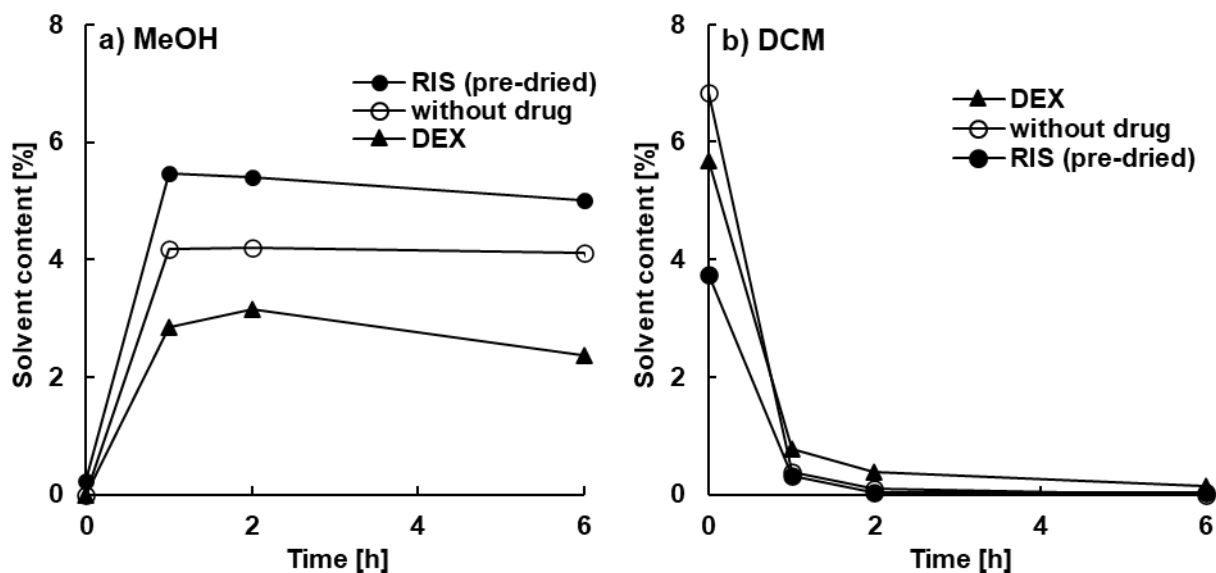


Figure 51: Effect of the drug loading during fluidized bed drying (140 mg/L methanol; 10 L/min) on the content of (a) absorbed methanol and (b) residual dichloromethane

Risperidone was molecularly dissolved in the PLGA matrix to a greater extent compared to dexamethasone and thus may have affected the affinity between the matrix and methanol and may itself act as a plasticizer. Dexamethasone had a very low solubility in PLGA and was present almost entirely in the form of dispersed crystals in the microparticles. Undissolved drug crystals absorbed probably neither dichloromethane nor alcohols but contributed to the mass of the microparticles and thereby reduced the calculated solvent contents. Furthermore, crystals may have acted as a diffusion barrier within the matrix. 140 mg/L methanol in the purge gas decreased the dichloromethane content of risperidone-loaded microparticles (after 1 h pre-drying) to 0.03 % (w/w) and of dexamethasone-loaded microparticles to 0.13 % (w/w) within 6 h (Figure 51b). Pre-drying was only necessary to prevent aggregation for risperidone-loaded microparticles. Despite pre-drying, risperidone-loaded microparticles had some dents (Figure 52). The surface morphology of dexamethasone-loaded microparticles was not altered.

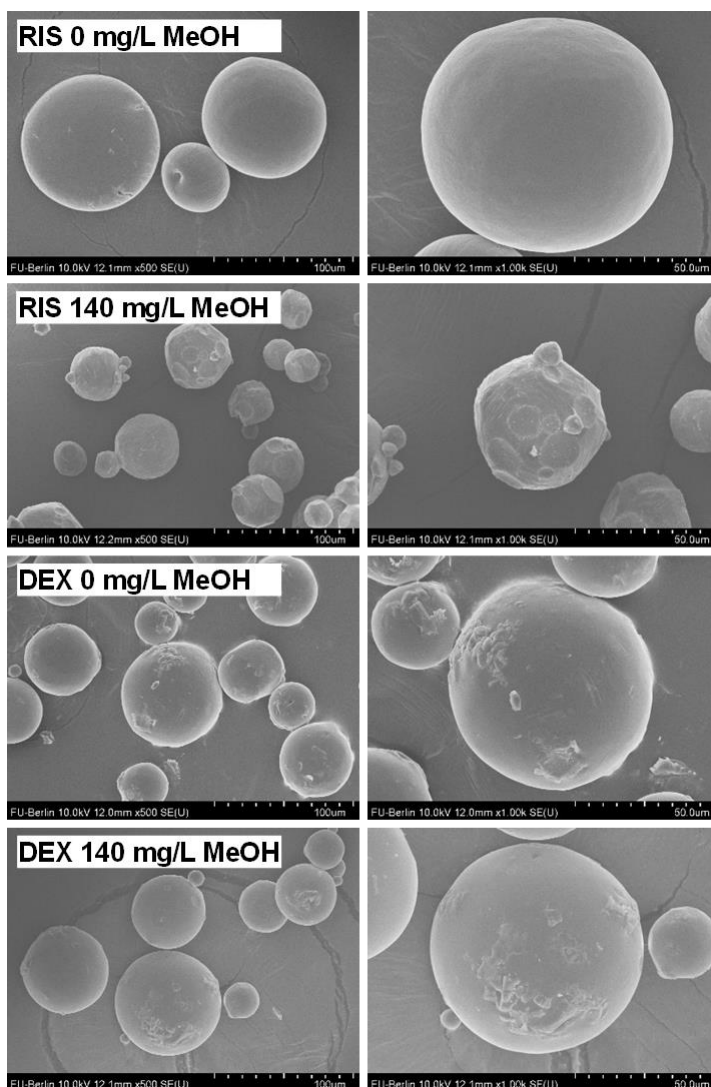


Figure 52: Effect of methanol vapor-assisted fluidized bed drying on the surface morphology of microparticles loaded with risperidone (1 h pre-dried) and dexamethasone

To investigate the potential effect of methanol vapor-assisted secondary drying on the recrystallization of drugs, PLGA films with a residual dichloromethane content of 8 - 10 % (w/w) were prepared. The films contained 2 % dexamethasone, or 10 % risperidone based on PLGA, which was slightly above each drug's solubility and dispersed crystals were observed. The films were purged with 1 L/min purge gas with different concentrations of methanol for 24 h. Alternatively, they were stored in a desiccator under an atmosphere saturated with methanol for 24 h. The absorbed methanol was finally removed by dry purging for a further 24 h. The appearance of dexamethasone-loaded films did not change compared to those dried exclusively under the hood even if they had absorbed 8 % (w/w) methanol. A pronounced

3.3. Secondary drying in an alcohol vapor-assisted fluidized bed

recrystallization of risperidone was observed even at a low methanol absorption of 2.6 % (w/w) achieved at 100 mg/L in the purge gas (Figure 53). Risperidone crystals grew needle-like from the edge of circular crystal spots into the PLGA, especially when absorbed methanol was removed again from the films. Both drugs have a similar solubility of 25 mg/L (dexamethasone) and 27 mg/L (risperidone) in pure methanol, resulting in similar improvements in solubility of these drugs in PLGA. Risperidone inherently had a higher solubility and diffusivity in PLGA and was initially dissolved in the dichloromethane:PLGA mixture, in contrast to dexamethasone.



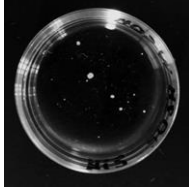
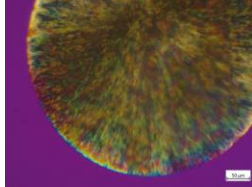

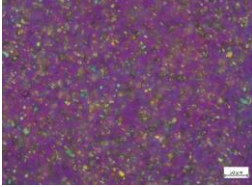
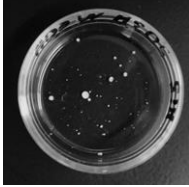
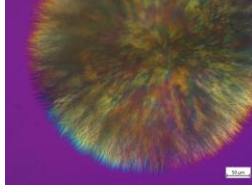

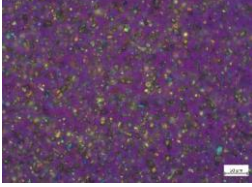
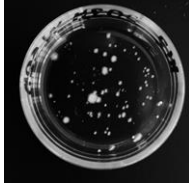


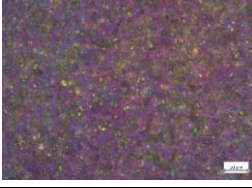
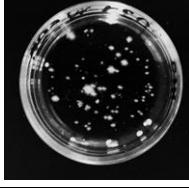

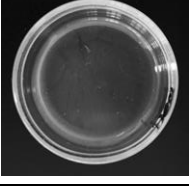
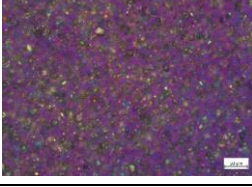
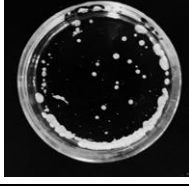
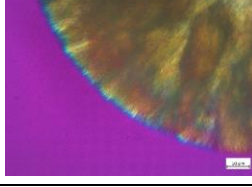
Drying condition	2 % Dexamethasone		10 % Risperidone	
	Macroscopic	Microscopic	Macroscopic	Microscopic
24h Hood				
24h Hood +6h MeOH				
24h Hood +24h MeOH				
24h Hood +24h MeOH +24h Hood				
72h Hood				

Figure 53: Effect of methanol vapor-assisted purge flow drying (100 mg/L; 1L/min) on the recrystallization of 2 % dexamethasone and 10 % risperidone in PLGA 503H films

3.3. Secondary drying in an alcohol vapor-assisted fluidized bed

An increasing content of methanol in the purge gas increased methanol absorption and recrystallization of risperidone (Figure 54), due to temporally higher solubility and diffusivity in the matrix. In 753S films, an increased number of risperidone crystal spots were observed covering a large area of the film, indicating a slightly lower solubility within this higher lactide content PLGA grade. The edges of the crystal spots were only slightly frayed due to weak recrystallization by methanol absorption and removal.

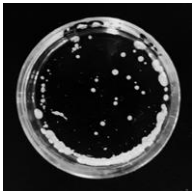
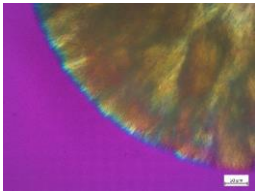
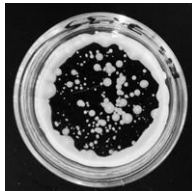
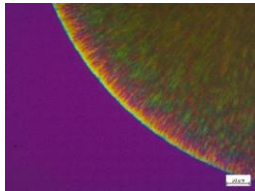
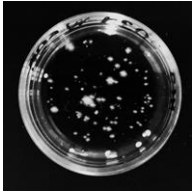
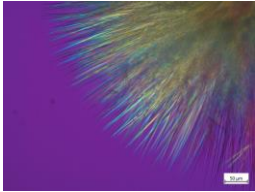
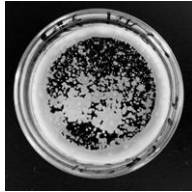
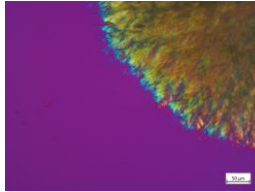
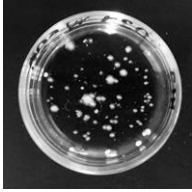
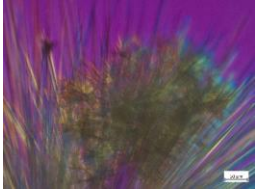
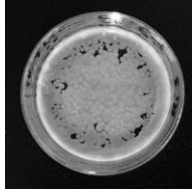
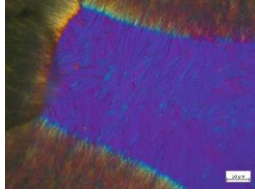
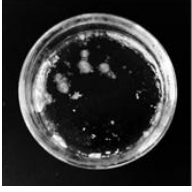
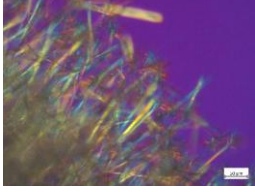

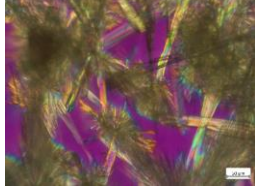
Methanol		PLGA 503H		PLGA 753S	
Gas [mg/L]	Films [mg/g]	Macroscopic	Microscopic	Macroscopic	Microscopic
0	0				
100	26				
170	57				
Sat.	80				

Figure 54: Effect of the methanol concentration in the purge gas on the methanol absorption and recrystallization of 10 % risperidone in PLGA 503H and 753S films

An increased methanol absorption caused a uniform precipitation of risperidone in crystal-free PLGA areas during methanol removal. Such a formation of new interfaces by precipitation is considered thermodynamically unfavorable. In 503H, risperidone precipitated only at pre-existing crystalline surfaces, when its solubility was decreased. There was no evidence that methanol was removed faster from 753S. Release studies indicated that risperidone had lower diffusivity in 753S (Figure 55). It was assumed that

3.3. Secondary drying in an alcohol vapor-assisted fluidized bed

the risperidone molecules in 753S were too slow to diffuse to existing crystalline interfaces when the solubility was decreased, due to the methanol removal. Recrystallization by methanol vapor-assisted secondary drying was identified as a potential risk for drugs that have inherently a good solubility and diffusivity in the PLGA grade used or whose solubility is greatly enhanced by methanol. This did not affect the investigated PLGA microparticles, because low methanol concentrations of 100 - 140 mg/L in the purge gas and short process times of a maximum of 6 h were sufficient for dichloromethane removal. Accordingly, the in-vitro release of risperidone and dexamethasone from microparticles was not changed by methanol vapor-assisted fluidized bed drying (Figure 55).

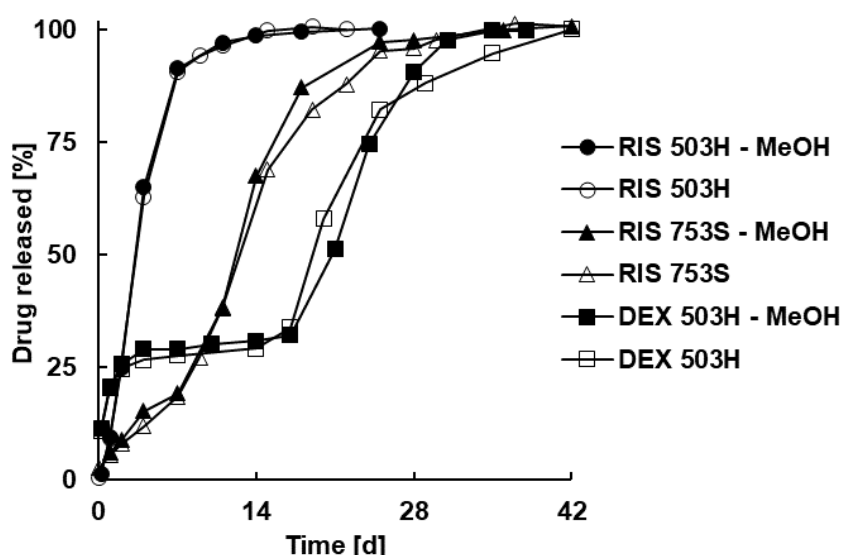


Figure 55: Effect of methanol assisted fluidized bed drying (6 h 140 mg/L 10 L/min + 18 h 0 mg/L 20 L/min 35 °C) on the in-vitro release of risperidone and dexamethasone from PLGA 503H and 753S microparticles compared to vacuum drying at 35 °C

In summary, the secondary drying of PLGA microparticles in a fluidized bed was investigated. The residual dichloromethane content was only slowly decreased under ambient conditions (from about 7 to 6.4 % (w/w) within 24 h), the solvent removal was improved by increasing the temperature up to 45 °C (0.7 % (w/w) after 24 h) and even more by 100 - 140 mg/mL alcohol vapor in the purge gas (0 - 0.11 % (w/w) after 6 h). By regulating the alcohol concentration and temperature of the purge gas, the alcohol absorption and the removal of residual solvent and alcohol were controlled. Methanol proved to be most effective in the present setup because its concentration could be adjusted over a wide range. The secondary drying was accelerated without affecting drug loading or in-vitro release of the encapsulated dexamethasone and risperidone.

3.4. Microfluidic microparticle preparation

Above, various aspects of the microparticle preparation by the solvent extraction/evaporation method were examined, particularly regarding the solvent removal. The initially necessary emulsification was carried out in a batch process by stirring. This step was replaced by a continuous microfluidic flow focusing process. Microfluidic offered precise control over droplet size and enabled the preparation of monodisperse microparticles, when operated in the so-called dripping regime (Chapter 1.4.2). Compared to the batch process, much smaller phase ratios are usually required for this. The influence of this peculiarity on solvent removal and drug encapsulation was examined in Chapter 3.4.1. The final microparticles were compared with those of the batch experiments in Chapter 3.4.2 and a process for continuous solvent removal was developed in Chapter 3.4.3.

3.4.1. Drug encapsulation in microfluidic microparticle preparation

Within the dripping regime, increasing the ratio of flow rates of continuous and dispersed phase decreased the size of monodisperse droplets (Table 8). The droplet size and the resulting shrunk solidified microparticles were not affected by increasing the theoretical risperidone loading from 10 to 30 %. Increasing the PVA concentration to 2 % (w/w) increased the viscosity of the continuous phase and decreased the interfacial tension. Due to the speed of droplet formation, no significant influence of the latter on droplet formation was expected, since the stabilizer molecules would first have to diffuse to the interface [80].

Table 8: Effect of PVA concentration and flow rate of the continuous phase (Q_{CP}) during microfluidic flow-focusing with a constant flow rate of the dispersed phase of 70 $\mu\text{L}/\text{min}$ on the particle size and the encapsulation efficiency (EE) of 10 % and 30 % risperidone in 503H

PVA concentration [%]	Q_{CP} [$\mu\text{L}/\text{min}$]	Particle size [μm]	EE [%]	
			TL 10 %	TL 30 %
1	140	45	50	21
1	490	32	37	19
2	560	80	62	-

Due to the increased viscosity and a further increase in the flow rate ratio to 1:8, droplets with a diameter significantly larger than the junction could also be produced in the present chip geometry (Figure 56). The reason for this was that due to the high flow rate the dispersed phase thread was pulled into the junction orifice and only then broke off, not as usual just before or in it.

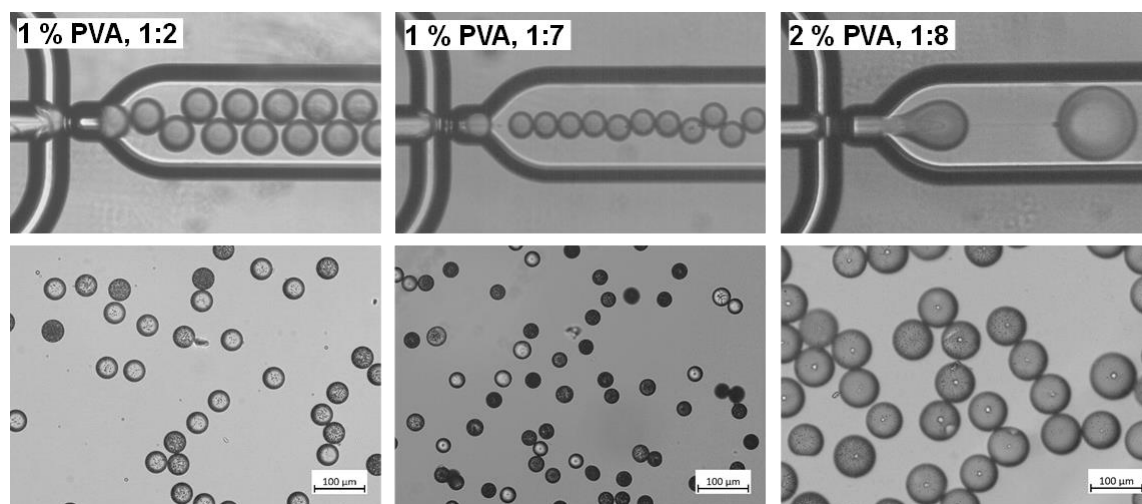


Figure 56: Effect of PVA concentration and flow rate ratio during microfluidic flow focusing on the microscopic appearance of droplet formation on the chip (top) and resulting solidified risperidone-loaded 503H microparticles (bottom)

The encapsulation efficiency of risperidone decreased with decreasing particle size and increasing theoretical drug loading (Table 8). Compared to microparticles produced by the batch process, the encapsulation efficiency was low. The droplets were solidified in a one-step dilution into microparticles by introducing them into 100 mL of continuous phase downstream of the chip. However, the tubing (inner diameter: 0.8 mm; length: 500 mm) between the chip and the solidification bath resulted in a solidification delay of 1.5 - 5 min depending on the total flow rate. Due to the small phase ratio, only a small amount of dichloromethane was extracted during this transfer passage. Risperidone was extracted by diffusion since the viscosity of the dispersed phase was not significantly increased. This was limited by the drug solubility in the continuous phase, which was increased by saturation with dichloromethane. In addition, an increasing diffusion distance slowed diffusion with increasing droplet size. An increase in the total flow rate reduced the solidification delay and thus the time available for diffusion.

Various modifications of the dispersed and continuous phases were investigated in the batch process to control solvent extraction and to improve the encapsulation efficiency (Chapter 3.1). The phase ratio of 1:20 was significantly larger than the one usually used in microfluidic flow focusing, but it was also not sufficient to completely dissolve dichloromethane. In summary, without dilution, the buffering of the continuous phase to an alkaline pH increased the encapsulation efficiency the most. Since only small phase ratios of usually 1:1 - 1:10 are used for droplet generation with microfluidic flow focusing, alkaline buffering for microfluidic encapsulation was also investigated. Increasing the pH of the continuous phase caused a change in the droplet formation regime, from dripping to jetting and led to the formation of large droplets (Figure 57).

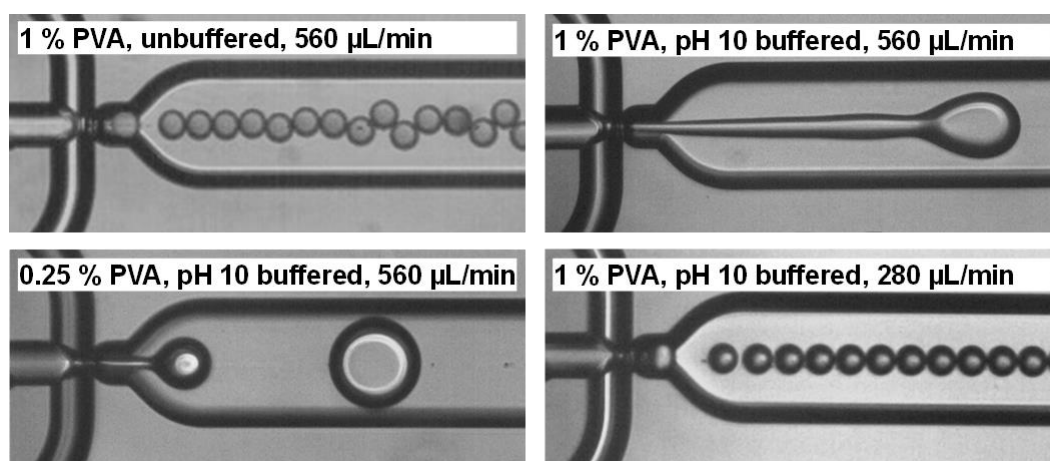


Figure 57: Effect of the composition of the continuous phase and total flow rate (phase ratio 1:7) on the microscopic appearance of microfluidic droplet formation

This transition of droplet formation regime was usually observed, if the capillary number Ca was ≥ 1 [80,82]. Since the flow rates were kept constant, such an increase could only be caused by an increase in viscosity or a decrease in interfacial tension (Equation 5). A pH-dependent change in viscosity, as described in the literature, was not observed at the low PVA concentration used. At a shear rate of $10 - 100 \text{ s}^{-1}$, the average viscosity of 1 % (w/V) PVA solution was $1.24 (\pm 0.01) \text{ mPas}$ regardless of buffering. The surface tension of the continuous phase increased slightly from 45 mN/m to 49 mN/m by increasing the pH. For droplet formation, however, the interfacial tension between both phases would be more important. An increase in pH of continuous phase probably led to dissociation of some PLGA carboxyl groups. The resulting negative charge caused a more hydrophilic surface of the PLGA phase and

reduced the interfacial tension to the continuous aqueous phase [183], causing an increase of the capillary number and a change of the droplet formation regime.

Reducing the PVA concentration to 0.25 % (w/V) was not enough to achieve the dripping regime, but shortened the jet length, due to a decrease in viscosity and an increase in interfacial tension. The stabilizer could not be completely omitted in order to avoid coalescence after the droplet formation. The reduction of the total flow rate (at a constant flow rate ratio of 1:7) enabled the preparation of monodisperse droplets with a particle size comparable to the droplet particle size without buffer in the dripping regime. Buffering the continuous phase and halving the total flow rate together led to a slight increase in particle size from 32 μm to 40 μm and a significant increase in the encapsulation efficiency at a 30 % theoretical risperidone loading from 19 to 93 %.

Using PLGA 753S instead of 503H did not change the particle size as both have approximately the same molecular weight and viscosity (Table 9). The encapsulation efficiency of risperidone was slightly lower for 753S than for 503H, consistent with the results of the classical batch process due to the slower solidification of 753S (Chapter 3.1.2). Adjusting the phase ratio to 1:1 or 1:10 at a constant flow rate of the dispersed phase of 35 $\mu\text{L}/\text{min}$ led to a particle size of 38 μm or 58 μm (Figure 58). The encapsulation efficiency was not affected by size due to the low solubility of risperidone in the alkaline-buffered continuous phase (Table 9).

Table 9: Effect of PLGA grade and flow rate of the continuous phase (pH 10 buffered 1 % (w/V) PVA) (Q_{CP}) in microfluidic flow focusing with a constant flow rate of dispersed phase of 35 $\mu\text{L}/\text{min}$ on the particle size and encapsulation efficiency (EE) of microparticles with 30 % theoretical risperidone loading

PLGA grade	Q_{CP} [$\mu\text{L}/\text{min}$]	Particle size [μm]	EE [%]
503H	245	40	93
753S	35	58	82
753S	245	40	83
753S	350	38	83

3.4.2. Comparison of microparticles prepared by microfluidic flow focusing and the classical batch process

Microparticles with a comparable d_{50} of 34 μm or 53 μm were produced by a batch process (including a one-step dilution after 15 min) with a stirring speed of 800 RPM and 1800 RPM (Figure 58 and 59). The particle size distributions were narrowed to the fractions 20 - 50 μm and 50 - 80 μm by wet sieving, these fractions were further investigated. The encapsulation efficiency of 30 % risperidone was 84 % and 87 % and thus only slightly higher compared to microfluidic flow focusing.

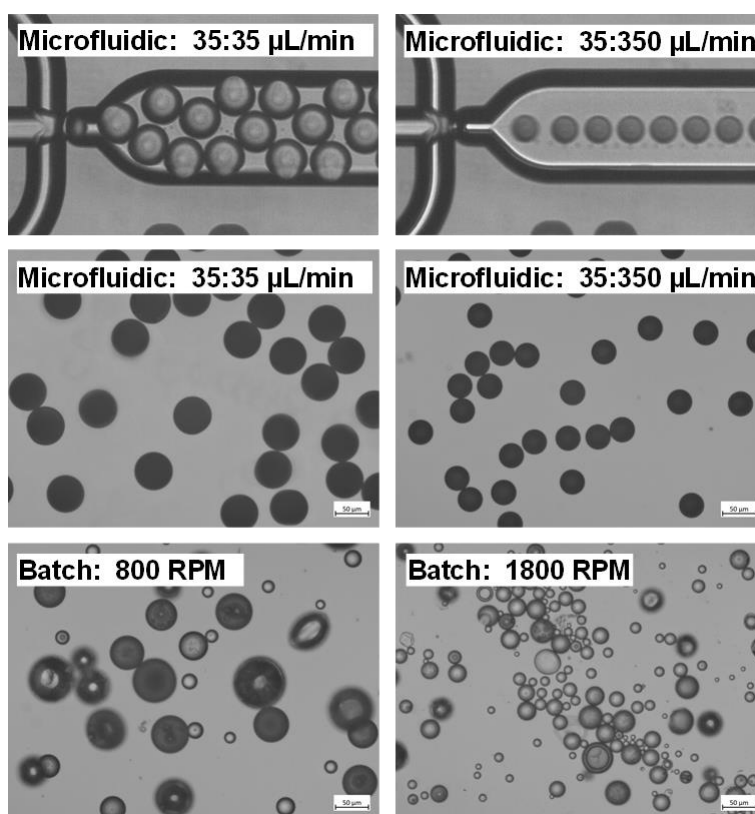


Figure 58: Effect of the flow rate ratio during microfluidic flow focusing on the microscopic appearance of droplet formation on chip (top) and resulting solidified microparticles (middle) and microparticles of comparable size produced by the batch process (bottom)

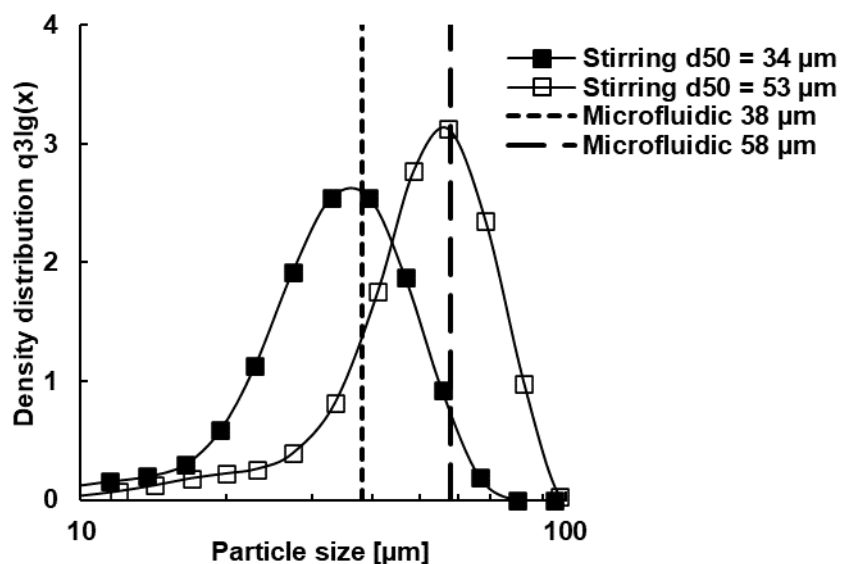


Figure 59: Comparison of the monodisperse particle size of microparticles prepared by microfluidic flow focusing (determined by microscopic size determination) and particle size distribution of comparable microparticles prepared by the batch process (determined by laser diffraction)

Both size fractions of microparticles prepared by the batch process released risperidone faster than microparticles prepared by microfluidic flow focusing (Figure 60). When comparing microparticles produced by the same method, an increase in size resulted in a decreased release in the first 7 days. Increased surface area and decreased diffusion pathways increased the release rate.

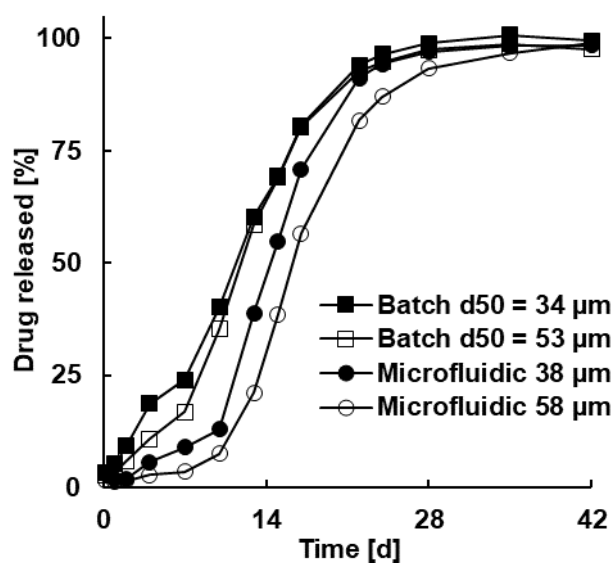


Figure 60: Effect of the particle size and manufacturing process on the in-vitro release of risperidone from 753S microparticles

In general, the fine fraction usually present in the batch could cause an increased burst and subsequent diffusional release [184]. However, especially the microparticles prepared by the batch process with $d_{50} = 53 \mu\text{m}$ contained only few small microparticles due to wet sieving and even these microparticles were released faster than those produced by microfluidic with a small particle size of only $38 \mu\text{m}$. The reason was probably a more homogeneous distribution of risperidone in the microparticles produced by microfluidic flow focusing. A higher content of drug close to the surface of microparticles, prepared by the batch process, may have increased burst and diffusional release [185].

3.4.3. Continuous solvent removal

Slow solidification of emulsion droplets into microparticles, due to a small phase ratio, was identified as a risk for high encapsulation efficiency (Chapter 3.1). Since the phase ratio during microfluidic flow focusing determined the droplet formation regime and the size of the droplets (Figure 56), a continuous dilution downstream of the microfluidic chip was investigated. $95 \mu\text{m}$ large droplets of 10 % 503H in dichloromethane were generated with a flow rate ratio of $70 \mu\text{L}/\text{min}$ dispersed phase to $140 \mu\text{L}/\text{min}$ continuous phase. The emulsion was continuously diluted downstream the microfluidic chip with water at flow rates of 3.5, 7, 14 or $35 \text{ ml}/\text{min}$ to increase the phase ratio from 1:2 to about 1:50, 1:100, 1:200 or 1:500 and thus enable fast extraction of dichloromethane. The liquid flow was then passed through a 150 or 450 cm long lag tube with an inner diameter of 1.6 mm, at the end of which was a planar flow cell in which microscopic images were taken. With this set-up, the shrinkage of the microparticles was evaluated. The diameter was reduced from 95 to $45 \mu\text{m}$, when the microparticles solidified completely due to subsequent solvent evaporation, independent of dilution (Figure 61).

With a short lag tubing of 150 cm, the droplet size decreased with increasing dilution until the final particle size was almost reached at a phase ratio of 1:200. Increasing the dilution further increased the droplet size again after 150 cm lag tubing. Due to the increased volume flow, the time available for extraction in the lag tubing decreased to approximately 5 s. Therefore, the extraction of dichloromethane was not sufficient for complete shrinkage, despite the increased dissolution capacity for dichloromethane in the continuous phase.

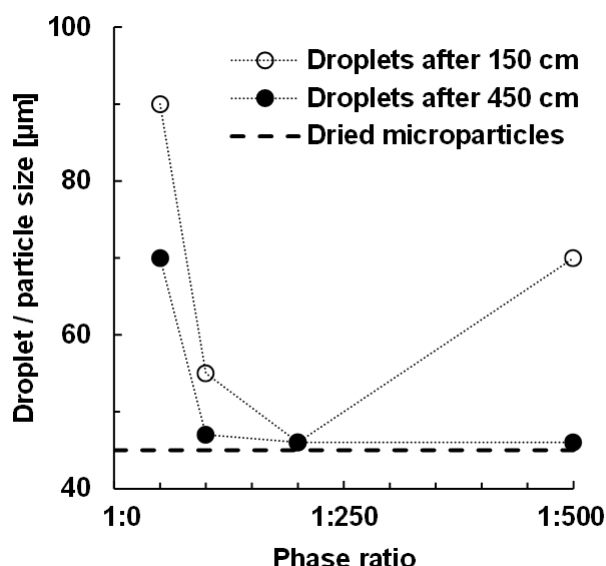


Figure 61: Effect of the phase ratio after dilution on the particle size of droplets after 150 cm or 450 cm lag tubing and of solidified microparticles

Increasing the diameter of the lag tubing would significantly increase the extraction time but would also increase the risk for accumulation of droplets and particles and thus favor coalescence or sticking. By extending the lag tubing, flow velocities and a certain distance between the droplets were maintained. The extension of the lag tubing to 450 cm resulted in almost complete shrinkage at a phase ratio of 1:100 – 1:500 due to the extended time available for extraction. Despite the apparently complete shrinkage, the microparticles still contained about 15 % (w/w) residual dichloromethane and were therefore still soft, deformable, and sticky. The increasing viscosity of the dispersed phase decreased the extraction rate already before complete solidification [97,120].

The addition of methanol to the continuous phase increased the shrinkage after 150 cm (Figure 62), due to an increased solubility of dichloromethane in the continuous phase and an increased extraction rate (Chapter 3.2.2).

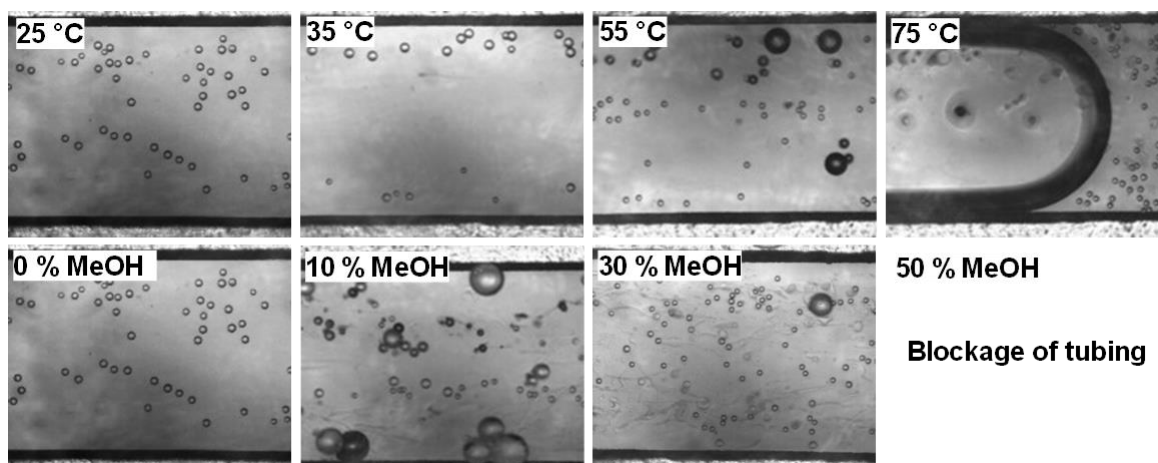


Figure 62: Effect of temperature (top) and methanol content (bottom) of the continuous phase on the microscopic appearance of droplets (generated by microfluidic flow focusing and subsequent 1:100 dilution) in a flow-cell after 150 cm lag tubing

However, with increasing methanol content, the tendency for the microparticles to stick to the tubing and flow cell walls increased. This endangered the process stability over the running time. As soon as some microparticles get stuck in the tubing, more and more adhere to them. With 50 % (w/w) methanol in the continuous phase, the tubing was completely blocked within seconds. Increasing the temperature also increased the shrinkage. From 55 °C on, i.e. well above the boiling point of dichloromethane of 40 °C, gas bubbles were formed. These disrupted the uniform flow and caused microparticle sticking to the tubing walls and to each other.

Elevated temperature and methanol in the continuous phase improved dichloromethane extraction but impaired process stability. To circumvent this and to reduce the residual solvent content further, the setup was adapted by installing a tangential flow filtration (TFF) module equipped with a 10 µm steel filter before the flow cell to concentrate the suspension and remove the majority of DCM (Figure 6). The removal of the filtrate was controlled with a peristaltic pump downstream of the filtrate outlet. Downstream of the flow cell, the suspension could be subsequently diluted again, if necessary, with heated or methanolic extractant. Continuous removal of the continuous phase with a commercial TFF unit (Vivaflow 200, Sartorius Lab Instruments GmbH & Co. KG, Goettingen, Germany) equipped with a 10 µm steel filter was not successful due to the obstructed flow path, large cross-section and limited solvent resistance (Figure 63a). Microparticles settled on walls and especially in corners at low flow rates or clogged the filter when they were still sticky due to the high residual

solvent content. A solvent resistant setup with a U-shaped flow path, small cross-section and a 10 μm steel sieve was prototyped (Figure 63b). Additional cooling of the continuous phase, which was added in the 1:100 dilution downstream of the microfluidic chip, to 10 $^{\circ}\text{C}$ prevented clogging of this setup completely. The residual dichloromethane content of the microparticles was reduced to 10 % (w/w) due to the improved dichloromethane solubility in water at lower temperature. For a further reduction of residual dichloromethane content, a lengthening of the extraction tubing and the combination of several TFF units might be advantageous.

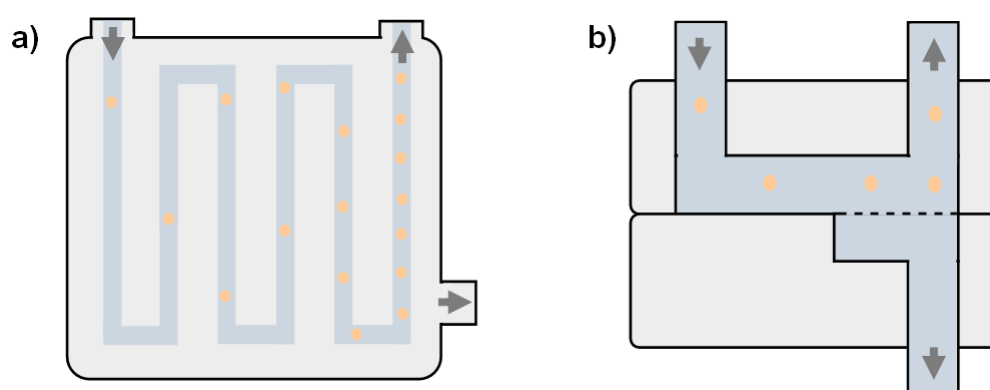


Figure 63: Comparison of the schematic design of (a) a commercial multi-angled tangential flow filtration with large cross-section that cause particle deposition and (b) self-built U-shaped tangential flow filtration device with small cross-section to maintain higher flow

In summary, a continuous process for the preparation of monodisperse microparticles with microfluidic flow focusing was investigated. For methodological reasons, smaller O/W phase ratios were used compared to the batch process. The limited initial solvent extraction and slower solidification of the dispersed phase led to a low risperidone encapsulation efficiency. Alkaline buffering of the continuous phase increased risperidone encapsulation, but also changed the droplet formation regime and thus microparticle size. This could be counteracted by reducing the overall flow rate. The in-vitro release of risperidone was delayed from microparticles produced by microfluidic compared to similarly sized polydisperse microparticles prepared by the batch process. Since the fine particle fraction was eliminated by sieving, a more homogeneous drug distribution within the microfluidically produced microparticles was probably the reason for an initially slower release. To improve solvent extraction, a

continuous downstream dilution process was developed. A phase ratio of at least 1:100 after dilution and a sufficiently long extraction time were necessary for complete shrinking of the droplets. Increasing the temperature or adding methanol to the continuous phase improved the dichloromethane extraction but also affected the process stability. A TFF process was developed to separate the dichloromethane-enriched continuous phase from the dispersed phase.

4. Summary

Biodegradable poly(lactide-co-glycolide) (PLGA) microparticles enable the controlled parenteral administration of drugs. Commonly used microencapsulation methods require the dissolution of PLGA in organic solvents. The removal of these solvents during the manufacturing process is essential to obtain solid microparticles. In addition, a low residual solvent content must be achieved in the final product to ensure storage stability and patient safety. In this dissertation the solvent removal during the preparation of microparticles with the O/W solvent extraction/evaporation method was investigated. In this method, an organic (O) phase containing drug, PLGA and organic solvent (dichloromethane or ethyl acetate) was emulsified in an aqueous polyvinyl alcohol solution (W) by a classical batch process or by microfluidic flow focusing. The effect of various formulation and process parameters was investigated in order to optimize the properties of PLGA microparticles with regard to minimal residual solvent levels at high drug loadings and encapsulation efficiencies and optimal drug release profiles.

The initial removal of organic solvent had a great effect on the properties of the microparticles and is usually controlled by two steps, the solvent dissolving in the continuous aqueous phase and the solvent evaporation rate. One-step dilution and continuous diafiltration were investigated to control the initial solvent extraction. The latter replaced the normally required large-volume manufacturing equipment and the O/W emulsion transfer. Accelerated extraction of the PLGA solvent dichloromethane shortened the process time until the microparticles were solidified and thus collectable. Increasing the diafiltration rate increased the particle size, porosity and drug loading of the microparticles. The encapsulation efficiency of risperidone was significantly increased from 62 % to up to 80 % in PLGA 503H microparticles and from 27 % to up to 75 % in PLGA 753S microparticles. A slower and more uniform solidification of the end-capped and higher lactide content PLGA 753S was identified as the reason for the increased drug loss without diafiltration. The residual dichloromethane content was not affected by diafiltration, but decreased by increasing the temperature, because the final solvent removal was limited by the diffusivity within the PLGA phase. Accelerated solvent extraction by diafiltration did not affect the in-vitro release of risperidone from both PLGA 503H and PLGA 753S microparticles. The effect of diafiltration on the extent of dexamethasone burst release depended on the drug loading. Increased porosity enhanced percolation if a large amount of undissolved drug crystals was present in the

PLGA matrix. By increasing the process temperature during diafiltration, the unwanted burst release could be reduced because of a reduced microparticle porosity.

Due to its complete miscibility with water, methanol as a co-solvent was extracted significantly faster than dichloromethane from the dispersed phase. Increasing the methanol content above 2.5 % (w/w) resulted in an increased porosity, drug loss and burst release. The final dichloromethane extraction was faster, although methanol had already been completely extracted from the PLGA-phase. The residual dichloromethane content after 24 h was reduced from 2.4 % (w/w) (without methanol) to below 0.5 % (w/w) if ≥ 2.5 % (w/w) methanol were used as a co-solvent. The resulting porosity did not explain this, because, if caused by diafiltration, it had no effect on the residual solvent content. Therefore, the effect of alcohols in the continuous phase on the solvent extraction was investigated further.

The final removal of the residual solvent from the microparticles was performed by wet extraction and secondary drying methods. With decreasing residual solvent content, the solvent removal became significantly slower as the diffusivity in the PLGA matrix decreased due to a decreasing plasticizing effect and free volume. A higher molecular weight and end-capping of PLGA increased the residual solvent content due to an increasing affinity for dichloromethane, viscosity and droplet/particle size. Increasing the lipophilicity of PLGA with a higher lactide content did not increase the residual dichloromethane content because a slower droplet solidification facilitated the final solvent extraction. The removal of residual dichloromethane was more efficient with alcoholic wet extraction, followed by aqueous wet extraction at elevated temperature and vacuum drying of the microparticles. Aqueous wet extraction reduced the residual dichloromethane content of risperidone-loaded PLGA 503H microparticles to 2.43 % (w/w) (20 °C) and 0.03 % (w/w) (35 °C) in 24 h. The elevated temperature promoted the risperidone-caused degradation of PLGA resulting in visible microparticle erosion and a decrease of risperidone encapsulation efficiency from 88 % to 75 %. Early filtration and subsequent vacuum drying of the solidified microparticles prevented this unwanted erosion of microparticles and drug loss. The residual dichloromethane content in filtered PLGA 503H microparticles was only reduced from about 5 % (w/w) to 4.34 % (w/w) (20 °C) and 3.20 % (w/w) (35 °C) after 18 h vacuum drying because of the missing plasticizing effect of water.

Redispersing filtered wet microparticles in alcoholic media improved the residual dichloromethane extraction. The potential of different extractants was explained by the Gordon-Taylor equation and Hansen solubility parameters. Short-chain monohydric alcohols decreased the glass transition temperature of PLGA more than polyhydric alcohols, water or dichloromethane. Ethanol had the greatest plasticizing effect of all investigated solvents. A higher chain length of monohydric alcohols increased the affinity to PLGA and thus the solvent absorption, but also the tendency of agglomeration of the microparticles. Extraction in methanol: or ethanol:water mixtures efficiently reduced the residual dichloromethane content from 4 - 7 % (w/w) to 0.5 - 2.3 % (w/w) within 1 h and 0.08 - 0.18 % (w/w) within 6 h. Increasing the alcohol content and temperature promoted microparticle aggregation and drug loss.

An alcohol vapor-assisted fluidized bed drying process for microparticles was developed to avoid the loss of encapsulated drug and thus utilize the potential of alcoholic extraction of the solvent residues from the microparticles. By regulating the alcohol concentration and the temperature of the purge gas, the alcohol absorption and the residual solvent and alcohol removal were controlled. Methanol proved to be particularly efficient in the developed setup due to its high volatility, molecular mobility and PLGA-affinity. The absorbed methanol was easily removed by alcohol-free fluidized bed or vacuum drying. While alcohol-free fluidized bed drying decreased the residual dichloromethane content only from about 7 % (w/w) to 6.4 % (w/w) (18 °C) or 0.7 % (w/w) (45 °C) within 24 h, 140 mg/L methanol vapor in the purge gas decreased the residual dichloromethane content to 0.11 % (w/w) in 2 h and removed it completely within 6 h. Methanol vapor also removed efficiently residual ethyl acetate from the microparticles (0.11 % (w/w) after 6 h), which is an alternative PLGA solvent to dichloromethane. Encapsulated risperidone increased the methanol absorption and thus contributed to microparticle plasticization. A high initial residual water content, which favored microparticle aggregation, was completely removed in less than 1 h by alcohol-free fluidized bed drying, which enabled the subsequent alcohol vapor-assisted removal of the residual organic solvent. Alcohol vapor-assisted fluidized bed drying was introduced as a promising alternative to established residual solvent removal methods, accelerating microparticle preparation without negatively affecting drug loading or release profile.

A continuous process for the preparation of monodisperse PLGA microparticles by microfluidic flow-focusing was developed as an alternative to the discontinuous preparation by the classical batch process. For methodological reasons, smaller O/W phase ratios (1:2 - 1:8) were used compared to the batch process ($\geq 1:20$). The resulting limited initial solvent extraction resulted in a low risperidone encapsulation efficiency of only 19 - 21 % at a theoretical drug loading of 30 %. The buffering of the continuous phase to alkaline pH increased encapsulation efficiency up to 93 % but led to a change in the microfluidic droplet formation and thus microparticle size. This could be counteracted by reducing the total flow rate and the amount of stabilizer in the continuous phase. The in-vitro release of risperidone was delayed from microparticles prepared by microfluidic compared to similar-sized polydisperse microparticles prepared by the batch process probably because of a more homogeneous drug distribution within the PLGA-matrix. A continuous dilution-based solvent extraction process was developed, and the effect on droplet shrinkage examined with flow microscopy. A phase ratio of at least 1:100 after dilution and a sufficient extraction time (75 s at 1:100 and 15 s at 1:500) were necessary to shrink the droplets to the particle size of the final microparticles. Increasing the temperature or adding methanol to the continuous phase improved the dichloromethane extraction but impaired the process stability due to the formation of gas bubbles or sticking of droplets/particles. A tangential flow filtration (TFF) process was developed to separate the dichloromethane-enriched continuous phase from the microparticles.

In conclusion, the effect of various formulation and process parameters on the removal of solvents in extraction/evaporation methods and on critical properties of the final microparticles such as drug loading and drug release was investigated. Methods were developed which accelerate both the initial and final removal of the organic solvents, thus shortening the total process time. In addition, high encapsulation efficiencies and desirable drug release profiles (e.g., low burst release) were achieved. This research contributes to know-how in the manufacturing of biodegradable PLGA microparticles by the solvent extraction/evaporation method through a detailed investigation of various single and combined solvent removal processes and their effects on the resulting properties of PLGA microparticles.

5. Zusammenfassung

Bioabbaubare Poly(lactid-co-glycolid) (PLGA) Mikropartikel ermöglichen die kontrollierte parenterale Gabe von Arzneistoffen. Die üblicherweise verwendeten Mikroverkapslungsverfahren erfordern das Auflösen von PLGA in organischen Lösungsmitteln. Die Entfernung dieser Lösungsmittel während des Herstellungsprozesses ist essenziell, um ausgehärtete Mikropartikel zu erhalten. Darüber hinaus muss ein niedriger Restlösungsmittelgehalt im Endprodukt erreicht werden, um Lagerstabilität und Patientensicherheit zu gewährleisten. In dieser Dissertation wurde die Lösungsmittelentfernung während der Mikropartikelherstellung mit der O/W Lösungsmittelextraktions/-verdampfungsmethode untersucht. In dieser Methode wurde eine organische (O) Phase aus Arzneistoff, PLGA und Lösungsmittel (Dichlormethan oder Ethylacetat) zunächst in einem klassischen Batchprozess oder durch mikrofluidische Flussfokussierung in eine wässrige Polyvinylalkohollösung (W) emulgiert. Der Einfluss verschiedener Formulierungs- und Prozessparametern wurde untersucht, um die Eigenschaften von PLGA-Mikropartikeln im Hinblick auf minimale Restlösungsmittelmengen bei hohen Wirkstoffbeladungen und Verkapselungseffizienzen sowie optimale Wirkstofffreisetzungprofile zu optimieren.

Die initiale Entfernung von organischem Lösungsmittel hat großen Einfluss auf die Eigenschaften der resultierenden Mikropartikel und ist in der Regel durch zwei Schritte gesteuert: das Lösen des Lösungsmittels in der kontinuierlichen wässrigen Phase und die Verdampfungsrate des Lösungsmittels. Eine einstufige Verdünnung und Diafiltration wurden zur Steuerung der initialen Lösungsmittelextraktion untersucht. Letzteres ersetzte das üblicherweise notwendige großvolumige Herstellungsequipment und den O/W-Emulsionstransfer. Die beschleunigte Extraktion des PLGA-Lösungsmittels Dichlormethan verkürzte die Prozesszeit, bis die Mikropartikel verfestigt und damit abtrennbar waren. Die Erhöhung der Diafiltrationsrate erhöhte die Partikelgröße, die Porosität und die Arzneistoffbeladung der Mikropartikel. Die Verkapselungseffizienz von Risperidon wurde erheblich erhöht, von 62 % auf bis zu 80 % in PLGA 503H Mikropartikeln bzw. von 27 % auf bis zu 75 % in PLGA 753S Mikropartikeln. Eine langsamere Verfestigung von Mikropartikeln aus PLGA 753S mit veresterten Endgruppen und erhöhtem Lactidgehalt wurde als Grund für den erhöhten Arzneistoffverlust ohne Diafiltration identifiziert. Der Restgehalt an Dichlormethan wurde nicht durch Diafiltration, sondern nur durch die Erhöhung der Temperatur gesenkt, da die finale Lösungsmittelentfernung durch die Diffusivität

innerhalb der PLGA-Phase limitiert war. Die beschleunigte Lösungsmittelextraktion durch Diafiltration hatte keinen Einfluss auf die in-vitro-Freisetzung von Risperidon sowohl aus PLGA 503H als auch aus PLGA 753S Mikropartikeln. Der Freisetzungsburst von Dexamethason nahm je nach Arzneistoffbeladung ab oder zu. Eine durch die schnelle Lösungsmittelextraktion erhöhte Porosität verstärkte die Perkolation ungelöster Arzneistoffkristalle bei hoher Arzneistoffbeladung. Durch eine Erhöhung der Prozesstemperatur während der Diafiltration konnte der unerwünschte Freisetzungsbursts aufgrund einer geringeren Porosität der Mikropartikel reduziert werden.

Aufgrund seiner vollständigen Mischbarkeit mit Wasser wurde das Co-Lösungsmittel Methanol schneller als Dichlormethan extrahiert. Die Erhöhung des Methanolanteils über 2,5 % (m/m) führte zu einer zunehmenden Mikropartikelporosität, sinkenden Dexamethasonbeladung und einer Erhöhung des Freisetzungsbursts. Die finale Dichlormethanextraktion verlief schneller, obwohl Methanol bereits vollständig aus der PLGA-Phase extrahiert war. Der Restdichlormethangehalt nach 24 h wurde von 2,4 % (m/m) (ohne Methanol) auf unter 0,5 % (m/m) gesenkt, wenn mindestens 2,5 % (m/m) Methanol als Co-Lösungsmittel verwendet wurden. Die resultierende Porosität erklärte dies nicht hinreichend, da sie, sofern durch Diafiltration verursacht, keinen Einfluss auf den Restlösungsmittelgehalt hatte. Daher wurde der Effekt von Alkoholen in der kontinuierlichen Phase auf die Lösungsmittelextraktion weiter untersucht.

Die finale Entfernung von Lösungsmittelrückständen aus den Mikropartikeln wurde mit Nassextraktions- und sekundären Trocknungsmethoden durchgeführt. Mit einem sinkendem Restlösungsmittelgehalt wurde die Lösungsmittelentfernung deutlich langsamer, da die Diffusivität in der PLGA-Matrix aufgrund eines sinkenden weichmachenden Effektes und freien Volumens abnahm. Die Erhöhung des Molekulargewichtes und die Endgruppenveresterung von PLGA führten zu einer leichten Erhöhung des Restlösungsmittelgehaltes, aufgrund der ansteigenden Affinität für Dichlormethan, Viskosität und Tröpfchen/Partikelgröße. Die Erhöhung der Lipophilie von PLGA durch einen höheren Lactidgehalt erhöhte den Restdichlormethangehalt nicht, da eine langsamere Tröpfchenverfestigung die finale Lösungsmittelextraktion erleichterte. Die Entfernung von Restdichlormethan war effizienter mit alkoholischer Nassextraktion, gefolgt von wässriger Nassextraktion bei

erhöhter Temperatur und Vakuumtrocknung der Mikropartikel. Durch die wässrige Nassextraktion wurde der Restdichlormethangehalt von Risperidonbeladenen Mikropartikeln aus PLGA 503H auf 2,43 % (m/m) (20 °C) bzw. 0,03 % (m/m) (35 °C) in 24 h reduziert. Die erhöhte Temperatur verstärkte den durch Risperidon verursachten Abbau von PLGA, was zu einer sichtbaren Mikropartikelerosion und der Senkung der Verkapselungseffizienz von 88 % auf 75 % führte. Eine frühzeitige Filtration und anschließende Vakuumtrocknung der verfestigten Mikropartikel verhinderte diese unerwünschte Erosion der Mikropartikel und den Verlust von Wirkstoffen. Der Restdichlormethangehalt in PLGA 503H Mikropartikeln wurde nach 18 h Vakuumtrocknung jedoch nur von etwa 5 % (m/m) auf 4,34 % (m/m) (20 °C) bzw. 3,20 % (m/m) (35 °C) gesenkt, da die weichmachende Wirkung des Wassers fehlt.

Das Redispergieren von abfiltrierten, nassen Mikropartikeln in alkoholischen Medien verbesserte die Restdichlormethanextraktion. Das Potenzial verschiedener Extraktionsmittel wurde mit der Gordon-Taylor-Gleichung und den Hansen-Löslichkeitsparametern erklärt. Kurzkettige einwertige Alkohole senkten die Glasübergangstemperatur von PLGA stärker als mehrwertige Alkohole, Wasser oder Dichlormethan. Ethanol hatte von allen untersuchten Lösungsmitteln die stärkste weichmachende Wirkung. Eine höhere Kettenlänge der einwertigen Alkohole erhöhte die Affinität zu PLGA und damit die Lösungsmittelabsorption, aber auch die Tendenz zur Agglomeration der Mikropartikel. Die Extraktion in Methanol: oder Ethanol:Wasser-Gemischen reduzierte den Restgehalt an Dichlormethan effizient von 4 - 7 % (m/m) auf 0,5 - 2,3 % (m/m) innerhalb von 1 h und auf 0,08 - 0,18 % (m/m) innerhalb von 6 h. Die Erhöhung des Alkoholgehaltes und der Temperatur führte vermehrt zu einer Aggregation der Mikropartikel und einem Verlust des verkapselten Arzneistoffes.

Ein Alkoholdampfunterstütztes Wirbelschichttrocknungsverfahren für Mikropartikel wurde entwickelt, um den Verlust von verkapseltem Arzneistoff zu vermeiden und so das Potenzial der alkoholischen Extraktion von Lösungsmittelrückständen aus Mikropartikeln zu nutzen. Durch Regulierung der Alkoholkonzentration und der Temperatur des Spülgases konnten die Alkoholabsorption und die Lösungsmittel- und Alkoholentfernung gesteuert werden. Methanol erwies sich in der entwickelten Versuchsanordnung aufgrund seiner hohen Volatilität, molekularen Mobilität und PLGA-Affinität als besonders effektiv und konnte mittels alkoholfreier Wirbelschicht-

oder Vakuumtrocknung leicht wieder entfernt werden. Während die alkoholfreie Wirbelschichttrocknung den Restdichlormethangehalt innerhalb von 24 h nur von etwa 7 % (m/m) auf 6,4 % (m/m) (18 °C) bzw. 0,7 % (m/m) (45 °C) senkte, reduzierten 140 mg/L Methanoldampf im Spülgas das Restdichlormethan auf 0.11 % (m/m) in 2 h und entfernten es vollständig in 6 h. Methanoldampf entfernte ebenfalls effizient Restethylacetat aus den Mikropartikeln (0,11 % (w/w) nach 6 Stunden), welches ein alternatives PLGA-Lösungsmittel zu Dichlormethan ist. Verkapseltes Risperidon erhöhte die Methanolabsorption der Mikropartikel und trug so zum Erweichen dieser bei. Ein hoher anfänglicher Restwassergehalt, der die Aggregation begünstigte, wurde durch eine alkoholfreie Wirbelschichttrocknung in unter 1 h vollständig entfernt, dies ermöglichte die anschließende alkoholdampfunterstützte Entfernung des organischen Restlösungsmittels ohne Mikropartikelaggregation. Die alkoholdampfunterstützte Wirbelschichttrocknung wurde als vielversprechende Alternative zu den etablierten Verfahren zur Entfernung von Lösungsmittelrückständen eingeführt, wodurch die Zeit zur Mikropartikelherstellung verkürzt wird, ohne die Arzneistoffbeladung oder das Freisetzungprofil negativ zu beeinflussen.

Ein kontinuierlicher Prozess zur Herstellung von monodispersen PLGA-Mikropartikeln mittels mikrofluidischer Flussfokussierung wurde als Alternative zur diskontinuierlichen Herstellung im Batchprozess entwickelt. Methodisch bedingt kamen dabei kleinere O/W-Phasenverhältnisse (1:2 - 1:8) zum Einsatz, verglichen mit dem Rührprozess ($\geq 1:20$). Die daraus resultierende begrenzte initiale Lösungsmittlextraktion und die langsamere Verfestigung der PLGA-Phase führten zu einer geringen Risperidonverkapslungseffizienz von nur 19 - 21 %, bei einer theoretischen Arzneistoffbeladung von 30 %. Die Pufferung der kontinuierlichen Phase auf einen alkalischen pH-Wert führte zu einer Erhöhung der Verkapslungseffizienz auf bis zu 93 %, aber auch der Änderung der mikrofluidischen Tröpfchenbildung und damit der Mikropartikelgröße. Dem konnte durch eine Reduzierung der Gesamtdurchflussrate und der Stabilisatorkonzentration in der kontinuierlichen Phase entgegengewirkt werden. Die in-vitro Freisetzung von Risperidon erfolgte verzögert aus mikrofluidisch hergestellten Mikropartikeln, verglichen mit ähnlich großen polydispersen Mikropartikeln, die im Batchprozess hergestellt wurden, wahrscheinlich wegen einer homogenen Arzneistoffverteilung in der PLGA-Matrix. Es wurde ein kontinuierliches, auf Verdünnung basierendes Lösungsmittlextraktionsverfahren entwickelt und die

Auswirkung auf die Tröpfchenschrumpfung mittels Durchflussmikroskopie untersucht. Ein Phasenverhältnis von mindestens 1:100 nach der Verdünnung und eine ausreichend lange Extraktionszeit (75 s bei 1:100 und 15 s bei 1:500) waren nötig, damit die Tröpfchen auf die Größe der finalen Mikropartikel schrumpften. Die Erhöhung der Temperatur oder der Zusatz von Methanol zur kontinuierlichen Phase verbesserte die Dichlormethanextraktion, beeinträchtigen jedoch die Prozessstabilität durch die Bildung von Gasblasen oder das Verkleben von Tröpfchen/Partikeln. Es wurde ein Tangentialflussfiltrations (TFF) -Prozess entwickelt, um die mit Dichlormethan angereicherte kontinuierliche Phase von den ausgehärteten Mikropartikeln abzutrennen.

Insgesamt wurden die Auswirkungen verschiedener Formulierungs- und Prozessparameter auf die Lösungsmittelentfernung in Extraktions-/Verdampfungsverfahren und auf die kritischen Eigenschaften der fertigen Mikropartikel wie die Arzneistoffbeladung und -freisetzung untersucht. Es wurden Verfahren entwickelt, die sowohl die initiale als auch die finale Entfernung von organischen Lösungsmitteln beschleunigen und damit die Gesamtprozesszeit verkürzen. Darüber hinaus wurden hohe Verkapselungseffizienzen und wünschenswerte Arzneistofffreisetzungprofile (z.B. geringe Burst-Freisetzung) erzielt. Diese Forschungsarbeit trägt zum Know-how bei der Herstellung biologisch abbaubarer PLGA-Mikropartikel durch die Lösungsmittelextraktions-/Verdampfungsverfahren bei, indem verschiedene einzelne und kombinierte Lösungsmittelentfernungsverfahren und ihre Auswirkungen auf die resultierenden Eigenschaften der PLGA-Mikropartikel eingehend untersucht werden.

6. Reference

-
- [1] Y.H. Yun, B.K. Lee, K. Park, Controlled Drug Delivery: Historical perspective for the next generation, *J. Control. Release* 219 (2015) 2–7.
- [2] K. Chaudhary, M.M. Patel, P.J. Mehta, Long-Acting Injectables: Current Perspectives and Future Promise, *Crit. Rev. Ther. Drug Carrier Syst.* 36 (2019) 137–181.
- [3] M. Dang, M.S. Shoichet, Long-Acting Ocular Injectables: Are We Looking In The Right Direction?, *Adv. Sci. (Weinh.)* 11 (2024) e2306463.
- [4] A.B. Jindal, A.R. Bhide, S. Salave, D. Rana, D. Benival, Long-acting parenteral drug delivery systems for the treatment of chronic diseases, *Adv. Drug Deliv. Rev.* 198 (2023) 114862.
- [5] C.I. Nkanga, A. Fisch, M. Rad-Malekshahi, M.D. Romic, B. Kittel, T. Ullrich, J. Wang, R.W.M. Krause, S. Adler, T. Lammers, W.E. Hennink, F. Ramazani, Clinically established biodegradable long acting injectables: An industry perspective, *Adv. Drug Deliv. Rev.* 167 (2020) 19–46.
- [6] H. Abdelkader, Z. Fathalla, A. Seyfoddin, M. Farahani, T. Thrimawithana, A. Allahham, A.W.G. Alani, A.A. Al-Kinani, R.G. Alany, Polymeric long-acting drug delivery systems (LADDs) for treatment of chronic diseases: Inserts, patches, wafers, and implants, *Adv. Drug Deliv. Rev.* 177 (2021) 113957.
- [7] M. Stielow, A. Witczyńska, N. Kubryń, Ł. Fijałkowski, J. Nowaczyk, A. Nowaczyk, The Bioavailability of Drugs-The Current State of Knowledge, *Molecules* 28 (2023).
- [8] M. Goldberg, I. Gomez-Orellana, Challenges for the oral delivery of macromolecules, *Nat. Rev. Drug Discov.* 2 (2003) 289–295.
- [9] D. Wang, J. Schneider-Thoma, S. Siafis, M. Qin, H. Wu, Y. Zhu, J.M. Davis, J. Priller, S. Leucht, Efficacy, acceptability and side-effects of oral versus long-acting- injectables antipsychotics: Systematic review and network meta-analysis, *Eur. Neuropsychopharmacol.* 83 (2024) 11–18.
- [10] L. Boyer, B. Falissard, P. Nuss, C. Collin, S. Duret, M. Rabbani, I. de Chefdebien, I. Tonelli, P.M. Llorca, G. Fond, Real-world effectiveness of long-acting injectable antipsychotic treatments in a nationwide cohort of 12,373 patients with schizophrenia-spectrum disorders, *Mol. Psychiatry* 28 (2023) 3709–3716.
- [11] Y. Shi, an Lu, X. Wang, Z. Belhadj, J. Wang, Q. Zhang, A review of existing strategies for designing long-acting parenteral formulations: Focus on underlying mechanisms, and future perspectives, *Acta Pharm. Sin. B* 11 (2021) 2396–2415.

-
- [12] K. Park, S. Skidmore, J. Hadar, J. Garner, H. Park, A. Otte, B.K. Soh, G. Yoon, D. Yu, Y. Yun, B.K. Lee, X. Jiang, Y. Wang, Injectable, long-acting PLGA formulations: Analyzing PLGA and understanding microparticle formation, *J. Control. Release* 304 (2019) 125–134.
- [13] E. Campos, J. Branquinho, A.S. Carreira, A. Carvalho, P. Coimbra, P. Ferreira, M.H. Gil, Designing polymeric microparticles for biomedical and industrial applications, *Eur. Polym. J.* 49 (2013) 2005–2021.
- [14] F. von Burkersroda, L. Schedl, A. Göpferich, Why degradable polymers undergo surface erosion or bulk erosion, *Biomaterials* 23 (2002) 4221–4231.
- [15] N.G. Kotla, A. Pandey, Y. Vijaya Kumar, F. Ramazani, A. Fisch, Polyester-based long acting injectables: Advancements in molecular dynamics simulation and technological insights, *Drug Discov. Today* 28 (2023) 103463.
- [16] C. Wischke, S.P. Schwendeman, Degradable Polymeric Carriers for Parenteral Controlled Drug Delivery, in: J. Siepmann, R.A. Siegel, M.J. Rathbone (Eds.), *Fundamentals and Applications of Controlled Release Drug Delivery*, Springer US, Boston, MA, 2012, pp. 171–228.
- [17] C. Bassand, L. Benabed, S. Charlon, J. Verin, J. Freitag, F. Siepmann, J. Soulestin, J. Siepmann, 3D printed PLGA implants: APF DDM vs. FDM, *J. Control. Release* 353 (2023) 864–874.
- [18] F. Sun, X. Sun, H. Wang, C. Li, Y. Zhao, J. Tian, Y. Lin, Application of 3D-Printed, PLGA-Based Scaffolds in Bone Tissue Engineering, *Int. J. Mol. Sci.* 23 (2022).
- [19] N.H. Shah, A.S. Railkar, F.C. Chen, R. Tarantino, S. Kumar, M. Murjani, D. Palmer, M.H. Infeld, A.W. Malick, A biodegradable injectable implant for delivering micro and macromolecules using poly (lactic-co-glycolic) acid (PLGA) copolymers, *J. Control. Release.* 27 (1993) 139–147.
- [20] C.B. Packhaeuser, J. Schnieders, C.G. Oster, T. Kissel, In situ forming parenteral drug delivery systems: an overview, *Eur. J. Pharm. Biopharm.* 58 (2004) 445–455.
- [21] R.A. Jain, C.T. Rhodes, A.M. Railkar, A.W. Malick, N.H. Shah, Comparison of various injectable protein-loaded biodegradable poly(lactide-co-glycolide) (PLGA) devices: in-situ-formed implant versus in-situ-formed microspheres versus isolated microspheres, *Pharm. Dev. Technol.* 5 (2000) 201–207.
- [22] H. Kranz, G.A. Brazeau, J. Napaporn, R.L. Martin, W. Millard, R. Bodmeier, Myotoxicity studies of injectable biodegradable in-situ forming drug delivery systems, *Int. J. Pharm.* 212 (2001) 11–18.

- [23] R. Bodmeier, Verfahren zur in-situ Herstellung von Partikeln, DE 19 724 784 A1 (1998).
- [24] P. Blasi, Poly(lactic acid)/poly(lactic-co-glycolic acid)-based microparticles: an overview, *J. Pharm. Investig.* 49 (2019) 337–346.
- [25] T. Kissel, Z. Brich, S. Bantle, I. Lancranjan, F. Nimmerfall, P. Vit, Parenteral depot-systems on the basis of biodegradable polyesters, *J. Control. Release.* 16 (1991) 27–41.
- [26] H.K. Makadia, S.J. Siegel, Poly Lactic-co-Glycolic Acid (PLGA) as Biodegradable Controlled Drug Delivery Carrier, *Polymers* 3 (2011) 1377–1397.
- [27] K. Avgoustakis, Polylactic- co -Glycolic Acid (PLGA), in: *Encyclopedia of Biomedical Polymers and Polymeric Biomaterials*, Taylor & Francis, 2015, pp. 6491–6500.
- [28] J. Sun, J. Walker, M. Beck-Broichsitter, S.P. Schwendeman, Characterization of commercial PLGAs by NMR spectroscopy, *Drug Deliv. Transl. Res.* 12 (2022) 720–729.
- [29] B. Wan, J.V. Andhariya, Q. Bao, Y. Wang, Y. Zou, D.J. Burgess, Effect of polymer source on in vitro drug release from PLGA microspheres, *Int. J. Pharm.* 607 (2021) 120907.
- [30] T.G. Park, Degradation of poly(lactic-co-glycolic acid) microspheres: effect of copolymer composition, *Biomaterials* 16 (1995) 1123–1130.
- [31] X.S. Wu, N. Wang, Synthesis, characterization, biodegradation, and drug delivery application of biodegradable lactic/glycolic acid polymers. Part II: biodegradation, *J. Biomater. Sci. Polym. Ed.* 12 (2001) 21–34.
- [32] F. Alexis, Factors affecting the degradation and drug-release mechanism of poly(lactic acid) and poly[(lactic acid)- co -(glycolic acid)], *Polym. Int* 54 (2005) 36–46.
- [33] E. Vey, C. Rodger, J. Booth, M. Claybourn, A.F. Miller, A. Saiani, Degradation kinetics of poly(lactic-co-glycolic) acid block copolymer cast films in phosphate buffer solution as revealed by infrared and Raman spectroscopies, *Polym. Degrad. Stab.* 96 (2011) 1882–1889.
- [34] S. Fredenberg, M. Wahlgren, M. Reslow, A. Axelsson, The mechanisms of drug release in poly(lactic-co-glycolic acid)-based drug delivery systems--a review, *Int. J. Pharm.* 415 (2011) 34–52.

- [35] J. Yoo, Y.-Y. Won, Phenomenology of the Initial Burst Release of Drugs from PLGA Microparticles, *ACS Biomater. Sci. Eng.* 6 (2020) 6053–6062.
- [36] F. Tamani, C. Bassand, M.C. Hamoudi, F. Danede, J.F. Willart, F. Siepmann, J. Siepmann, Mechanistic explanation of the (up to) 3 release phases of PLGA microparticles: Diprophylline dispersions, *Int. J. Pharm.* 572 (2019) 118819.
- [37] H. Gasmi, F. Siepmann, M.C. Hamoudi, F. Danede, J. Verin, J.-F. Willart, J. Siepmann, Towards a better understanding of the different release phases from PLGA microparticles: Dexamethasone-loaded systems, *Int. J. Pharm.* 514 (2016) 189–199.
- [38] X. Luan, M. Skupin, J. Siepmann, R. Bodmeier, Key parameters affecting the initial release (burst) and encapsulation efficiency of peptide-containing poly(lactide-co-glycolide) microparticles, *Int. J. Pharm.* 324 (2006) 168–175.
- [39] S.H.S. Koshari, X. Shi, L. Jiang, D. Chang, K. Rajagopal, A.M. Lenhoff, N.J. Wagner, Design of PLGA-Based Drug Delivery Systems Using a Physically-Based Sustained Release Model, *J. Pharm. Sci.* 111 (2021) 345–357.
- [40] Y. Yeo, N. Baek, K. Park, Microencapsulation methods for delivery of protein drugs, *Biotechnol. Bioprocess Eng.* 6 (2001) 213–230.
- [41] S. Freitas, H.P. Merkle, B. Gander, Microencapsulation by solvent extraction/evaporation: reviewing the state of the art of microsphere preparation process technology, *J. Control. Release.* 102 (2005) 313–332.
- [42] M. Li, O. Rouaud, D. Poncelet, Microencapsulation by solvent evaporation: state of the art for process engineering approaches, *Int. J. Pharm.* 363 (2008) 26–39.
- [43] A. Schoubben, M. Ricci, S. Giovagnoli, Meeting the unmet: from traditional to cutting-edge techniques for poly lactide and poly lactide-co-glycolide microparticle manufacturing, *J. Pharm. Investig.* 49 (2019) 381–404.
- [44] C. Thomasin, N.T. Hô, H.P. Merkle, B. Gander, Drug microencapsulation by PLA/PLGA coacervation in the light of thermodynamics. 1. Overview and theoretical considerations, *J. Pharm. Sci.* 87 (1998) 259–268.
- [45] C. Thomasin, H.P. Merkle, B. Gander, Drug microencapsulation by PLA/PLGA coacervation in the light of thermodynamics. 2. Parameters determining microsphere formation, *J. Pharm. Sci.* 87 (1998) 269–275.
- [46] F. Wan, M. Yang, Design of PLGA-based depot delivery systems for biopharmaceuticals prepared by spray drying, *Int. J. Pharm.* 498 (2016) 82–95.

- [47] M.A. Tracy, Development and scale-up of a microsphere protein delivery system, *Biotechnol. Prog.* 14 (1998) 108–115.
- [48] R. Bodmeier, H.G. Chen, Preparation of biodegradable poly(+/-)lactide microparticles using a spray-drying technique, *J. Pharm. Pharmacol.* 40 (1988) 754–757.
- [49] F.J. Wang, C.-H. Wang, Effects of fabrication conditions on the characteristics of etanidazole spray-dried microspheres, *J. Microencapsul.* 19 (2002) 495–510.
- [50] J. Bleich, B.W. Müller, W. Waßmus, Aerosol solvent extraction system — a new microparticle production technique, *Int. J. Pharm.* 97 (1993) 111–117.
- [51] R. Bodmeier, H. Wang, D.J. Dixon, S. Mawson, K.P. Johnston, Polymeric microspheres prepared by spraying into compressed carbon dioxide, *Pharm. Res.* 12 (1995) 1211–1217.
- [52] C. Böhm, B. Tandon, A. Hrynevich, J. Teßmar, P.D. Dalton, Processing of Poly(lactic- co -glycolic acid) Microfibers via Melt Electrowriting, *Macromol. Chem. Phys.* 223 (2022).
- [53] P. Orsolini, Pharmaceutical composition in the form of microparticles, U.S. 5,225,205A (1993).
- [54] G. Nykamp, U. Carstensen, B.W. Müller, Jet milling--a new technique for microparticle preparation, *Int. J. Pharm.* 242 (2002) 79–86.
- [55] S. Farinha, C. Moura, M.D. Afonso, J. Henriques, Production of Lysozyme-PLGA-Loaded Microparticles for Controlled Release Using Hot-Melt Extrusion, *AAPS PharmSciTech* 21 (2020) 274.
- [56] J.-M. Ruiz, Preparation process of sustained release compositions and the compositions thus obtained, US5213812A (1993).
- [57] J.-M. Ruiz, Process for the preparation of microballs and microballs thus obtained, U.S. 5,569,467A (1996).
- [58] L.-H. Hung, S.-Y. Teh, J. Jester, A.P. Lee, PLGA micro/nanosphere synthesis by droplet microfluidic solvent evaporation and extraction approaches, *Lab Chip* 10 (2010) 1820–1825.
- [59] N. Kiss, G. Brenn, H. Pucher, J. Wieser, S. Scheler, H. Jennewein, D. Suzzi, J. Khinast, Formation of O/W emulsions by static mixers for pharmaceutical applications, *Chem. Eng. Sci.* 66 (2011) 5084–5094.

-
- [60] R.K. Thakur, C. Vial, K. Nigam, E.B. Nauman, G. Djelveh, Static Mixers in the Process Industries—A Review, *Chem. Eng. Res. Des.* 81 (2003) 787–826.
- [61] T. Kawakatsu, Y. Kikuchi, M. Nakajima, Regular-sized cell creation in microchannel emulsification by visual microprocessing method, *J. Americ. Oil Chem. Soc.* 74 (1997) 317–321.
- [62] S. Sugiura, M. Nakajima, N. Kumazawa, S. Iwamoto, M. Seki, Characterization of Spontaneous Transformation-Based Droplet Formation during Microchannel Emulsification, *J. Phys. Chem. B* 106 (2002) 9405–9409.
- [63] K. Shiga, N. Muramatsu, T. Kondo, Preparation of poly(D,L-lactide) and copoly(lactide-glycolide) microspheres of uniform size, *J. Pharm. Pharmacol.* 48 (1996) 891–895.
- [64] G. Ma, M. Nagai, S. Omi, Preparation of uniform poly(lactide) microspheres by employing the Shirasu Porous Glass (SPG) emulsification technique, *Colloids Surf. A: Physicochem. Eng. Asp* 153 (1999) 383–394.
- [65] E. Amstad, M. Chemama, M. Eggersdorfer, L.R. Arriaga, M.P. Brenner, D.A. Weitz, Robust scalable high throughput production of monodisperse drops, *Lab Chip* 16 (2016) 4163–4172.
- [66] P. Walstra, Principles of emulsion formation, *Chem. Eng. Sci.* 48 (1993) 333–349.
- [67] P. Sansdrap, A.J. Moës, Influence of manufacturing parameters on the size characteristics and the release profiles of nifedipine from poly(DL-lactide-co-glycolide) microspheres, *Int. J. Pharm.* 98 (1993) 157–164.
- [68] F. Gabor, B. Ertl, M. Wirth, R. Mallinger, Ketoprofen-poly(D,L-lactic-co-glycolic acid) microspheres: influence of manufacturing parameters and type of polymer on the release characteristics, *J. Microencapsul.* 16 (1999) 1–12.
- [69] S. Fathi Roudsari, R. Dhib, F. Ein-Mozaffari, Mixing effect on emulsion polymerization in a batch reactor, *Polym. Sci. Eng.* 55 (2015) 945–956.
- [70] R. Bodmeier, J.W. McGinity, Polylactic acid microspheres containing quinidine base and quinidine sulphate prepared by the solvent evaporation technique. I. Methods and morphology, *J. Microencapsul.* 4 (1987) 279–288.
- [71] D. Noviendri, I. Jaswir, M. Taher, F. Mohamed, H.M. Salleh, I.A. Noorbatcha, F. Octavianti, W. Lestari, R. Hendri, H. Ahmad, K. Miyashita, A. Abdullah, Fabrication of Fucoxanthin-Loaded Microsphere(F-LM) By Two Steps Double-Emulsion Solvent Evaporation Method and Characterization of Fucoxanthin

- before and after Microencapsulation, *Journal of oleo science* 65 (2016) 641–653.
- [72] Y. Yang, Morphology, drug distribution, and in vitro release profiles of biodegradable polymeric microspheres containing protein fabricated by double-emulsion solvent extraction/evaporation method, *Biomaterials* 22 (2001) 231–241.
- [73] R.V. Calabrese, T.P.K. Chang, P.T. Dang, Drop breakup in turbulent stirred-tank contactors. Part I: Effect of dispersed-phase viscosity, *AIChE J.* 32 (1986) 657–666.
- [74] C. Desnoyer, O. Masbernat, C. Gourdon, Experimental study of drop size distributions at high phase ratio in liquid–liquid dispersions, *Chem. Eng. Sci.* 58 (2003) 1353–1363.
- [75] H. Sah, Microencapsulation techniques using ethyl acetate as a dispersed solvent: effects of its extraction rate on the characteristics of PLGA microspheres, *J. Control. Release.* 47 (1997) 233–245.
- [76] R. Jeyanthi, R.C. Mehta, B.C. Thanoo, P.P. Deluca, Effect of processing parameters on the properties of peptide-containing PLGA microspheres, *J. Microencapsul.* 14 (1997) 163–174.
- [77] Y. Yeo, K. Park, Control of encapsulation efficiency and initial burst in polymeric microparticle systems, *Arch. Pharm. Res.* 27 (2004) 1–12.
- [78] G.F. Christopher, S.L. Anna, Microfluidic methods for generating continuous droplet streams, *J. Phys. D: Appl. Phys.* 40 (2007) R319-R336.
- [79] J.K. Nunes, S.S.H. Tsai, J. Wan, H.A. Stone, Dripping and jetting in microfluidic multiphase flows applied to particle and fiber synthesis, *J. Phys. D: Appl. Phys.* 46 (2013).
- [80] R.M. Erb, D. Obrist, P.W. Chen, J. Studer, A.R. Studart, Predicting sizes of droplets made by microfluidic flow-induced dripping, *Soft Matter* 7 (2011) 8757.
- [81] S. Damiani, U.B. Kompella, S.A. Damiani, R. Kodzius, *Microfluidic Devices for Drug Delivery Systems and Drug Screening*, *Genes* 9 (2018).
- [82] T. Cubaud, T.G. Mason, Capillary threads and viscous droplets in square microchannels, *Phys. Fluids* 20 (2008) 53302.
- [83] Z. Nie, M. Seo, S. Xu, P.C. Lewis, M. Mok, E. Kumacheva, G.M. Whitesides, P. Garstecki, H.A. Stone, Emulsification in a microfluidic flow-focusing device: effect of the viscosities of the liquids, *Microfluid Nanofluid* 5 (2008) 585–594.

- [84] D. Hernández-Cid, V.H. Pérez-González, R.C. Gallo-Villanueva, J. González-Valdez, M.A. Mata-Gómez, Modeling droplet formation in microfluidic flow-focusing devices using the two-phases level set method, *Mater. Today Proc.* 48 (2022) 30–40.
- [85] F. Mardani, S. Falahatian, M. Taghipoor, Mapping flow-focusing microfluidic droplet formation to determine high-throughput droplet generation configurations, *Results Eng.* 18 (2023) 101125.
- [86] L. Peng, M. Yang, S. Guo, W. Liu, X. Zhao, The effect of interfacial tension on droplet formation in flow-focusing microfluidic device, *Biomed. Microdevices* 13 (2011) 559–564.
- [87] B. Amoyav, O. Benny, Controlled and tunable polymer particles' production using a single microfluidic device, *Appl. Nanosci.* 8 (2018) 905–914.
- [88] R. Bodmeier, J.W. McGinity, Solvent selection in the preparation of poly(DL-lactide) microspheres prepared by the solvent evaporation method, *Int. J. Pharm.* 43 (1988) 179–186.
- [89] F. Ito, H. Fujimori, H. Honnami, H. Kawakami, K. Kanamura, K. Makino, Study of types and mixture ratio of organic solvent used to dissolve polymers for preparation of drug-containing PLGA microspheres, *Eur. Polym. J.* 45 (2009) 658–667.
- [90] A. Otte, F. Sharifi, K. Park, Interfacial tension effects on the properties of PLGA microparticles, *Colloids Surf. B: Biointerfaces* 196 (2020) 111300.
- [91] C. Wischke, Y. Zhang, S. Mittal, S.P. Schwendeman, Development of PLGA-based injectable delivery systems for hydrophobic fenretinide, *Pharm. Res.* 27 (2010) 2063–2074.
- [92] A. Rawat, D.J. Burgess, Effect of ethanol as a processing co-solvent on the PLGA microsphere characteristics, *Int. J. Pharm.* 394 (2010) 99–105.
- [93] K. Dixit, R.B. Athawale, S. Singh, Quality control of residual solvent content in polymeric microparticles, *J. Microencapsul.* 32 (2015) 107–122.
- [94] C. B'Hymer, Residual solvent testing: a review of gas-chromatographic and alternative techniques, *Pharm. Res.* 20 (2003) 337–344.
- [95] J. Wang, S.P. Schwendeman, Mechanisms of solvent evaporation encapsulation processes: prediction of solvent evaporation rate, *J. Pharm. Sci.* 88 (1999) 1090–1099.

- [96] H. Katou, A.J. Wandrey, B. Gander, Kinetics of solvent extraction/evaporation process for PLGA microparticle fabrication, *Int. J. Pharm.* 364 (2008) 45–53.
- [97] W.-I. Li, K.W. Anderson, R.C. Mehta, P.P. Deluca, Prediction of solvent removal profile and effect on properties for peptide-loaded PLGA microspheres prepared by solvent extraction/ evaporation method, *J. Control. Release.* 37 (1995) 199–214.
- [98] Y.-Y. Yang, T.-S. Chung, X.-L. Bai, W.-K. Chan, Effect of preparation conditions on morphology and release profiles of biodegradable polymeric microspheres containing protein fabricated by double-emulsion method, *Chem. Eng. Sci.* 55 (2000) 2223–2236.
- [99] S. Mao, Y. Shi, L. Li, J. Xu, A. Schaper, T. Kissel, Effects of process and formulation parameters on characteristics and internal morphology of poly(D,L-lactide-co-glycolide) microspheres formed by the solvent evaporation method, *Eur. J. Pharm. Biopharm.* 68 (2008) 214–223.
- [100] R. Jeyanthi, B.C. Thanoo, R.C. Metha, P.P. Deluca, Effect of solvent removal technique on the matrix characteristics of polylactide/glycolide microspheres for peptide delivery, *J. Control. Release.* 38 (1996) 235–244.
- [101] R.A. Mensah, S.B. Kirton, M.T. Cook, I.D. Styliari, V. Hutter, D.Y.S. Chau, Optimising poly(lactic-co-glycolic acid) microparticle fabrication using a Taguchi orthogonal array design-of-experiment approach, *PloS one* 14 (2019) e0222858.
- [102] J.W. Gibson, R.J. Holl, A.J. Tipton, Emulsion-based processes for making microparticles, U.S. 6,291,013 (2001).
- [103] Y. Bahl, H. Sah, Dynamic changes in size distribution of emulsion droplets during ethyl acetate-based microencapsulation process, *AAPS PharmSciTech* 1 (2000) E5.
- [104] K.S. Soppimath, T.M. Aminabhavi, Ethyl acetate as a dispersing solvent in the production of poly(DL-lactide-co-glycolide) microspheres: effect of process parameters and polymer type, *J. Microencapsul.* 19 (2002) 281–292.
- [105] R.C. Mehta, R. Jeyanthi, S. Calls, B.C. Thanoo, K.W. Burton, P.P. Deluca, Biodegradable microspheres as depot system for parenteral delivery of peptide drugs, *J. Control. Release.* 29 (1994) 375–384.
- [106] T.R. Tice, D.H. Lewis, Microencapsulation Process, U.S. 4,389,330 (1983).
- [107] D.H. Lewis, Growth promoters for animals, U.S. 5,288,496 (1994).

-
- [108] W.-I. Li, K.W. Anderson, P.P. Deluca, Kinetic and thermodynamic modeling of the formation of polymeric microspheres using solvent extraction/evaporation method, *J. Control. Release.* 37 (1995) 187–198.
- [109] L. Besslich, Formulation and process development of biodegradable microparticles for controlled parenteral drug delivery. Doctoral dissertation, Berlin, 2020.
- [110] T.W. Chung, Y.Y. Huang, Y.Z. Liu, Effects of the rate of solvent evaporation on the characteristics of drug loaded PLLA and PDLLA microspheres, *Int. J. Pharm.* 212 (2001) 161–169.
- [111] T.-W. Chung, Y.-Y. Huang, Y.-L. Tsai, Y.-Z. Liu, Effects of solvent evaporation rate on the properties of protein-loaded PLLA and PDLLA microspheres fabricated by emulsion-solvent evaporation process, *J. Microencapsul.* 19 (2002) 463–471.
- [112] S.L. Lyons, S.G. Wright, Method and apparatus for preparing microparticles using in-line solvent extraction, U.S. 6,705,757 B2 (2004).
- [113] M.C. Operti, A. Bernhardt, V. Sincari, E. Jager, S. Grimm, A. Engel, M. Hruby, C.G. Figdor, O. Tagit, Industrial Scale Manufacturing and Downstream Processing of PLGA-Based Nanomedicines Suitable for Fully Continuous Operation, *Pharmaceutics* 14 (2022) 276.
- [114] E.W.Q. Yeap, D.Z.L. Ng, D. Lai, D.J. Ertl, S. Sharpe, S.A. Khan, Continuous Flow Droplet-Based Crystallization Platform for Producing Spherical Drug Microparticles, *Org. Process Res. Dev.* 23 (2019) 93–101.
- [115] E.F. Leonard, A.C. West, C.P. Aucoin, E.E. Nanne, Systems and methods of microfluidic membraneless exchange using filtration of extraction outlet streams, U.S. 8,097,153 B2 (2012).
- [116] T. Suzuki, Y. Matsukawa, A. Suzuki, Method and apparatus for preparing microspheres, U.S. 7,011,776 B2 (2006).
- [117] J.M. Ramstack, Method for preparing microparticles using liquid-liquid extraction, U.S. 6,884,372 B2 (2005).
- [118] E.P. Chang, R.D. Braatz, T.A. Hatton, Pervaporation of emulsion droplets for the templated assembly of spherical particles: A population balance model, *AIChE J.* 59 (2013) 3975–3985.
- [119] J.L. Atkinson, B.K. Chambers, Solvent extraction microencapsulation with tunable extraction rates, U.S. 8,703,843 B2 (2014).

- [120] W.R. Foss, J.N. Anderl, A.L. Clausi, P.A. Burke, Diffusivities of dichloromethane in poly(lactide-co-glycolide), *J. Appl. Polym. Sci.* 112 (2009) 1622–1629.
- [121] P. Blasi, S.S. D'Souza, F. Selmin, P.P. Deluca, Plasticizing effect of water on poly(lactide-co-glycolide), *J. Control. Release.* 108 (2005) 1–9.
- [122] J.S. Vrentas, J.L. Duda, Diffusion in polymer–solvent systems. I. Reexamination of the free-volume theory, *J. Polym. Sci. Polym. Phys. Ed.* 15 (1977) 403–416.
- [123] J.S. Vrentas, J.L. Duda, Diffusion in polymer–solvent systems. II. A predictive theory for the dependence of diffusion coefficients on temperature, concentration, and molecular weight, *J. Polym. Sci. Polym. Phys. Ed.* 15 (1977) 417–439.
- [124] E. Di Maio, S. Iannace, G. Mensitieri, Mass transport of low molecular weight compounds in polymers, in: E. Kiran (Ed.), *Foaming with Supercritical Fluids*, 1st ed., Elsevier, 2021, pp. 179–230.
- [125] D.R. Sturm, R.P. Danner, J.D. Moser, S.-W. Chiu, Application of the Vrentas-Duda free-volume theory of diffusion below the glass-transition temperature: Application to hypromellose acetate succinate-solvent systems, *J. Appl. Polym. Sci.* 136 (2019) 47351.
- [126] B. Wang, T. Yamaguchi, S.-I. Nakao, Solvent diffusion in amorphous glassy polymers, *J. Polym. Sci. B Polym. Phys.* 38 (2000) 846–856.
- [127] A. Rawat, D.J. Burgess, Effect of physical ageing on the performance of dexamethasone loaded PLGA microspheres, *Int. J. Pharm.* 415 (2011) 164–168.
- [128] K. Park, A. Otte, F. Sharifi, J. Garner, S. Skidmore, H. Park, Y.K. Jhon, B. Qin, Y. Wang, Potential Roles of the Glass Transition Temperature of PLGA Microparticles in Drug Release Kinetics, *Mol. Pharm.* 18 (2021) 18–32.
- [129] H. Eser, F. Tihminlioglu, Determination of thermodynamic and transport properties of solvents and non solvents in poly(L-lactide-co-glycolide), *J. Appl. Polym. Sci.* 102 (2006) 2426–2432.
- [130] J.S. Vrentas, J.L. Duda, A free-volume interpretation of the influence of the glass transition on diffusion in amorphous polymers, *J. Appl. Polym. Sci.* 22 (1978) 2325–2339.
- [131] N. Ramesh, P.K. Davis, J.M. Zielinski, R.P. Danner, J.L. Duda, Application of free-volume theory to self diffusion of solvents in polymers below the glass

- transition temperature: A review, *J. Polym. Sci. B Polym. Phys.* 49 (2011) 1629–1644.
- [132] L. Wang, J.-P. Corriou, C. Castel, E. Favre, Transport of Gases in Glassy Polymers under Transient Conditions: Limit-Behavior Investigations of Dual-Mode Sorption Theory, *Ind. Eng. Chem. Res.* 52 (2013) 1089–1101.
- [133] J.S. Vrentas, C.M. Vrentas, Predictive methods for self-diffusion and mutual diffusion coefficients in polymer–solvent systems, *Eur. Polym. J.* 34 (1998) 797–803.
- [134] J.S. Vrentas, J.L. Duda, H.-C. Ling, Self-diffusion in polymer-solvent-solvent systems, *J. Polym. Sci. Polym. Phys. Ed.* 22 (1984) 459–469.
- [135] W. Schabel, P. Scharfer, M. Kind, I. Mamaliga, Sorption and diffusion measurements in ternary polymer–solvent–solvent systems by means of a magnetic suspension balance—Experimental methods and correlations with a modified Flory–Huggins and free-volume theory, *Chem. Eng. Sci.* 62 (2007) 2254–2266.
- [136] W. Schabel, I. Ludwig, M. Kind, Measurements of Concentration Profiles in Polymeric Solvent Coatings by Means of an Inverse Confocal Micro Raman Spectrometer—Initial Results, *Dry. Technol.* 22 (2004) 285–294.
- [137] S.P. Chamarthy, R. Pinal, Plasticizer concentration and the performance of a diffusion-controlled polymeric drug delivery system, *Colloids Surf. A: Physicochem. Eng. Asp* 331 (2008) 25–30.
- [138] S. Schenderlein, M. Lück, B.W. Müller, Partial solubility parameters of poly(D,L-lactide-co-glycolide), *Int. J. Pharm.* 286 (2004) 19–26.
- [139] K. Vay, S. Scheler, W. Friess, Application of Hansen solubility parameters for understanding and prediction of drug distribution in microspheres, *Int. J. Pharm.* 416 (2011) 202–209.
- [140] D.J. van Drooge, W.L.J. Hinrichs, M.R. Visser, H.W. Frijlink, Characterization of the molecular distribution of drugs in glassy solid dispersions at the nano-meter scale, using differential scanning calorimetry and gravimetric water vapour sorption techniques, *Int. J. Pharm.* 310 (2006) 220–229.
- [141] F. Siepman, V. Le Brun, J. Siepman, Drugs acting as plasticizers in polymeric systems: a quantitative treatment, *J. Control. Release.* 115 (2006) 298–306.
- [142] C. Thomasin, P. Johansen, R. Alder, R. Bemsel, G. Hottinger, H. Altorfer, D.M. Wright, G. Wehrli, H.P. Merkle, B. Gander, A contribution to overcoming the

- problem of residual solvents in biodegradable microspheres prepared by coacervation, *Eur. J. Pharm. Biopharm.* 42 (1996) 16–24.
- [143] M.E. Rickey, J.M. Ramstack, R. Kumar, Residual solvent extraction method and microparticles produced thereby, U.S. 6,824,822 B2 (2003).
- [144] A.R. Ahmed, M. Ciper, R. Bodmeier, Reduction in Burst Release from Poly(D,L-Lactide-Co-Glycolide) Microparticles by Solvent Treatment, *Lett. Drug Des. Discov.* 7 (2010) 759–764.
- [145] K. Vay, W. Frieß, S. Scheler, A detailed view of microparticle formation by in-process monitoring of the glass transition temperature, *Eur. J. Pharm. Biopharm.* 81 (2012) 399–408.
- [146] V.A. Philip, R.C. Mehta, P.P. Deluca, In vitro and in vivo respirable fractions of isopropanol treated PLGA microspheres using a dry powder inhaler, *Int. J. Pharm.* 151 (1997) 175–182.
- [147] M.E. Rickey, J.M. Ramstack, D.H. Lewis, Preparation of biodegradable, biocompatible microparticles containing a biologically active agent, U.S. 5,792,477 A (1999).
- [148] A. Otte, B.K. Soh, K. Park, The Impact of Post-Processing Temperature on PLGA Microparticle Properties, *Pharm. Res.* 40 (2023) 2677–2685.
- [149] J. Shen, S. Choi, W. Qu, Y. Wang, D.J. Burgess, In Vitro-In Vivo Correlation of Parenteral Risperidone Polymeric Microspheres, *J. Control. Release* 218 (2015) 2–12.
- [150] M. Igartua, R.M.A. Hernández, J.E. Rosas, M.E. Patarroyo, J.L. Pedraz, Gamma-irradiation effects on biopharmaceutical properties of PLGA microspheres loaded with SPf66 synthetic vaccine, *Eur. J. Pharm. Biopharm.* 69 (2008) 519–526.
- [151] M.J. Alonso, S. Cohen, T.G. Park, R.K. Gupta, G.R. Siber, R. Langer, Determinants of release rate of tetanus vaccine from polyester microspheres, *Pharm. Res.* 10 (1993) 945–953.
- [152] G. Della Porta, E. Reverchon, Nanostructured microspheres produced by supercritical fluid extraction of emulsions, *Biotechnol. Bioeng.* 100 (2008) 1020–1033.
- [153] G. Della Porta, N. Falco, E. Reverchon, Continuous supercritical emulsions extraction: a new technology for biopolymer microparticles production, *Biotechnol. Bioeng.* 108 (2011) 676–686.

- [154] H. Park, J.-S. Kim, S. Kim, E.-S. Ha, M.-S. Kim, S.-J. Hwang, Pharmaceutical Applications of Supercritical Fluid Extraction of Emulsions for Micro-/Nanoparticle Formation, *Pharmaceutics* 13 (2021).
- [155] K. Koushik, U.B. Kompella, Preparation of large porous deslorelin-PLGA microparticles with reduced residual solvent and cellular uptake using a supercritical carbon dioxide process, *Pharm. Res.* 21 (2004) 524–535.
- [156] H. Kamali, M. Atamanesh, E. Kaffash, F. Mohammadpour, E. Khodaverdi, F. Hadizadeh, Elimination of residual solvent from PLGA microspheres containing risperidone using supercritical carbon dioxide, *J. Drug Deliv. Sci. Technol.* 57 (2020) 101702.
- [157] D. Liu, D.L. Tomasko, Carbon dioxide sorption and dilation of poly(lactide-co-glycolide), *J. Supercrit. Fluids* 39 (2007) 416–425.
- [158] T.H. Kim, T.G. Park, Critical effect of freezing/freeze-drying on sustained release of FITC-dextran encapsulated within PLGA microspheres, *Int. J. Pharm.* 271 (2004) 207–214.
- [159] P. Fonte, S. Reis, B. Sarmiento, Facts and evidences on the lyophilization of polymeric nanoparticles for drug delivery, *J. Control. Release* 225 (2016) 75–86.
- [160] Z. Wu, M. Zhao, W. Zhang, Z. Yang, S. Xu, Q. Shang, Influence of drying processes on the structures, morphology and in vitro release profiles of risperidone-loaded PLGA microspheres, *J. Microencapsul.* 36 (2019) 21–31.
- [161] H.K. Kim, H.J. Chung, T.G. Park, Biodegradable polymeric microspheres with "open/closed" pores for sustained release of human growth hormone, *J. Control. Release.* 112 (2006) 167–174.
- [162] K.B. Shepard, A.M. Dower, A.M. Ekdahl, M.M. Morgen, J.M. Baumann, D.T. Vodak, Solvent-Assisted Secondary Drying of Spray-Dried Polymers, *Pharm. Res.* 37 (2020) 156.
- [163] K.J. Chua, S.K. Chou, New Hybrid Drying Technologies, in: D.-W. Sun (Ed.), *Emerging Technologies for Food Processing*, 1st ed., Academic Press, 2005, pp. 535–551.
- [164] The International Council for Harmonisation of Technical Requirements for Pharmaceuticals for Human Use, *Impurities: Guideline for Residual Solvents: ICH Q3C (R9)*, 2024.
- [165] J. Kay, R. Thomas, J. Gruenhagen, C.J. Venkatramani, Simultaneous quantitation of water and residual solvents in pharmaceuticals by rapid

- headspace gas chromatography with thermal conductivity detection (GC-TCD), *Journal of pharmaceutical and biomedical analysis* 194 (2021) 113796.
- [166] H. Shim, H. Sah, Assessment of Residual Solvent and Drug in PLGA Microspheres by Derivative Thermogravimetry, *Pharmaceutics* 12 (2020).
- [167] K. Vay, W. Frieß, S. Scheler, Understanding reflection behavior as a key for interpreting complex signals in FBRM monitoring of microparticle preparation processes, *Int. J. Pharm.* 437 (2012) 1–10.
- [168] F. Bach, Physical Stability of and In-vitro Drug Release from Biodegradable PLGA Matrices. Doctoral dissertation, Berlin, 2021.
- [169] A.S. Zidan, Z. Rahman, M.A. Khan, Online monitoring of PLGA microparticles formation using Lasentec focused beam reflectance (FBRM) and particle video microscope (PVM), *AAPS J.* 12 (2010) 254–262.
- [170] M. Muhaimin, A.Y. Chaerunisaa, R. Bodmeier, Real-time particle size analysis using focused beam reflectance measurement as a process analytical technology tool for continuous microencapsulation process, *Sci. Rep.* 11 (2021) 19390.
- [171] J. Panyam, D. Williams, A. Dash, D. Leslie-Pelecky, V. Labhasetwar, Solid-state solubility influences encapsulation and release of hydrophobic drugs from PLGA/PLA nanoparticles, *J. Pharm. Sci.* 93 (2004) 1804–1814.
- [172] F. Bach, S. Staufenbiel, R. Bodmeier, Implications of changes in physical state of drugs in poly(lactide-co-glycolide) matrices upon exposure to moisture and release medium, *J. Drug Deliv. Sci. Technol.* 80 (2023) 104115.
- [173] T. Ehtezazi, C. Washington, Controlled release of macromolecules from PLA microspheres: using porous structure topology, *J. Control. Release.* 68 (2000) 361–372.
- [174] C. Zhang, Biodegradable microparticles and in situ forming implants/microparticles containing drugs in different physical states. Doctoral dissertation, Berlin, 2022.
- [175] A.F.M. Barton, *CRC handbook of solubility parameters and other cohesion parameters*, 2 ed., CRC Press, Boca Raton, Fla., 1991.
- [176] M. Sugisaki, H. Suga, S. Seki, Calorimetric Study of the Glassy State. III. Novel Type Calorimeter for Study of Glassy State and Heat Capacity of Glassy Methanol, *Bull. Chem. Soc. Jpn.* 41 (1968) 2586–2591.

-
- [177] S. Benkhof, A. Kudlik, T. Blochowicz, E. Rössler, Two glass transitions in ethanol: a comparative dielectric relaxation study of the supercooled liquid and the plastic crystal, *J. Phys.: Condens. Matter* 10 (1998) 8155–8171.
- [178] C. Talón, M.A. Ramos, S. Vieira, I. Shmyt'ko, N. Afonikova, A. Criado, G. Madariaga, F.J. Bermejo, Thermodynamic and structural properties of the two isomers of solid propanol, *J. Non-Cryst. Solids* 287 (2001) 226–230.
- [179] A. Toxqui-Terán, C. Leyva-Porras, M.Á. Ruíz-Cabrera, P. Cruz-Alcantar, M.Z. Saavedra-Leos, Thermal Study of Polyols for the Technological Application as Plasticizers in Food Industry, *Polymers* 10 (2018).
- [180] S. D'Souza, J.A. Faraj, R. Dorati, P.P. Deluca, Enhanced Degradation of Lactide-co-Glycolide Polymer with Basic Nucleophilic Drugs, *Adv. Pharm. 2015* (2015) 1–10.
- [181] S. D'Souza, J.A. Faraj, S. Giovagnoli, P.P. Deluca, Development of Risperidone PLGA Microspheres, *J. Drug Deliv. 2014* (2014) 620464.
- [182] G. Liu, K. McEnnis, Glass Transition Temperature of PLGA Particles and the Influence on Drug Delivery Applications, *Polymers* 14 (2022).
- [183] J.-W. Yoo, S. Mitragotri, Polymer particles that switch shape in response to a stimulus, *Proceedings of the National Academy of Sciences of the United States of America* 107 (2010) 11205–11210.
- [184] W. Chen, A. Palazzo, W.E. Hennink, R.J. Kok, Effect of Particle Size on Drug Loading and Release Kinetics of Gefitinib-Loaded PLGA Microspheres, *Mol. Pharm.* 14 (2017) 459–467.
- [185] Q. Xu, M. Hashimoto, T.T. Dang, T. Hoare, D.S. Kohane, G.M. Whitesides, R. Langer, D.G. Anderson, Preparation of monodisperse biodegradable polymer microparticles using a microfluidic flow-focusing device for controlled drug delivery, *Small (Weinh.)* 5 (2009) 1575–1581.

List of Figures

Figure 1: Synthesis of PLGA by ring-opening polymerization of lactide and glycolide (adapted from [27]).....	5
Figure 2: Schematic representation of different flow regimes in (a) coaxial, (b) flow focusing and (c) T-junction microfluidic devices [79]	15
Figure 3: Initial sub-processes around a single droplet after emulsification during the solvent extraction/evaporation method [12]	19
Figure 4: Schematic representation of the different contributions to the polymer volume as a function of temperature based on the free volume theory [124]	24
Figure 5: Schematic setup for diafiltration-controlled extraction for microparticle preparation, equipped with probes for in-process video microscopy (PVM) and focused beam reflectance measurement (FBRM).....	36
Figure 6: Schematic setup for continuous solvent extraction downstream to microfluidic emulsification	38
Figure 7: Schematic setup for alcohol vapor-assisted fluidized bed drying of microparticles	39
Figure 8: Distribution of dichloromethane during the solvent evaporation controlled microparticle preparation with an initial phase ratio of 1:20 (50 mL batch size). Closed symbols represent values determined by gas chromatography (dispersed and continuous phase) or mass loss (evaporated), while open symbols are calculated ..	47
Figure 9: Effect of initial phase ratio and dilution after 15 min on the particles size distribution.....	48
Figure 10: Effect of one-step dilution, 15 min after emulsification and buffering of the continuous phase, on the encapsulation efficiency of risperidone	49
Figure 11: Effect of relative diafiltration rate and drug loading on the dichloromethane content in (a) the continuous phase and (b) the dispersed phase (200 mL batch size)	50
Figure 12: Effect of diafiltration and temperature on the dichloromethane content in the dispersed phase (50 mL batch size)	50
Figure 13: Effect of relative diafiltration rate and drug loading on square weighted media chord length (200 mL batch size).....	51
Figure 14: Number of chord counts of size fractions during encapsulation of 30 % risperidone with the solvent evaporation method (200 mL batch size).....	52
Figure 15: Microscopic appearance (in-situ) during encapsulation of risperidone in PLGA 503H (circles mark first appearance of needle-shaped risperidone crystals) ..	52

Figure 16: Effect of relative diafiltration rate and drug loading on the particle size distribution of microparticles loaded with (a) 30 % dexamethasone and (b) 30 % risperidone	53
Figure 17: Effect of relative diafiltration rate and drug loading on the morphology of microparticle cross-sections	54
Figure 18: Effect of relative diafiltration rate, drug loading and PLGA grade on the encapsulation efficiency	55
Figure 19: Effect of PLGA grade and risperidone loading on the square weighted media chord length during the solvent evaporation process (200 mL batch size)	56
Figure 20: Microscopic appearance (in-situ) during encapsulation of risperidone in PLGA RG 753S (circles mark first appearance of needle-shaped risperidone crystals)	56
Figure 21: Effect of relative diafiltration rate on the in-vitro release of (a) dexamethasone as a function of the theoretical drug loading and (b) risperidone as a function of the PLGA grade	57
Figure 22: Effect of temperature during diafiltration-assisted preparation of dexamethasone-loaded microparticles (30 % theoretical drug loading) on the morphology of microparticle cross-sections	58
Figure 23: Effect of temperature during diafiltration assisted preparation of dexamethasone-loaded microparticles (30 % theoretical drug loading) (a) on the in-vitro drug release and (b) on the correlation of the water content before drying and the burst release within 48 h	59
Figure 24: Effect of the methanol content in the dispersed phase on the residual dichloromethane content of dexamethasone-loaded microparticles.....	60
Figure 25: Effect of the methanol content in the dispersed phase on the microscopic appearance (top) and the morphology of cross-sections (bottom) of microparticles with 30 % dexamethasone.....	61
Figure 26: Effect of the theoretical dexamethasone loading and the methanol content in the dispersed phase on the encapsulation efficiency of microparticles	62
Figure 27: Effect of the theoretical dexamethasone loading and the methanol content in the dispersed phase on the in-vitro release of microparticles.....	62
Figure 28: Effect of extraction conditions on the residual dichloromethane content of blank PLGA 503H microparticles	65
Figure 29: Effect of the extraction time at 35 °C on the microscopic appearance of risperidone-loaded 503H microparticles	66
Figure 30: Effect of PLGA grade on the particle size distribution of risperidone-loaded microparticles	68

Figure 31: Effect of PLGA grade and the extraction temperature on the microscopic appearance of risperidone-loaded microparticles	69
Figure 32: Effect of increased extraction temperature and modification of PLGA grade, i.e. (a) molecular weight, (b) end-capping and (c) lactide content on the in-vitro release of 30 % risperidone (n=1)	70
Figure 33: Effect of the amount of methanol (a, b), ethanol (c, d) or isopropanol (e, f) in the continuous phase on the content of absorbed alcohol (a, c, e) and residual dichloromethane (b, d, f) in blank microparticles.....	73
Figure 34: Effect of the type and amount of absorbed (non-)solvent on the glass-transition temperature of PLGA, calculated with the Gordon Taylor equation	74
Figure 35: Effect of the type and amount of alcohol in the continuous phase on the microscopic appearance of blank microparticles after 6h (the red line marks the limit when sticking occurred).....	75
Figure 36: Effect of the type and amount of alcohol in the continuous phase on the content of (a) absorbed alcohol and (b) residual dichloromethane in microparticles (30 % theoretical dexamethasone loading).....	76
Figure 37: Effect of the theoretical dexamethasone loading and type and amount of alcohol in the continuous phase on the encapsulation efficiency	76
Figure 38: Effect of the type and amount of alcohol in the continuous phase on the appearance of microparticles (30 % theoretical dexamethasone loading) after 6 h extraction under polarized light microscope (left) and scanning electron microscope (mid and right).....	77
Figure 39: Effect of the type and amount of alcohol in the continuous phase on the content of (a) alcohol and (b) dichloromethane in microparticles (30 % theoretical risperidone loading).....	78
Figure 40: Effect of the type and amount of alcohol in the continuous phase on the appearance of microparticles (30 % theoretical risperidone loading) after 6 h extraction under polarized light microscope (left) and scanning electron microscope (mid and right).....	79
Figure 41: Effect of the type and amount of alcohol in the continuous phase on the encapsulation efficiency of 30 % risperidone	80
Figure 42: Effect of the purge gas temperature on the residual dichloromethane content of blank PLGA 503H microparticles during fluidized bed drying	81
Figure 43: Effect of the purge gas temperature on the microscopic appearance of blank PLGA 503H microparticles during fluidized bed drying	82
Figure 44: Effect of the alcohol concentration and flow rate during fluidized bed drying, on the content of (a) absorbed alcohol and (b) residual dichloromethane of blank 503H microparticles (6 h alcohol purge, followed by 18 h dry purge (20 L/min, 35 °C)).....	84

Figure 45: Effect of the stabilizer and ethyl acetate content in the continuous phase on the microscopic appearance of blank 503H microparticles	85
Figure 46: Effect of the stabilizer and ethyl acetate content in the continuous phase on the particle size distribution of blank 503H microparticles.....	85
Figure 47: Effect of the methanol concentration in the purge gas during fluidized bed drying, on the content of (a) absorbed methanol and (b) residual ethyl acetate of blank PLGA 503H microparticles	86
Figure 48: Effect of PLGA grade and pre-drying during fluidized bed drying (100 mg/L methanol; 10 L/min) on the content of (a) absorbed methanol and (b) residual dichloromethane of risperidone-loaded microparticles.....	87
Figure 49: Effect of PLGA grade and pre-drying during fluidized bed drying (100 mg/L methanol; 10 L/min) on the microscopic appearance of risperidone-loaded microparticles	87
Figure 50: Effect of PLGA grade and 30 % risperidone loading on the DSC thermogram of microparticles	88
Figure 51: Effect of the drug loading during fluidized bed drying (140 mg/L methanol; 10 L/min) on the content of (a) absorbed methanol and (b) residual dichloromethane	89
Figure 52: Effect of methanol vapor-assisted fluidized bed drying on the surface morphology of microparticles loaded with risperidone (1 h pre-dried) and dexamethasone.....	90
Figure 53: Effect of methanol vapor-assisted purge flow drying (100 mg/L; 1L/min) on the recrystallization of 2 % dexamethasone and 10 % risperidone in PLGA 503H films	91
Figure 54: Effect of the methanol concentration in the purge gas on the methanol absorption and recrystallization of 10 % risperidone in PLGA 503H and 753S films .	92
Figure 55: Effect of methanol assisted fluidized bed drying (6 h 140 mg/L 10 L/min + 18 h 0 mg/L 20 L/min 35 °C) on the in-vitro release of risperidone and dexamethasone from PLGA 503H and 753S microparticles compared to vacuum drying at 35 °C	93
Figure 56: Effect of PVA concentration and flow rate ratio during microfluidic flow focusing on the microscopic appearance of droplet formation on the chip (top) and resulting solidified risperidone-loaded 503H microparticles (bottom)	95
Figure 57: Effect of the composition of the continuous phase and total flow rate (phase ratio 1:7) on the microscopic appearance of microfluidic droplet formation.....	96
Figure 58: Effect of the flow rate ratio during microfluidic flow focusing on the microscopic appearance of droplet formation on chip (top) and resulting solidified microparticles (middle) and microparticles of comparable size produced by the batch process (bottom)	98

Figure 59: Comparison of the monodisperse particle size of microparticles prepared by microfluidic flow focusing (determined by microscopic size determination) and particle size distribution of comparable microparticles prepared by the batch process (determined by laser diffraction)99

Figure 60: Effect of the particle size and manufacturing process on the in-vitro release of risperidone from 753S microparticles99

Figure 61: Effect of the phase ratio after dilution on the particle size of droplets after 150 cm or 450 cm lag tubing and of solidified microparticles 101

Figure 62: Effect of temperature (top) and methanol content (bottom) of the continuous phase on the microscopic appearance of droplets (generated by microfluidic flow focusing and subsequent 1:100 dilution) in a flow-cell after 150 cm lag tubing 102

Figure 63: Comparison of the schematic design of (a) a commercial multi-angled tangential flow filtration with large cross-section that cause particle deposition and (b) self-built U-shaped tangential flow filtration device with small cross-section to maintain higher flow..... 103

List of Tables

Table 1: Dissolution of 2.5 % (w/V) PLGA in different solvents depending on the lactide:glycolide ratio at a constant molecular weight of around 80 kDa [12]	17
Table 2: Classification and permitted daily exposure (PDE) of organic solvents commonly used for preparation of PLGA microparticles by solvent extraction/evaporation method (adapted from [164])	31
Table 3: Density and glass transition temperature of excipients (references in parenthesis) used to calculate the glass transition temperature of binary systems with the Gordon-Taylor equation	65
Table 4: Effect of PLGA grade and extraction temperature on the encapsulation efficiency (EE) of 35 % risperidone and residual water and solvent content	67
Table 5: Effect of the type and amount of alcohol in the continuous phase on the dichloromethane solubility	71
Table 6: Hansen solubility parameters of the investigated drugs and excipients (references in parenthesis) and their HSP distance R_a to PLGA.....	72
Table 7: Effect of the purge flow rate and bubbler temperature on the concentration of methanol and ethanol in the purge gas	83
Table 8: Effect of PVA concentration and flow rate of the continuous phase (Q_{CP}) during microfluidic flow-focusing with a constant flow rate of the dispersed phase of 70 $\mu\text{L}/\text{min}$ on the particle size and the encapsulation efficiency (EE) of 10 % and 30 % risperidone in 503H.....	94
Table 9: Effect of PLGA grade and flow rate of the continuous phase (pH 10 buffered 1 % (w/V) PVA) (Q_{CP}) in microfluidic flow focusing with a constant flow rate of dispersed phase of 35 $\mu\text{L}/\text{min}$ on the particle size and encapsulation efficiency (EE) of microparticles with 30 % theoretical risperidone loading.....	97

Publications

F. Kias, R. Bodmeier, Control of encapsulation efficiency and morphology of poly(lactide-co-glycolide) microparticles with a diafiltration-driven solvent extraction process. *Submitted to Eur. J. Pharm. Biopharm.*

F. Kias, R. Bodmeier, Acceleration of final residual solvent extraction from poly(lactide-co-glycolide) microparticles. *Submitted to Pharm. Res.*

F. Kias, R. Bodmeier, Accelerated removal of solvent residuals from PLGA microparticles by alcohol vapor-assisted fluidized bed drying. *Submitted to Int. J. Pharm.*